



VCU

Virginia Commonwealth University
VCU Scholars Compass

Theses and Dissertations


Graduate School

2015

POLYSACCHARIDE-BASED SHEAR THINNING HYDROGELS FOR THREE-DIMENSIONAL CELL CULTURE

Vasudha Surampudi
Virginia Commonwealth University

Follow this and additional works at: <https://scholarscompass.vcu.edu/etd>

 Part of the [Biochemical and Biomolecular Engineering Commons](#), [Biological Engineering Commons](#), [Biomaterials Commons](#), [Biomechanics and Biotransport Commons](#), and the [Polymer Science Commons](#)

© The Author

Downloaded from

<https://scholarscompass.vcu.edu/etd/3872>

This Dissertation is brought to you for free and open access by the Graduate School at VCU Scholars Compass. It has been accepted for inclusion in Theses and Dissertations by an authorized administrator of VCU Scholars Compass. For more information, please contact libcompass@vcu.edu.

©Vasudha Surampudi 2015

All Rights Reserved

POLYSACCHARIDE-BASED SHEAR THINNING HYDROGELS FOR
THREE-DIMENSIONAL CELL CULTURE

A dissertation submitted in partial fulfillment of the requirements for the degree of Doctor of
Philosophy at Virginia Commonwealth University.

By

Vasudha Surampudi

M.S., Virginia Commonwealth University, U.S.A, 2011

B. Tech, Jawaharlal Nehru Technological University, India, 2008

Director: Dr. Xuejun Wen, M.D., Ph.D., AIMBE Fellow

Alice T. and William H. Goodwin Jr. Endowed Chair Professor in Regenerative Medicine
Chemical and Life Sciences Engineering

Virginia Commonwealth University

Richmond, Virginia

May, 2015

ACKNOWLEDGEMENT

I would like to start by thanking Dr. Xuejun Wen to agreeing to let me join his lab and opening up the Pandora box of research. The creative and scientific freedom given by Dr. Wen helped me explore the crevices of science, doing things with a passion I thought I almost lost. Thank you for helping me at the time when I needed it the most. This PhD would not have been possible without the knowledge and resources provided by Dr. Wen. Also, I would like to know the secret to his eternal state of zen. I would like to thank Dr. Ning Zhang for her wonderful guidance and feedback during my dissertation writing.

I would like to thank Dr. B. Frank Gupton, our department Chair and my committee member, for having faith in my abilities and ensuring that I was placed in a lab that was a wonderful fit to my personality as well as my research interests. The insightful discussions I had with Dr. Gupton, along with all the life advice I received, helped me become a mature individual. I would like to thank the committee members, Dr. Michael Peters, Dr. Hu Yang and Dr. Dong Sun for sticking with me during the change of course in my graduate studies and their wonderful questions brought out the better researcher in me. I would also like to thank Dr. Daniel Conway to taking time out of schedule to provide assistance with the photobleaching experiments.

I would like to thank my on-call advice group of friends and researchers, consisting of Dr. Giuseppe Pettinato, Dr. Xiaowei Li, Dr. Rajender Reddy Mallepally, Dr. Venkat Sundar Gadepalli, Dr. Joe Riggs, Dr. Vijender Chaitankar, and, Dr. Aditi Mulgaonkar. Also, I would have been in school forever, if not for the help of Ganesh Sosale. A huge part of keeping me sane

during this roller-coaster of graduate school are my friends, who became a family, Aditi, Soni, Leena, Sudha, Ancy, Bhanu and Vijay. I want to add my cousin/sister/best friend Akhila Singaraju here too. Thank you for praying for me as I have been praying for you too. Thank you, Babatunde and Kendra for being my running mates in the program. I am happy to be finishing this journey with you guys.

A special shout-out goes to my new family of my supporting in-laws and sister-in-law, Swetha. Words cannot express the gratitude and love I have for my parents and my brother for always believing in me and giving me the freedom to think and develop into an independent person. Playing an equally important role in my development into a dedicated student is my husband, Pratik. Thank you for telling me to never lose hope and teaching me to always stay positive. You are my biggest cheer leader and this PhD would not have been possible without you being on my side always.

To everyone facing difficulty achieving their goals, “*Just keep swimming*”.

This dissertation and my whole career are dedicated to my family.

To my parents, my brother and my husband, Pratik.

TABLE OF CONTENTS

ACKNOWLEDGEMENTS	ii
DEDICATION	iv
LIST OF FIGURES	x
LIST OF TABLES	xviii
ABSTRACT	
1. INTRODUCTION AND DISSERTATION OVERVIEW	
1.1. Three dimensional <i>In Vitro</i> models	1
1.2. Shear-thinning hydrogels for tissue engineering and regenerative medicine	2
1.3. Limitations	3
1.4. Project Objective, Significance and Innovation	4
1.5. Specific Aims and Rationale	5
1.6. Dissertation Organization	6
1.7. Design of Experiments	7
2. SHEAR THINNING HYDROGELS AND THEIR BIOMEDICAL APPLICATIONS	
2.1. Introduction	9
2.2. Shear-thinning hydrogels introduction	10
2.3. Properties and Characterization of shear-thinning hydrogels	11
2.3.1. Fluid Classification	11
2.3.2. Non-newtonian flow models	14
2.3.3. Rheological Analysis	16
2.3.4. Physical characteristics of Shear-thinning fluids	19
2.3.5. Gelation Kinetics	21

2.4. Classification of shear-thinning hydrogels based on their chemical composition	
2.4.1. Natural	
2.4.1.1. Polysaccharide-based	23
2.4.1.2. Peptide-Based Hydrogels	27
2.4.2. Synthetic/Synthetic-Natural Blend Polymers	30
2.4.2.1. Photocrosslinkable polymers	30
2.4.2.2. Polyelectrolyte-based polymers	32
2.4.2.3. PolyHIPEs: Polymerization of High internal Phase Emulsions	32
2.4.2.4. Polymers as delivery vehicles for microsphere/nanoparticles	35
2.5. Conclusions	38
2.6. REFERENCES	39
3. PREPARATION AND CHARACTERIZATION OF GELLAN GUM-BASED SHEAR-THINNING HYDROGELS	
3.1. Introduction	50
3.2. Materials And Methods	53
3.2.1. Materials	53
3.2.2. Preparation of hydrogels	53
3.2.3. Aerogel synthesis and Scanning electron microscope	54
3.2.4. Rheological characterization of hydrogels	54
3.2.5. Swelling of hydrogels	56
3.2.6. Degradation studies	56
3.2.7. In vitro growth factor release studies	57
3.2.8. Fluorescence Recovery after Photobleaching (FRAP)	57
3.3. Results	58
3.3.1. Hydrogel formation and gel morphology	58
3.3.2. Scanning electron microscopy for porosity	59
3.3.3. Rheological characterization of the hydrogels	60
3.3.4. Swelling studies	70

3.3.5. Degradation studies	70
3.3.6. In vitro release of VEGF	71
3.3.7. Fluorescence Recovery After Photobleaching for Diffusion Coefficient	74
3.4. Discussion	76
3.5. Conclusions	78
3.6. References	79
4. APPLICATION OF GELLAN GUM-BASED SHEAR THINNING HYDROGELS FOR THREE-DIMENSIONAL CELL CULTURE	
4.1. Introduction	83
4.2. Materials And Methods	85
4.2.1. Materials	85
4.2.2. Cell Culture	86
4.2.3. Silk Fibroin Extraction	88
4.2.4. Cell Viability	88
4.2.5. Cellular Actin Cytoskeleton Organization	89
4.2.6. Rheological Characterization Of Hydrogels	89
4.2.7. Statistical Analysis	90
4.3. Results And Discussion	90
4.3.1. General Cell Culture Model And Material Characterization With Cells	91
4.3.2. Btc-3 Cell Culture	95
4.3.3. Human Endothelial Cell Culture	98
4.3.4. Human Induced Pluripotent Stem Cells	103
4.3.5. Human Neural Stem Cells	105
4.4. Conclusions	110
4.5. References	110
5. GELLAN GUM-BASED SHEAR-THINNING HYDROGELS AS SUBSTRATES IN SCALABLE ROBOTIC FABRICATION OF IDENTICAL CELL SPHEROIDS FOR TISSUE ENGINEERING	

5.1. Introduction	114
5.2. Materials And Methods	119
5.2.1. Materials	119
5.2.2. Preparation of hydrogels	120
5.2.3. Rheological characterization of hydrogels	120
5.2.4. Swelling of hydrogels	121
5.2.5. Human neural stem cell culture	122
5.2.6. Human induced pluripotent stem cell maintenance culture	122
5.2.7. Cell viability	122
5.2.8. Embryoid body formation	123
5.2.9. Embryonic body suspension culture and growth evaluation	124
5.2.10. Human Neurosphere Formation	124
5.2.11. Immunofluorescence	125
5.2.12. Statistical analysis	126
5.3. Results	126
5.3.1. Gellan gum based microwell fabrication	126
5.3.2. Rheological analysis	127
5.3.3. Swelling studies	128
5.3.4. Human Embryoid body formation	130
5.3.5. Human neurosphere formation	135
5.4. Discussion	139
5.5. Conclusions	141
5.6. References	142
6. OVERALL CONCLUSIONS AND FUTURE DIRECTIONS	
6.1. Conclusions	146
6.2. Future Directions	148

LIST OF FIGURES

- 1.1: The “Blackbox” process model schematic
- 2.1: Two dimensional model of Newtonian fluids and the parameters involved in shear stress and shear rates contributing towards the definition of the fluid viscosity
- 2.2: Graphical representation of the different types of fluids based on their relationship between shear stress and rate of shear strain with shear stress as y-axis and shear rate as x-axis.
- 2.3: Rheological characteristics of PEG–silica gels. a, Typical G' , G'' and δ of gels without fumed silica as a function of increasing shear stress τ applied with time.
- 2.4: Chemical structure of polymers as building blocks of hybrid hydrogels
- 2.5: The versatility of gellan gum structures that can be used for simple polymer processing techniques: (A) Discs (B) Membranes (C) Fibers (D) Particles (E) (F) Lyophilized scaffolds
- 2.6: Construction of BCM-integrated HA hydrogels with force-modulated DEX release capacity. (A): Chemical structures of hydrogel building blocks: (1) glycidyl
- 2.7: Dynamic rheological study of h9e hydrogel A. Storage modulus G' of shear-thinning and recovery test of 1, 2, and 3 mM peptide hydrogel. B. Amplitude sweep test with shear strain from 1% to 500% and 1- 5-, and 10-minute breaks. (Four times) C. Multiple
- 2.8: a. Schematic representation of the process to fabricate a polymerized high internal phase emulsion [84]. (A) The emulsion is composed of a hydrophobic organic phase and an aqueous phase. (B) High internal phase emulsion (HIPE) is defined by the aqueous volume phase greater than 74% and exhibits a whipped mayonnaise consistency before cure. b. Injectable PFDMA polyHIPEs can be used *in situ* to space fill complex defects c. 24 hour 3T3 Live/Dead analysis of

5 wt% PGPR polyHIPEs. A) Fluorescent image (green = live, red = dead) B) Comparison of viable cells on tissue culture polystyrene and HIPE (n=15). No significant difference was observed between the polystyrene ($96 \pm 3\%$) and HIPE ($95 \pm 6\%$).

2.9: (a) Schematic representation of the preparation of polymer–nanoparticle (PNP) hydrogels utilizing non-covalent interactions between core-shell nanoparticles (NPs) and (b) hydrophobically modified hydroxypropylmethylcellulose. (c) The NPs can be composed of either poly(styrene) (PS; non-degradable) or poly(ethylene glycol)-*block*-poly(lactic acid)

3.1: Hydrogel morphology A. Gellan gum with and without cell culture medium, B. Hydrogel can be injected into the desired shapes or patterns, C. The gellan gum sets into gels

3.2: The porosity and textural properties were studied by observing the microscale features using the scanning electron microscopy of supercritical CO₂ dried hydrogels at

3.3: The sol-gel transition was observed by the changes in the storage and loss moduli (G' and G'') and phase angle (δ)

3.4: The addition of cell culture medium added the cationic interactions which made the gellan gum gels stronger as observed by the difference in the storage modulus (G') with red data points for gellan gum only (1.4%) and blue data points for gellan gum (1.4%) with

3.5: The storage modulus (G') increased with an increase in the number of days of incubation in the cell culture medium when loaded with cells (Mean \pm Std. Dev)

3.6: Shear thinning effect of the hydrogels was measured by the change in the viscosity with an increase in shear rate and the similar trend was recorded in the gels with (A) and

3.7: Oscillatory time sweep and flow sweep were used in combination to get the time needed for the gelation proceeding shear thinning, inset: the viscosity reading of the

3.8: Shear stress and relaxation test was used to observe the effect of shear-thinning and consequent thixotropic recovery of the initial state with the removal of the shear stress

3.9: Swelling studies were performed in cell culture medium and PBS in the lower to high gel stiffness range as quantified from the prior rheology experiments and the gel

3.10: Cumulative release of the VEGF was recorded over a period of two weeks in two different concentrations of gellan gum, one representing the lower limit of the stiffness

3.11: The cumulative release trend of the VEGF was confirmed by the release of VEGF from two different loading concentrations of condition 1, 500 ng/ml and condition 2, 100 ng/ml

3.12: Fluorescence recovery after photobleaching was used to get the values of D, diffusion coefficient of the different molecular weights of FITC-dextran in the gellan gum hydrogels to get an idea of the range of the sizes of proteins and cells to be housed in the

4.1: Schematic for the development of the *in-vitro* gellan-gum based three-dimensional cell propagation model

4.2: Schematic for the silk fibroin extraction from silk worm cocoons

4.3: The rheological analysis showed a gradual increase in the storage modulus of the hydrogels with the ETC-3 cells being cultured in them for a time period of 7 days (Mean \pm Std. Dev.)

4.4: Scanning electron microscopic images of the supercritical dried hydrogel samples with day 5 human endothelial cells, the images show various magnifications of the scaffold and potential extracellular matrix generated by the cells within the scaffold

- 4.5: Phase contrast microscopic images of the three-dimensional culture of the different cell types in the gellan-gum hydrogels with A. hiPSC B. hNSCs C. β TC-3 D. hECs
- 4.6: The effect of gel stiffness and cell seeding density were observed for the β TC3 cells seeded at 500k/100 μ l seeding density. Conditions: Hydrogels without Silk Fibroin (A-
- 4.7: The individual islet-like structures seen at close using a 40X objective with AlexaFluor 488 staining for Actin and DAPI for cell nuclei
- 4.8: Cell proliferation was observed for a time period of four days by using AlamarBlue™ to correlate the percent reduction of the dye as the cell number per time point
- 4.9: Cell viability assay was used to conclude that the hydrogel showed negligible number of dead cells at the cell seeding densities of 50k (A, D, G), 100k (B, E, H) and 500k (C, F, I) per 100 μ l with the viable live cells seen A-C; dead cells seen in D-F; Merge (G-I)
- 4.10: The effect of cell seeding density is observed by staining for actin using AlexaFluor 546 and DAPI for cell nuclei for two different hydrogels with initial gellan gum concentration of 1.1% (A-C) and 1.4% (D-F). The cell seeding densities were 125k/100 μ l (A,D); 500k/ μ l (B,E); 1000k/100 μ l (C,F)
- 4.11: The actin morphology of the cells shows the tubular assembly of the cells within the 1.1% initial concentration of gellan gum and silk fibroin added hydrogel
- 4.12: Orthogonal sectioning confirmed the hollow tubular structure of the formed vessel-like cell assembly with A. The cross section of the tubular structure, B. DAPI, C. AlexaFluor 546 Phalloidin

4.13: The tubular assembly was further enhanced with the addition of VEGF to the cell culture medium in which the hydrogel was incubated

4.14: The role of VEGF in the cell adhesion and proliferation is proven with the incorporation of VEGF in the hydrogel directly. A. hECs growing in the hydrogel with no VEGF and B, C.

Hydrogel with VEGF added to the hydrogel directly to get a final concentration of 100 ng/ml.

4.15: Live-Dead assay was performed to identify the hydrogel concentration favorable to the hiPSC survival. Also the effect silk fibroin was observed in the different hydrogel stiffness as well. Conditions without silk fibroin (A-C), conditions with silk fibroin (D-F). The starting concentration of gellan gum used is 1.1% (A, D), 1.4% (B, E) and 1.7% (C, F)

4.16: The cell morphology of the hiPSCs was observed by staining for actin and DAPI for nuclei in two different cell seeding densities, A. 50k cells/100 μ l and B. 100k cells/100 μ l

4.17: The effect of cell seeding density is observed by staining for actin using AlexaFluor 488 and DAPI for cell nuclei for two different hydrogels with initial gellan gum concentration of 1.1% (A-C) and 1.4% (D-F). The cell seeding densities were 125k/100 μ l

Figure 4.18: A closer look at the human neurosphere as seen using a 40X objective

4.19: The effect of gel stiffness and cell seeding density were observed for the hNSCs seeded at 200k/100 μ l (A-C), 500k/100 μ l (D-F) seeding density, initial gellan gum concentrations of gellan gum, 1.1% (A, D), 1.4% (B, E), 1.7% (C, F)

4.20: The effect of adding silk fibroin to the hNSCs was observed in 1.4% (A, C) and 1.7% (B, D) was observed with the conditions A, B without silk fibroin and B, D with silk fibroin added

4.21: An extensive study on the effect of cell seeding density was performed on hNSCs with cell morphology observed by AlexaFluor 488 staining for actin and DAPI for cell nuclei during different time points: day 1 (A, E, I, M), day 3 (B, F, J, N), day 5 (C, G, K, O), day 10 (D, H, L, P) with cell densities being 125k (A-D), 250k (E-H), 500k (I-L), 1000k (M-P) per 100 μ l

4.22: Nestin marker expression was observed to confirm the stemness of the hNSCs seeded in the 1.4% initial concentration of gellan gum hydrogels for two different seeding densities of 250k (A) and 500k (B) per 100 μ l with silk fibroin

4.23: A closer look at the spheroid structures formed within the 1.4% gellan gum hydrogels with different initial seeding densities 250k (A, B) and 500k (C, D) per 100 μ l

5.1: (a) Layer by layer fabrication of cell sheets with embedded spheroids as building blocks. (b) Toxicology testing of multiple drug concentrations and time points simultaneously performed on multiple spheroids per condition

5.2: Schematic for the gellan gum based microwell fabrication

5.3: A. The Computer controlled spheroid maker, B and C. Process of microwells fabrication, D. Gellan gum Microwells

5.4: Dynamic swelling of the hydrogels of 3% and 4% was evaluated in cell culture medium (a) and PBS (b) to up to 21 days. Similar experiment was conducted simultaneously in DI water (c) as a negative control to observe the effect of cations on the swelling and potential degradation of the hydrogel

5.5: Condensation of the hiPSC suspension within the microwells immediately after seeding (A, B, C, D, E) and the compact core development within 24 hours of culture in the microwells (F, G, H, I, J) for various cell seeding densities (top-bottom; 20k, 25k, 30k, 35k, 40k cells/microwell)

5.6: Compact and spherical hEBs were formed at various seeding densities and the size is directly proportional to the cell number per microwell, A-E, 20k, 25k, 30k, 35k, 40k cells/microwell and stayed intact after 24 hours of suspension culture with gentle agitation. F. The rate of formation of hEB was dependent on the cell seeding density to the microwells and the optimum range of cell seeding density was observed to be within 25k-40k cells/microwell; Scale bar: 500 μm

5.7: Cell viability of the hEBs was assessed by using Live-Dead assay with live cells stained with green fluorescent SYTO 10 (A) and dead cells with compromised cell membranes stained with red fluorescent ethidium homodimer-2 (B), DAPI staining for nuclei (C) and merge (D); Scale bar: 100 μm

5.8: hEBs expressed the proteins specific to the three germ layer lineages with Alpha fetoprotein (AFP, endoderm-specific) (A-C), SOX1 (ectoderm-specific) (D-F) and brachiury (mesoderm-specific) (G-I); Scale bar: 100 μm

5.9: A. Freshly extracted human neurospheres from the microwells B-D. Increase in the size of the core and the overall size increase observed in the neurosphere from day 1 (B), day 2 (B) and day 4 (D) in suspension following the extraction from the microwells; Scale bar: 200 μm

5.10: Compact and spherical human neurospheres were formed at various seeding densities and the size is directly proportional to the cell number per microwell, A-F, 125k, 250k, 500k, 750k, 1000k, 3000k cells per microwell; Scale bar: 200 μm

5.11: Cell viability of the neurospheres was assessed by using Live-Dead assay with live cells stained with green fluorescent SYTO 10 (A) and dead cells with compromised cell membranes stained with red fluorescent ethidium homodimer-2 (B), DAPI staining for nuclei (C) and merge (D); Scale bar: 100 μm

5.12: Human neurospheres expressed the nestin protein specific to the human neural stem cells with DAPI for nuclei (A), nestin antibody (B) and merge (C); Scale bar: 100 μm

5.13: CMFDA stained cell bodies and DAPI stained nuclei of the human neurospheres were visible uniformly dispersed in the cross section of the human neurospheres proving the uniform cell distribution within the spheroids

LIST OF TABLES

- 1.1: Different test conditions and potential array of experiments to run
- 3.1: The G' values of the different concentrations of gellan gum hydrogels were evaluated from the oscillatory time sweep studies
- 3.2: The zero-rate viscosity increased with an increase in gellan gum concentration
- 5.1: Rheological analysis of gellan gum concentrations to be used for microwell fabrication

ABSTRACT

POLYSACCHARIDE-BASED SHEAR THINNING HYDROGELS FOR THREE-DIMENSIONAL CELL CULTURE

By Vasudha Surampudi, M.S.

A dissertation submitted in partial fulfillment of the requirements for the degree of Doctor of Philosophy at Virginia Commonwealth University.

Virginia Commonwealth University, 2015.

Major Director: Dr. Xuejun Wen, M.D., Ph.D., AIMBE Fellow
Alice T. and William H. Goodwin Jr. Endowed Chair Professor in Regenerative Medicine
Chemical and Life Sciences Engineering

The recreation of the complicated tissue microenvironment is essential to reduce the gap between *in vitro* and *in vivo* research. Polysaccharide-based hydrogels form excellent scaffolds to allow for three-dimensional cell culture owing to the favorable properties such as capability to absorb

large amount of water when immersed in biological fluids, ability to form “smart hydrogels” by being shear-thinning and thixotropic, and eliciting minimum immunological response from the host. In this study, the biodegradable shear-thinning polysaccharide, gellan-gum based hydrogel was investigated for the conditions and concentrations in which it can be applied for the adhesion, propagation and assembly of different mammalian cell types in an unmodified state, at physiological conditions of temperature. Cell studies, to show successful propagation and assembly into three-dimensional structures, were performed in the range of hydrogels which were deemed to be optimum for cell culture and the cell types were chosen to represent each embryonic germ layer, i.e., human neural stem cells for ectoderm, human brain microvasculature cells for mesoderm, and murine β -cells for endoderm, along with a pluripotent cell line of human induced pluripotent stem cells, derived from human foreskin fibroblasts. Three-dimensional cell organoid models, to allow for gellan gum based bioprinting, were also developed using human induced pluripotent stem cells and human neural stem cells.

1. INTRODUCTION AND DISSERTATION OVERVIEW

1.1 Three Dimensional *In Vitro* Models

The environment of the cells in their native tissues is far-removed from the present *in vitro* two-dimensional flat dish models used for the propagation of the mammalian cells. They agreeably help in the organized development of the cells required for providing the first set of solutions to the pressing research questions, leading to the *in vivo* studies. However, there is an urgent need for moving the technology towards making the three-dimensional *in vitro* culture of cells a norm. In order to develop an ideal biomimetic environment to the cells, it is essential to have a porous scaffold that has a larger surface area in a smaller volume, should be responsive to the changes in temperature and shear forces, should have the ability to retain and supply growth factors and it is crucial to have a “breathing” material, i.e., the material should be diffusive to the supply for gases, nutrients and waste materials, both, into and out of the scaffold. The extracellular matrix of the native tissue is comprised of an organized, intricate meshwork of polysaccharides and polypeptides. Two main classes of macromolecules make up the majority of the matrix; polysaccharides called Glycosaminoglycans, which are usually bound together with proteins to give rise to Proteoglycans; and fibrous protein network of collagen, elastin, laminin and fibronectin. These two classes give rise to an extensive array of scaffolds of varying biomechanical properties, as per the cell type to be housed in them, ranging from the soft tissues like synovia, to hard, mineralized tissues of bone, tendon or cartilage. They allow for the organization of cells into complex three-dimensional organoids to do their programmed tasks. The stiffness and the associated mechanical

properties of the tissue are dependent on this ground substance, which, in turn, affects the cell survival, migration and proliferation.

An ideal *in vitro* model should allow for cell encapsulation and growth factor loading at room temperature and physiological conditions at 37 °C and should be reverted to the solution using simple techniques, in order to develop a potentially, enzyme-free passaging model. Shear-thinning and thixotropic hydrogels fit this requirement by being injectable under the application of varying degrees of shear-forces and show sol-gel transitions.

For the future *in vivo* studies, the hydrogels can be injected directly at the site of injury so as to reduce the probability of scar formation. Hydrogels, with their three-dimensional scaffold and the hydrophilic ability to retain water from the biological solutions is a promising approach towards the development of the ideal three dimensional model.

1.2 Shear-Thinning Hydrogels for Tissue Engineering and Regenerative Medicine

Shear-thinning hydrogels are Non-Newtonian fluids that show a decrease in fluid viscosity with an increase in shear-stress and some of them are self-healing by showing a recovery in the viscosity over a period of time. The self-healing property is due to the fluid property called thixotropy. These hydrogels are also referred to as “Smart hydrogels” as they respond to the external stimuli along with being reversible in the properties retaining their original structure over a period of time or with the removal of external stimulus. Growth factors, drugs or cells can be mixed with the hydrogel before injection for the *in vivo* experiments. Most of the polymers used in the biomedical applications and also the natural biomaterials existing in the body are visco-elastic,

showing both viscous and elastic nature during the state of flow or deformation. Recent experiments show shear-thinning hydrogels that resemble extracellular matrix in its chemical and mechanical properties, with their high permeability for metabolites, oxygen, nutrients and assist in intercellular chemical signaling. Shear-thinning hydrogels show varying levels of viscous and elastic components in response to external mechanical stimulus, shear stress. In human body, some of the prime examples of shear-thinning fluids include cytoplasm, blood, mucus, vitreous humor, tears, synovial fluid and ground substance of tissues which adds to the increasing interest in the understanding and further development of shear-thinning hydrogels targeted towards biomedical applications.

1.3 Limitations

Some of the challenges faced in the development of an ideal shear-thinning hydrogel based *in vitro* propagation system is that the material needs to be a biocompatible hydrogel with shorter duration for the shear-thinning and recovery. The scaffold should remain stable and not be prone to the changes caused due to the cell metabolites and, more importantly, should not lose the diffusivity due to the cell propagation. The transparency of the biomaterial is important to allow for tracking the proliferation of the cells. Also, the shear forces required to break down the gel to the solution should not be too high, as it risks causing mechanical damage to the cells and associated cell structures. The cross-linking of the gels should not use any toxic linkers, which may release free radicals, leading to oxidative stress. The material should be sufficiently inert in order to be developed into a direct injectable model for *in vivo* studies. The current research is at a state where in the shear-thinning models are lacking in, at least, one of the above mention

criteria. This is a void that needs to be filled in order to allow for more accurate solutions to the problems being faced in the fields of tissue engineering and regenerative medicine.

1.4 Project Objective, Significance, and Innovation

The objectives of this research were to use develop a polysaccharide based shear-thinning hydrogel to imitate the extracellular matrix of the native tissues in order to allow for the cell adhesion and propagation of a wide spectrum of mammalian cell types. To achieve this, gellan-gum based model was developed and characterized in order to develop a shear-thinning hydrogel cell culture system. A wide spectrum of gellan gum concentrations were analyzed in order to find the optimum range of concentrations which give rise to a shear-thinning hydrogel, in combination with the cell culture medium. Other combinations with peptides and growth factors were also studied, to improve and functionalize the biomaterial to be developed into unique cell-specific niches. This research aims to provide a gold standard for the three-dimensional *in vitro* cell propagation models by means of tunable biomechanical properties of the cell scaffold, along with the convenience of being able to translate directly into regenerative medicine and drug delivery applications for *in vivo* studies. Gellan gum provides an advantage of working with an FDA approved biomaterial. The presence of side chains of the sugars composed in the gellan-gum is beneficial in developing modified versions of the polysaccharide. In the current study, the novel application of gellan gum as a shear-thinning *in vitro* cell culture model is shown by using a representative cell type from each embryonic germ layer in order to test the concept. Also, a pluripotent cell line has been used to perform a well-rounded study. This study will significantly impact the current *in*

in vitro cell propagation models and pave path towards establishment of the three-dimensional systems in research.

1.5 Specific Aims and Rationale

Hypothesis: The hypothesis of this project is that, the polysaccharide, gellan gum forms an ideal three-dimensional propagation system mimicking the physical, chemical and mechanical properties of extracellular matrix and provides the necessary microenvironment for the cellular survival and proliferation *in vitro* and the shear-thinning ability of the polysaccharide is useful for the development of an enzyme-free cell passaging system.

Aim 1: To develop and characterize a gellan-gum based shear-thinning hydrogel for cell culture applications

Rationale: Gellan-gum is an anionic polysaccharide and is a relatively inert biomaterial with applications in biomedical industry. In this study, we aim to identify the optimum concentrations and conditions required for the development of a three-dimensional cell propagation model which will show shear-thinning even with the addition of cell suspension in the cation-rich cell culture medium. The shear-thinning ability should be ideally retained even after a prolonged period of cell culture within the scaffold.

Aim 2: To optimize the gellan gum based shear-thinning hydrogels for three dimensional cell culture

Rationale: The goal is to use the gellan gum based hydrogels in the concentrations and conditions optimized in the specific aim 1 for cell studies. Specifically, it is aimed to develop cell-specific niches by means of growth factors in order to see the development

and assembly of cells to the three-dimensional structures unique to the natural environment of the tissues. It is aimed to use a representative cell type from each embryonic germ layer and a pluripotent cell type.

Aim 3: To develop a high-throughput model for the generation of large-scale micro-tissue aggregates to improve cell survival for transplantation applications

Rationale: It is hypothesized that the cell spheroids improve the ability of cell survival and proliferation rates for *in vivo* studies in comparison to adding single cell suspension directly. In this aim, the goal is to construct a high-throughput automated technology in order to use the gellan-gum hydrogels to imprint patterns to generate three-dimensional organized structures, which are hypothesized to improve the cell growth and survival.

1.6 Dissertation Organization

The following manuscript is arranged into different chapters that showcase individual studies relating to the overall aims of the project. In Chapter 2, a comprehensive literature review is presented to introduce shear-thinning hydrogels. This chapter focuses on the characterization of the properties of the shear-thinning hydrogels, along with a classification of the shear-thinning biomaterials used for biomedical applications. Chapter 3 provides the methodology of preparation and characterization of gellan-gum based shear-thinning hydrogels. The results from this chapter will be used to get the optimum range of the concentrations and combinations of the gellan-gum to be applied for the cell studies. In Chapter 4, the previously optimized range of gellan-gum will be used to test the efficiency to be used as a biomimetic biomaterial. The results from this can be used to extrapolate the data that the gellan gum based hydrogels give rise to an efficient three-dimensional propagation system with similarities to the extracellular matrix of the native

tissue. In Chapter 5, it is aimed to develop an automated high-throughput model to use gellan gum based hydrogels for imprinting features by a robotic arm in order to develop three-dimensional cellular models, which are aimed to be used for applications in tissue engineering and regenerative medicine. Chapter 6 summarizes the overall conclusions drawn from the body of work and discusses challenges and future directions related to the progress of the presented research.

1.7 Design of Experiments

In order to improve the efficiency of the experiments (DOE), the design of experiments is performed to do controlled experimentation. DOE is useful to determine the relationship between the factors affecting a process and the output of the process. This is useful to manage the process inputs in order to optimize the output. In this current study, the controlled inputs (Factors) are identified as the gellan gum concentration, growth factor/silk fibroin concentration and cell seeding density. The uncontrolled inputs (Co-factors) are the cationic interactions with the gellan gum modifying the storage modulus of the hydrogel and the different cell types being tested for showing the cytocompatibility. The continuous inputs are physiological conditions of temperature and humidity in the form of the incubation conditions of 37 °C and CO₂. The outputs (Response) are cell proliferation and cell survival.

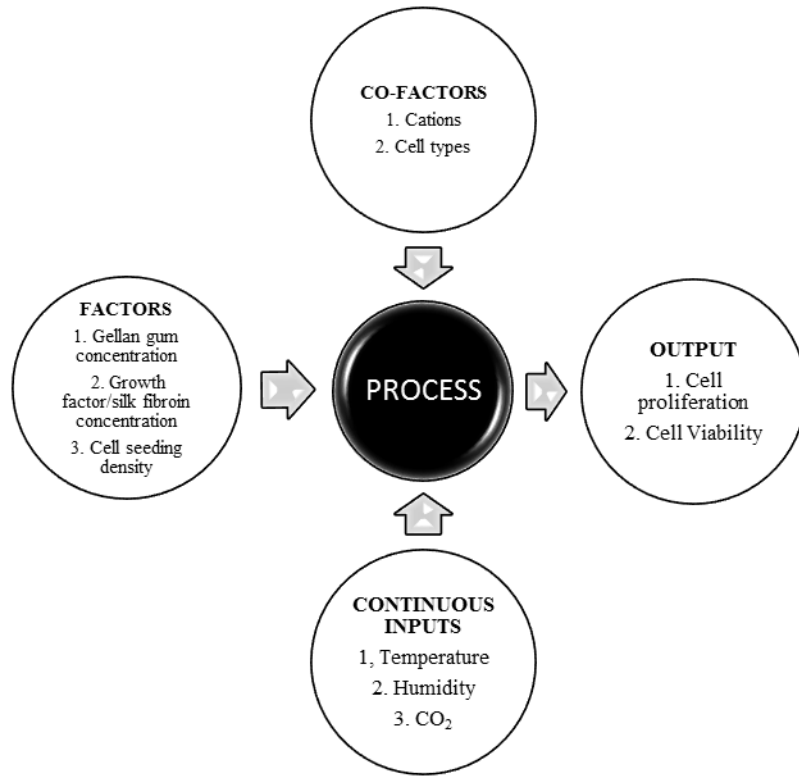


Figure 1.1: The “Blackbox” process model schematic

Table 1.1: Different test conditions and potential array of experiments to run

	Run Order	Gel conc (A)	Silk fibroin (B)	Cell seeding (C)	AxB	AxC	BxC	AxBxC
1	6	C _{Low}	SF _{Low}	Cell# _{Low}	1	1	1	-1
2	8	C _{Low}	SF _{Low}	Cell# _{High}	1	-1	-1	1
3	1	C _{Low}	SF _{High}	Cell# _{Low}	-1	1	-1	1
4	4	C _{Low}	SF _{High}	Cell# _{High}	-1	-1	1	-1
5	2	C _{High}	SF _{Low}	Cell# _{Low}	-1	-1	1	1
6	5	C _{High}	SF _{Low}	Cell# _{High}	-1	1	-1	-1
7	3	C _{High}	SF _{High}	Cell# _{Low}	1	-1	-1	-1
8	7	C _{High}	SF _{High}	Cell# _{High}	1	1	1	1

2. SHEAR-THINNING HYDROGELS: PROPERTIES, CLASSIFICATION, AND BIOMEDICAL APPLICATIONS

2.1 Introduction

Hydrogels are three-dimensional networks which are formed as a result of crosslinking of hydrophilic polymer chains and can store high water content (50-99%) with physical characteristics similar to human tissues[1]. The hydrogels show tunable mechanical and physical characteristics and porosity by changing the polymer concentration, cross linking density and mechanism. Both natural and synthetic polymers can be used as the hydrophilic chains for providing the backbone to the hydrogels.

In nature, hydrogel based scaffolds can be seen in plant and animal kingdom, including examples like cellulose, chitosan, polysaccharide based extracellular matrix (ECM) in tissues, elastin and collagen. For biomedical applications like regenerative medicine, tissue engineering and drug delivery, it is highly desirable to synthesize scaffolds that mimic the naturally existing hydrogels or if possible, using the similar polymer backbone to generate the scaffold. Synthetic hydrogels, such as, poly (ethylene glycol) (PEG), poly (vinyl alcohol) (PVA), poly (methyl methacrylate) (PMMA) possess stronger mechanical properties and tunability. Various biomedical applications of hydrogels include drug delivery, wound dressings, soft contact lenses, medical electrodes, hemo-compatible surfaces for medical devices, scaffolds for tissue engineering[2-7]. Naturally-derived hydrogels have an added advantage over the synthetic hydrogels due to their properties like biocompatibility and biodegradability.

One of the key features to be taken into consideration while deciding the hydrogels primarily for biomedical applications is their ability to be injected into the body in order to be delivered *in vivo* via injection, thereby, reducing pain, scarring, healing time and chances of infection that

arrive from surgical administration of hydrogels[8]. Some of the hydrogels are injected as liquid and undergo gelation *in situ* at the target site whereas the other type of hydrogels are injected as is owing to their changing mechanical properties. The injectable hydrogels are used to fill irregular shapes and increase the interaction between the surrounding tissue and the scaffold.

The latter kind of hydrogels are called shear-thinning hydrogels. In this review, we focus more on the shear-thinning hydrogels and their biomedical applications in the field of tissue engineering and regenerative medicine. Shear-thinning hydrogels are an attractive contender for the injectable hydrogels by changing the viscosity with changing shear-stress.

2.2 Shear-thinning hydrogels

Shear-thinning hydrogels are Non-Newtonian fluids that show a decrease in fluid viscosity with an increase in shear-stress and some of them are self-healing by showing a recovery in the viscosity over a period of time. The self-healing property is due to the fluid property called thixotropy. These hydrogels are also referred to as “Smart hydrogels” as they respond to the external stimuli along with being reversible in the properties retaining their original structure over a period of time or with the removal of external stimulus. Growth factors, drugs or cells can be mixed with the hydrogel before injection for the *in vivo* experiments. Recent experiments show shear-thinning hydrogels that resemble extracellular matrix in its chemical and mechanical properties, with their high permeability for metabolites, oxygen, nutrients and assist in intercellular chemical signaling. All hydrogels are basically visco-elastic materials. Shear-thinning hydrogels show varying levels of viscous and elastic components in response to external mechanical stimulus, shear stress. Oscillatory testing using dynamic oscillatory rheology is used to analyze the varying properties of these hydrogels. Storage modulus, loss modulus, phase angle are generally quantified to get a measure of the change in viscoelasticity of the shear-thinning

hydrogels. Stress-relaxation tests are used to identify the time-dependency of the hydrogels which are in turn, characterized as thixotropic. In human body, some of the prime examples of shear-thinning fluids include cytoplasm, blood, mucus, vitreous humor, tears, synovial fluid and ground substance of tissues which adds to the increasing interest in the understanding and further development of shear-thinning hydrogels targeted towards biomedical applications[9-15]. The increasing knowledge on the physical and mechanical properties of the body fluids is enabling the development of improved solutions to the existing problems in the field of tissue engineering in the form of improved biomaterials.

In the current review, we discuss the molecular mechanisms involved in shear-thinning behavior of the hydrogels, physical characteristics, and dependency on time and temperature, gelation kinetics, rheometric analysis, followed by a detailed classification of the shear-thinning hydrogels based on the chemical composition. In the end, we look at the ongoing research for the biomedical applications of the shear-thinning hydrogels and potential problems faced, leading to an insight towards the future directions of the research.

2.3 Properties and characterization of shear-thinning hydrogels

2.3.1 Fluid classification

A fluid is categorized as the substance that cannot resist deformation forces and flows in the direction of applied shear forces. As seen in figure 1, under the action of shear forces on the top face at a distance, H , the initial state of fluid as denoted by the solid rectangle changes to the sheared or deformed state, as seen as the dotted lined parallelogram, at a velocity, V . Shear stress (τ) is defined as the force per unit area creating the flow. The gradient of the velocity in the direction at right angles to the direction of the flow is termed as shear rate or strain rate or velocity gradient ($\dot{\gamma}$). The fluid viscosity (μ) is a measure of the resistance of fluids to gradual

deformation by shear stress. Newton's law of viscosity states that the ratio of shear stress to shear rate is constant, for a given temperature and pressure and is defined as the fluid viscosity or coefficient of viscosity. The fluids that obey Newton's law of viscosity are termed as Newtonian fluids. The shear stress is always proportional to the shear rate for a Newtonian fluid and the constant of proportionality is given by the value of viscosity. Non-Newtonian fluids do not follow Newton's law and their viscosity is dependent on the shear rate.

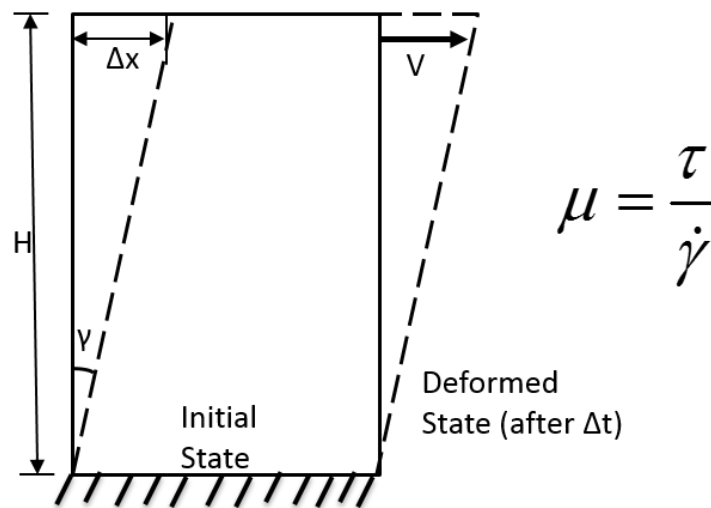


Figure 2.1: Two dimensional model of Newtonian fluids and the parameters involved in shear stress and shear rates contributing towards the definition of the fluid viscosity. Under the applied shear forces, the top face of fluid, which is at a distance H from the bottom face, moves under a spatial velocity, V, giving rise to the sheared or deformed state and according to the Newton's law of viscosity, the viscosity, μ , is the proportionality of shear stress to the rate of shear strain.

There are different types of Non-Newtonian behavior classified based on the dependency on shear rate or time[16]. Based on the dependency on shear rate, they are either shear-thickening or shear-thinning. Shear-thickening fluids are those whose viscosity increases with the increase in shear rate. Shear-thinning hydrogels are the viscoelastic fluids that behave like a solid when the material does not undergo enough shear stress, but behave like a liquid with an increase in the yield stress. Bingham plastics are those that require a finite yield stress after which they show the Newtonian behavior. The flow properties of some Non-Newtonian fluids are dependent on both rate of shear strain and time. Based on the dependency on time, there are two types of Non-Newtonian fluids, rheopectic and thixotropic fluids. Rheopectic fluids show increase in viscosity under a constant shear stress over an increase in time period, whereas, thixotropic fluids show a decrease in the fluid viscosity under a constant shear stress over an increase in time period. When they are sheared at a constant shear rate followed by a period of rest, their apparent viscosity gradually decreases, which is due to a progressive break down of their internal structure. Thixotropy helps to generate reversible hydrogels that can be injected in the form of a solution, but can end up as a hydrogel at the target site.

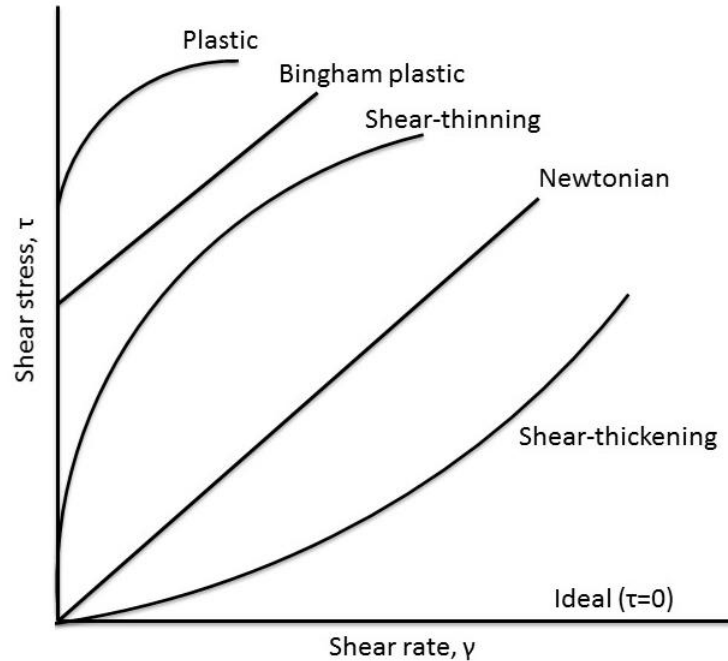


Figure 2.2: Graphical representation of the different types of fluids based on their relationship between shear stress and rate of shear strain with shear stress as y-axis and shear rate as x-axis.

2.3.2 Non-Newtonian flow models:

Different models have been proposed to describe the flow and transport mechanisms of shear-thinning fluids, both qualitatively and quantitatively. Modeling the flow and transport phenomena helps in a better classification of the polymeric shear-thinning fluids that simulate the naturally existing biological materials in the body. The size of the monomer and the concentration of the polymer also effect the yield stress to be considered for the rheological models. Some of the models used to describe the shear-thinning fluids are Power law model, Ellis model, Cross model and Carreau model.

The power-law model is a simple model used to describe the rheology of shear-thinning fluids.

$$\tau = \mu \dot{\gamma}^n$$

The power-law index, n , is less than unity for shear-thinning fluids, 1 for Newtonian fluids and greater than unity for the shear-thickening fluids. However, the power-law model does not account for the Newtonian plateau occurring at the lower and higher shear rates[17].

The Ellis model is another model that accounts for the Newtonian plateau at lower shear rates and is, essentially, the power-law model at higher shear rates[18].

$$\frac{\mu_0}{\mu} = 1 + \left(\frac{\tau}{\tau_{1/2}} \right)^{n-1}$$

μ_0 is the zero shear rate viscosity, $\tau_{1/2}$ is the value of shear stress when the viscosity is half of the zero shear rate viscosity and n is the power component.

The Cross model is based on the assumption that the shear-thinning behavior is a result of formation and breakage of the structural units of the fluid[19]. The cross model is denoted by the equation:

$$\frac{\mu - \mu_\infty}{\mu_0 - \mu_\infty} = \frac{1}{\left[1 + \left(\lambda \dot{\gamma} \right)^{2/3} \right]}$$

where μ_0 is zero shear rate viscosity, μ_∞ is infinite shear rate limiting viscosity.

The Carreau model attempts to describe a wide range of fluids by establishing a curve-fit model for both Newtonian and shear-thinning models, taking into consideration, the zero shear rate viscosity (μ_0), and infinite shear rate limiting viscosity (μ_∞)[20, 21].

$$\frac{\mu - \mu_\infty}{\mu_0 - \mu_\infty} = \left[1 + \left(\lambda \dot{\gamma} \right)^2 \right]^{\frac{n-1}{2}}$$

2.3.3 Rheological Analysis

Rheology is the science of flow properties of various materials. Eugene Bingham first coined the term “Rheology”, which comes from the Greek words, *rheos*, to flow and, *logia*, the study of. It is used to quantify the shear stress needed to produce the flow or deformation of the fluids at various shear rates. Rheology is used to define a material as viscous, elastic, visco-elastic, plastic or visco-plastic. Most of the polymers used in the biomedical applications and also the natural biomaterials existing in the body are visco-elastic, showing both viscous and elastic nature during the state of flow or deformation. The viscous nature of a material enables the flow by resisting the shear strain linearly with respect to time under the application of shear stress and the elasticity is defined as the ability of the material to stretch but return to its original state at the removal of shear stress. The storage modulus and loss modulus give an estimate of the proportion of elastic and viscous portion of the visco-elastic fluids. The storage modulus, G' , is the energy that is required to deform the elastic portion of the visco-elastic fluids, while, the loss modulus, G'' , is the heat energy dissipated at the deformation of the viscous portion. The goal of the rheological analysis is to determine the constitutive equation for the hydrogel in question and it relates the molecular properties to the flow response.

Rheometers are the instruments designed to study the rheological properties of the materials. A dynamic oscillatory rheometer is used to measure the value of dynamic modulus, which is the ratio of shear stress to shear strain in an oscillatory field. Oscillatory curves give a unique mapping of the microstructure of a material. Under the application of shear force in the form of a sinusoidal wave, the elastic response of shear stress is in phase with the input sinusoidal wave, and the viscous response is $\pi/2$ or 90° out of the phase with the input wave. The loss angle or the

phase angle, δ , is given by $\tan^{-1} G''/G'$. In the solid-like state of the visco-elastic fluid, the storage modulus (G') is greater than the loss modulus, (G'') and the phase angle is less than 45° . The point at which G' is equal to G'' is the point of liquefaction and at this point, the phase angle is equal to 45° . Once this point is crossed, the material is a liquid and its loss modulus (G'') is greater than the storage modulus (G') and its phase angle is larger than 45° .

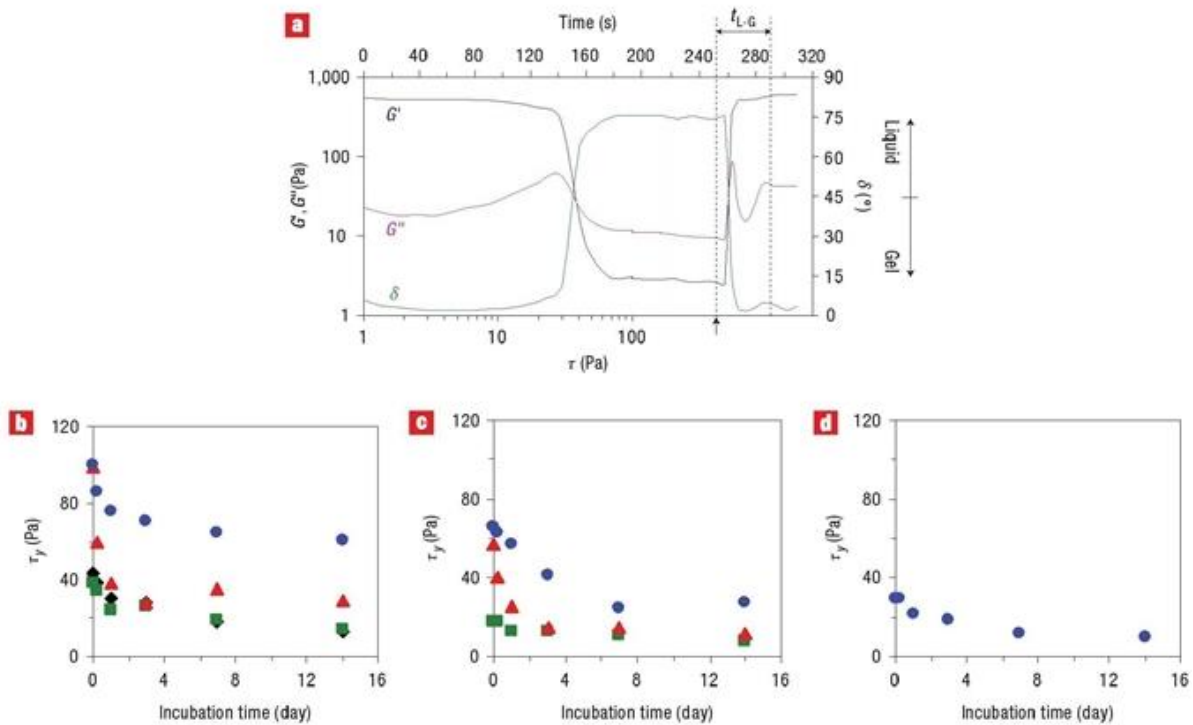


Figure 3: Rheological characteristics of PEG–silica gels. a, Typical G' , G'' and δ of gels without fumed silica as a function of increasing shear stress t applied with time. At 150 s, when $G' = G''$, liquefaction occurs and $\tau = \tau_\gamma =$ liquefaction stress. The time taken for G' , G'' and δ to return to their original levels when shear stress was removed ($t = 251$ s, indicated by the double arrow) is the liquid–gel transition time (t_{L-G}). b–d, Effect of gel incubation time in cell culture media at 37 °C on the τ_γ of the gels for 10 (b), 20 (c) and 30 (d) days.

vol% (d) of medium (black diamonds, 0 wt% FS; green squares, 5 wt% FS; red triangles, 10 wt% FS; blue circles, 15 wt% FS) [22].

Some of the common rheological test methods used for studying shear-thinning hydrogels are strain sweep, frequency sweep, stress ramp, temperature ramp, flow curves, and thixotropic loop. Usually, the rheological testing of a novel polymer or body fluid is initiated by a strain sweep to get the critical strain value, beyond which the material shows non-linear behavior and the storage modulus decreases. The range of strain during which the material shows linear response in terms of both storage and loss moduli is termed as the Linear Visco-elastic Range (LVR). After the critical strain, the material is no longer highly structured and shows the deformation or flow. Once the LVR is established, the frequency sweep is used to understand the colloidal dynamics or interaction between the phase components of the hydrogel at a strain which is usually at 50% of the critical strain. This is used to understand the sol-gel transition by investigating the changes in G' and G'' . Flow curve determines the viscosity, which is the rate at which the material is sheared. Temperature ramp is used to understand the storage and stability of a hydrogel inside the body at 37°C and to understand the changes in the mechanical properties of a hydrogel at room temperature to give an idea of the shelf life and storage conditions and the subsequent changes inside the body. Thixotropic loop is used to identify the effect of time-dependent Non-Newtonian behavior.

The readings from the dynamic oscillatory rheometer can vary with the changes in the polymer or the concentration of the polymer or crosslinking mechanism being used. The monomeric rearrangement can give rise to a shift in the viscous to elastic proportions. The mechanism of crosslinking and the introduction of salts, which leads to stronger ionic bonding can change the

elastic portions considerably and mostly, irreversibly. Rheological testing is widely used to simulate the biomechanical properties of extracellular matrix and tissues using hydrogels, which are, in turn, used in the research and development of medical, pharmaceutical and personal products. It is used to understand the gelation kinetics, storage stability and degradation studies at body temperature.

2.3.4 Physical characteristics of Shear-thinning fluids

Shear-thinning behavior is shown by different fluids, pure substances, solutions, mixtures, and dispersions. A pure substance or a solution has a uniform phase and is termed as a simple fluid. Dispersions and mixtures show more than a single phase. For instance, solid particles dispersed in liquid, emulsion of immiscible liquids. One of the components may be Newtonian, but together, the material may show Non-Newtonian characteristics. For example, in blood, the plasma by itself is a Newtonian fluid, but with the presence of red blood cells, white blood cell, platelets and thrombocytes, it shows shear-thinning behavior and is described by Non-Newtonian homogenous continuum models[23]. For dispersions, the viscosity depends on the particle size, shape, concentration, surface charges and interaction with the continuous phase in which they are suspended [24]. Other factors like Brownian motion, inertia, interactions due to electrostatic, van der Waals or steric forces also play an important role in determining the hydrogel rheology[25]. During the solid-like phase of the hydrogels, the macromolecules are present as the highly entangled ball-like structures appearing like spheres. With an increase in the yield stress, the Brownian motion randomizes the macromolecule organization giving rise to more linear chain-like structures, which in turn, leads to lower viscosity, thereby being a shear-thinning fluid [26,

27]. The viscosity for the polymeric models is best described by Graessley theory and the shear-induced reduction in the viscosity is given by the following formula [28]:

$$\frac{\mu}{\mu_0} = \frac{2}{\pi} \left[\cot^{-1} \alpha + \frac{\alpha(1-\alpha^2)}{(1+\alpha^2)^2} \right]$$

where, $\alpha = \left(\frac{\mu}{\mu_0} \right) \left(\frac{\dot{\gamma} \theta_0}{2} \right)$ and θ_0 is a time-constant for the formation of entanglements at low shear rates.

Shear-thinning behavior is still seen in dilute and semi-dilute poly-electrolyte solutions with weak cations in low concentrations [29]. The effect of cations is another criterion to be considered for the sol-gel transitions. The cations form hydrogen bond bridges between the double-stranded polysaccharide chains of gellan gum [30]. The critical interactions taking place between the polymer chains, cations and water molecules determine the physical properties of hydrogel, like, setting temperature, strength and firmness. The pore size of the hydrogels is reduced due to the cation-water bridges. In turn, the values of μ , G' and G'' are modified with the electrolyte or the salt solutions. The size of the cation matters as well [31, 32]. The cation concentration is important for cell culture based *in vitro* and *in vivo* experiments where the hydrogel may either be incubated in cell culture medium or injected with the cell culture medium.

In cells, along with cytoplasm acting as a Non-Newtonian fluid, the internal cytoskeleton comprised of proteins like F.actin lead to further strain-softening [33]. The linear visco-elastic responses of the F-actin filaments in response to the stress can be explained by the linear reorganization of the actin filaments, which are in the form of entangled balls at the onset of

shear stress and via strongly aligned hair pin structures, they lead to the linear organized filaments that slide over one another, in order to facilitate the lamellar flow, which is at the end of the strain softening. This model can be further extended to other cytoskeleton filaments, thereby, explaining a complicated biological model which shows Non-Newtonian behavior.

2.3.5 Gelation Kinetics

The general transition of the gel to solution is due to the reorganization of the polymer chains within the hydrogel in the presence of shear-forces. The recovery is dependent on the material and the extent of damage done to the polymeric chains. If the chain structure is broken, then the gelation is not reversible. Polysaccharide-based hydrogels like gellan gum can form gels at different conditions like high temperatures and in the presence of cations. At high temperatures, gellan gum is in the coil form and upon decrease in temperature, a thermally reversible coil to double-helix transition occurs, which is a prerequisite for gel formation [30, 34-36]. The anti-parallel double helices are self-assembled to form oriented bundles, called junction zones and the untwined regions of polysaccharide chains, in the form of extended helical chains, connect the junction zones, leading to the formation of a three dimensional network, that creates the gel [37]. The gelation of gellan gum solutions is strongly influenced by the chemical nature and quantity of cations present in the solution. The introduction of cations shields the electrostatic repulsion and thereby allows the tight binding and aggregation of helices[38].

The β - peptide based shear-thinning hydrogels show the gelation and transformation into the solution owing to the amphiphilic peptides that display both hydrophobic and charged hydrophilic face [39]. The hydrophobic faces are packed together, giving the material an entropic gain and form β -sheet sandwiches. Shear forces break these hydrophobic interactions and result

in the low viscosity fibrillary solution. Novel self-healing peptide based hydrogels were designed by the Burdick group with the self-assembly derived from the dock and lock mechanism [40].

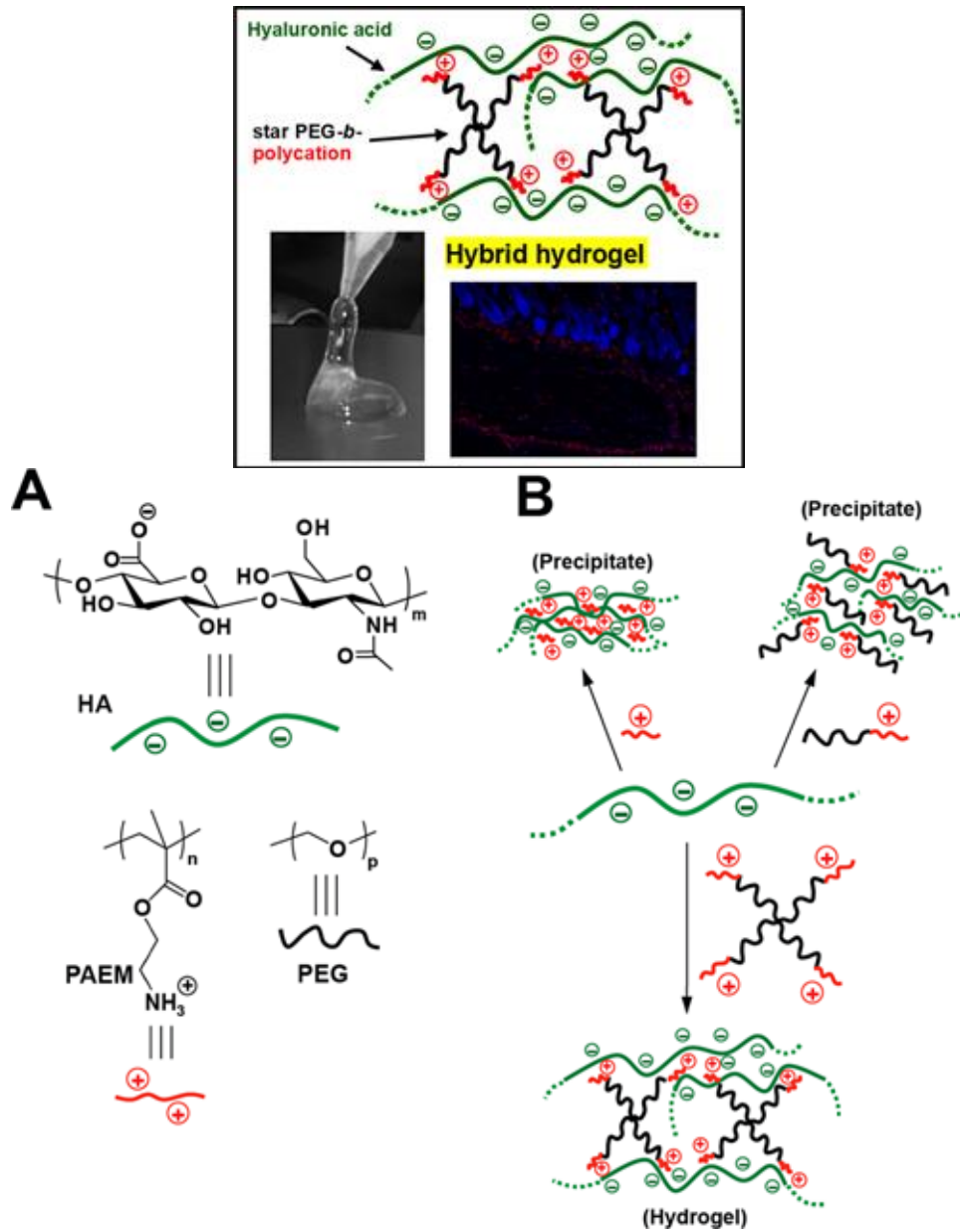


Figure 4: Chemical structure of polymers as building blocks of hybrid hydrogels A) and a schematic illustration of interactions between structurally diverse cationic polymers and anionic HA B). Star, rather than linear, polycations would favor hydrogel formation.

2.4 Classification of shear-thinning hydrogels based on their chemical composition

2.4.1 Natural

The extracellular matrix of human tissues is a complex amalgamation of different peptides and polysaccharides like fibrous proteins, type II collagen, elastin, laminin, fibronectin, glycosaminoglycans (GAGs), and the combination of the GAGs with the peptides to give rise to proteoglycans[41]. Hyaluronic acid is also present alongside the proteoglycans in many body fluids. Different natural hydrogels of bacterial origin have shown structural similarities with the natural ECM and have been investigated for their cytocompatibility. The natural hydrogels used for biomedical applications are described in the following sections.

2.4.1.1 Polysaccharide-based

Polysaccharide based hydrogels are excellent candidates for biomedical applications, due to the properties like higher polarity, varied chemical composition giving a stereological advantage, biocompatible and show no cytotoxicity. Availability of multiple side chains is beneficial for electrostatic interactions with peptides and growth factors and help in the development of the cell niches by means of the growth-factor reserves. Also, the side chains play an important role in order to develop novel modified hydrogel based scaffolds in order to improve their biomechanical features. The coiled-coil or the complex double helix arrangement of the polysaccharide moieties in the hydrogels leads to the shear-thinning at different conditions of temperature or change in the cations concentration. Their viscoelastic properties were investigated early on by the researchers [42, 43].

Gums are anionic, hydrophilic extracellular secretions from bacteria like *Sphingomonas*, *Agrobacterium* and are a glucose- rich backbone for *in-vitro* cell culture with applications in regenerative medicine and pharmaceutical industry. Gums are hydrocolloids, i.e., suspension of

hydrophilic polymers in aqueous solution. Some of the popular gums used in cell culture are gellan and xanthan gum. Gellan gum was initially described by Moorhouse et al. from the Kelco group of the Merck and is a high molecular weight, linear anionic polysaccharide composed of tetrasaccharide (1,3- β -D-glucose, 1,4- β -D-glucuronic acid, 1,4- β -D-glucose, 1,4- α -L-rhamnose) repeating units, containing one carboxyl side group [44]. With primary applications in food industry and the subsequent FDA and EPA approval, gellan gum is used in the biomedical industry due to the transparent gels, resistant to heat and pH changes [45, 46]. Both acylated and deacylated versions of gellan gum form thermo-reversible hydrogels, with deacylated being the more commonly used version. Novel in-situ gelling gellan-gum based nanostructured lipid carriers were generated taking the shear-thinning property of the gellan into consideration [47]. Xanthan gum is similar to gellan gum but has a pentameric repeat unit of two molecules each of glucose, mannose and one molecule glucuronic acid. These gums show shear-thinning viscoelastic properties in the range of temperature suitable for physiological applications [48]. The early experiments using xanthan gum were done by Oviatt et. al. to simulate natural hyaluronic acid for ophthalmic applications [49]. Xanthan gum forms synergistic hydrogels when mixed with other polysaccharides like gluco- or galacto-mannans via specific interactions of β 1, 4-linkages [50, 51].

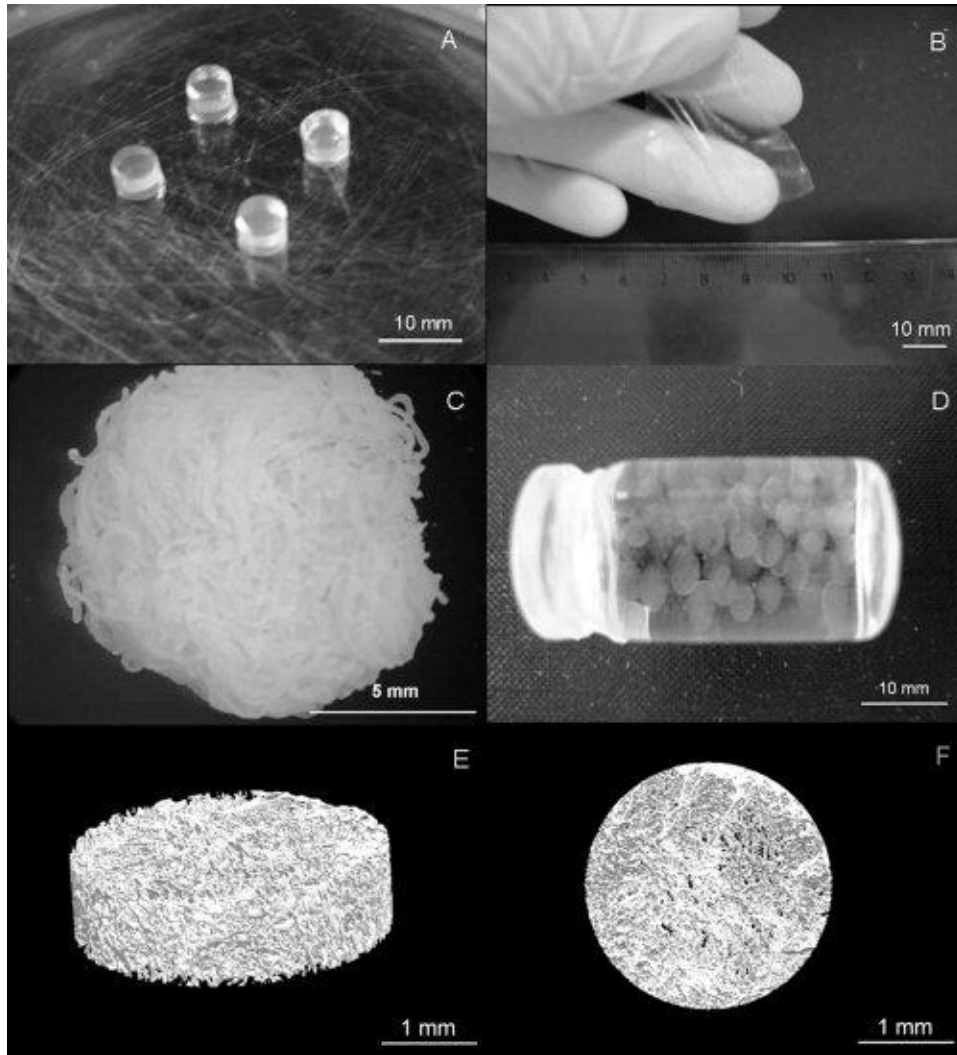


Figure 5: The versatility of gellan gum structures that can be used for simple polymer processing techniques: (A) Discs (B) Membranes (C) Fibers (D) Particles (E) (F) Lyophilized scaffolds

Hyaluronic acid

Hyaluronic acid (HA) is a linear, anionic, non-sulfated glycosaminoglycan (GAG) consisting of repeating disaccharides of β -1,4-linked glucuronic acid and β -1,3-linked *N*-acetyl-d-glucosamine present in the extracellular matrix (ECM) of all connective tissues, and is popular biomaterial

due to its properties like biocompatibility, biodegradability and lack of immunogenicity [52-54]. HA contributes to cell proliferation and growth by promoting cell adhesion and helps in wound healing by playing a role early inflammatory response [53]. There are many chemically modified forms of HA used, like amides, thiols, hydrazides and are used to make novel therapeutic biomaterials and drug delivery systems [55-60]. Apart from the chemically modified HA, there are a lot of researchers who investigated the ionic modifications of HA [61-63]. Dodecyl chain-substituted HA was shown to have longer lasting gelation to be applied for chondrocyte culture and cartilage repair [64]. Polyelectrolyte form of HA seen as a blend with synthetic polymers is discussed in a later section.

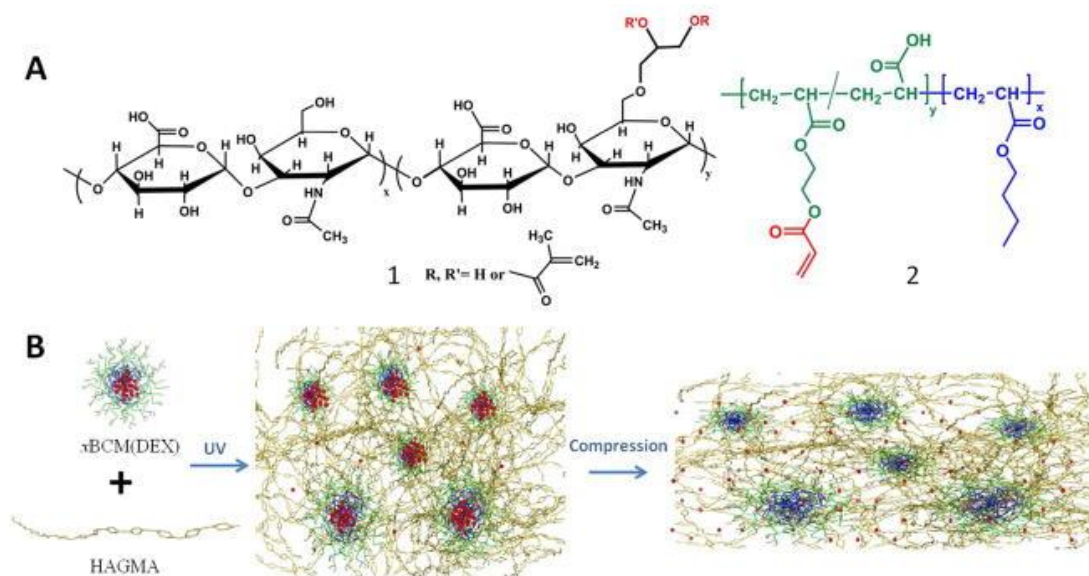


Figure 6: Construction of BCM-integrated HA hydrogels with force-modulated DEX release capacity. (A): Chemical structures of hydrogel building blocks: (1) glycidyl methacrylate-modified HA (HAGMA) and (2) the precursor of crosslinkable block copolymer micelles (x BCM), P(AA₁₀₀-*g*-HEA₂₀)-*b*-PnBA₄₀. (B): Photocrosslinking of HAGMA in the presence of DEX-loaded x BCMs [x BCM(DEX)] resulted in the covalent

immobilization of x BCMs in the crosslinked HA network. Compressive stress imposed on the hydrogel was transmitted to the integrated x BCMs, resulting in the release and re-distribution of DEX via the deformation of the rubbery PnBA core [54].

Others

Alginate is an anionic copolymer from mannuronic acid (M) and guluronic acid (G) and is extracted mainly from the seaweed *Laminaria hyperborea* in a large-scale industrial production. An initial assessment of the rheology of calcium alginate was performed for the applications of treating aneurysms by injectability with grugs through a microcatheter systems [65]. Hydrophobic modification of the alginate allowed for improving the protein holding abilities over the calcium alginate and the shear-thinning ability was retained in the modified hydrogels as well [66].

A fast-gelling, non-cell adhesive, degradable, and biocompatible blend of hyaluronan and methylcellulose (HAMC) was designed as injectable intrathecal drug delivery system. It is injectable due to its shear-thinning property, and its gel strength increases with temperature [67].

2.4.1.2 Peptide-Based Hydrogels

A tunable peptide-based scaffold, composed of a pair of mutually-attractive but self-repulsive peptide modules were found to form viscoelastic materials when mixed with each other at very low concentrations. It has a fibrillar structure and can act as morphogenetic guide to cells. It is dynamically responsive to repeated strains caused either by cell motility, orientation or proliferation, might foster the growth of the developing tissue constructs [68].

Another peptide model incorporates the pH-dependent intramolecular folding of beta-hairpin peptides to their propensity to self-assemble, affording hydrogels rich in beta-sheet. The peptide-based model, MAX-1 was specifically engineered to include chemical responsiveness by linking intramolecular folding to changes in solution pH, and mechanical responsiveness, by linking hydrogelation to self-assembly. The intramolecular folding takes place under basic conditions, affording amphiphilic beta-hairpins that intermolecularly self-assemble. Rheology shows that the resulting hydrogel is rigid but is shear-thinning [69].

A 20-residue peptide, MAX8 was designed by the same group to fold and self-assemble in response to DMEM resulting in mechanically rigid hydrogel. This smart, polymeric system allows for the gelation with the addition of the cell suspension and the gel shows shear-thinning when the appropriate shear stress is applied. However, after the application of shear has stopped, the gel quickly resets and recovers its initial mechanical rigidity in a near quantitative fashion. This property allows gel/cell constructs to be delivered via syringe with precision to target sites [70].

A dual-component Dock-and-Lock (DnL) self-assembly mechanism has been used to construct shear-thinning, self-healing, and injectable hydrogels in which, one component is derived from the RII α subunit of cAMP-dependent kinase A and is engineered as a telechelic protein with end groups that dimerize (docking step) and the second component is derived from the anchoring domain of A-kinase anchoring protein (AD) and is attached to multi-arm crosslinker polymers and binds to the docked proteins (locking step) and give rise to robust physical hydrogels instantaneously and under physiological conditions when mixed.. With high recovery rates and resistance to yield at high strains, the DnL gels have been used for mesenchymal stem cell

encapsulation and delivery. However, it needs to be noted that the cells are prone to mechanical damage at the high strain values [40].

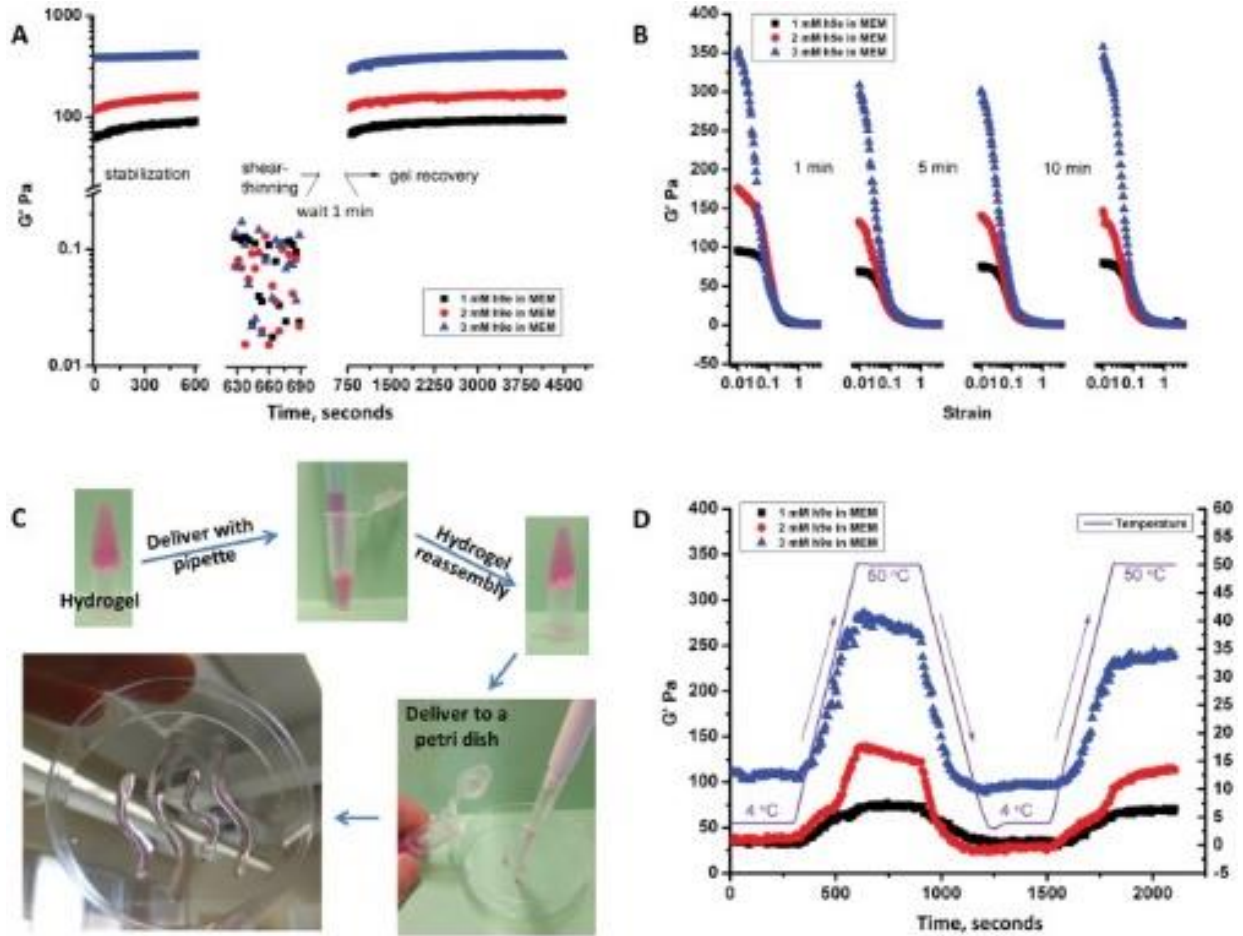


Figure 7: Dynamic rheological study of h9e hydrogel [71] A. Storage modulus G' of shear-thinning and recovery test of 1, 2, and 3 mM peptide hydrogel. B. Four times amplitude sweep test with shear strain from 1% to 500% and 1- 5-, and 10-minute breaks. C. Multiple times delivery of peptide hydrogel via pipette; hydrogel was shear thinning but reassembled quickly without permanently destroying hydrogel architecture. D. Temperature profile test of 1, 2, and 3 mM peptide hydrogel between 4°C and 50°C.

2.4.2 Synthetic/Synthetic-Natural Blend Polymers

2.4.2.1 Photocrosslinkable polymers

The photocrosslinking is a complicated procedure. In some cases, it leads to the breakdown of the hydrogel to lead to shear-thinning and in others, vice versa. An example of the first scenario is the photo-assisted breakdown of the riboflavin-loaded alginate hydrogels leading to the decrease in the viscosity of the hydrogels and changing the rheological properties towards shear-thinning hydrogels at high polymer concentrations [72].

Combining a crystallite-based physical network and a crosslink-based chemical network, photocrosslinked Poly (ϵ -caprolactone fumarate) (PCLF) conduits are synthesized from poly(ϵ -caprolactone) (PCL) diols. The PCLF conduits had shown cell attachment and proliferation of Schwann cell precursor line, SPL201 cells and the nerve conduit with the best crystallinity and mechanical properties was chosen for *in vivo* studies using a 1-cm gap rat sciatic nerve model. The histological evaluation revealed that the material is biocompatible and strong enough to hold the sutures and developed a nerve cable with myelinated axons at the end of 17 weeks after implantation [73]. Photo-crosslinking was initiated with ultraviolet (UV) light ($\lambda=315-380$ nm) in the presence of a photo-initiator, phenyl bis(2,4,6-trimethyl benzoyl) phosphine oxide (BAPO, IRGACURE 819™, Ciba Specialty Chemicals, Tarrytown, NY). Uncrosslinked PCLF shows shear thinning properties and in the presence of the UV light, it undergoes crosslinking *in situ*. The increased surface roughness, higher stiffness and change in the microtopography of the crosslinked PCLF is favorable for the SPL201 attachment and proliferation. However, it must be ensured that the crosslinking takes place only after the PCLF and the photoinitiator with cells is at the desired site of implantation. Angiogenesis is essential in the ischemic environment of the nerve conduit and to enable this, VEGF-encapsulated poly-lactic-co-glycolic acid (PLGA)

microspheres are generated and introduced into the photocrosslinked PCLF conduit. PLGA is metabolized into the non-toxic lactic acid and glycolic acid without leading to cytotoxicity [74]. Novel modified HA with self-assembled block copolymer micelles (BCMs) are synthesized by Jia et. al. as the dynamic building blocks and microscopic crosslinkers for anti-inflammatory drug release studies in osteoarthritic patients [54, 75]. They incorporate nanoscopic, mechano-responsive drug depots strategically within the hydrogel, allowing to fine-tune the gel mechanics and convert the exerted mechanical forces on the gel matrix to biochemical signals with a desired spatial distribution. They used amphiphilic block copolymer of poly(*n*-butyl acrylate) (P*n*BA) and glycidyl methacrylate (GMA) modified HA (HAGMA), which was photochemically modified to incorporate the hydrophobic anti-inflammatory drug, Dexamethasone (DEX) to form resultant HA gels (HA_xBCM) contain covalently integrated micellar compartments with DEX being sequestered in the hydrophobic core. Transmission electron microscopy (TEM) imaging revealed that the covalently integrated BCMS underwent strain-dependent reversible deformation. The covalent incorporation of the block copolymer in the HA matrix is important for the stability of the overall assembled micelles. The release mechanisms for the hydrophobic drug molecules could be in two ways, one is through diffusion through the hydrogel matrix at a rate of diffusion dependent on the concentration gradient. The other way is the perpendicular deformation of the block copolymer micelles in the presence of compression forces, which are covalently linked to the hydrogel matrix, consequently, leading to the weakening of the hydrophobic association between DEX and the micelle core and leading to the drug release.

Another photocrosslinkable polymer is a modified form of Poly ethylene glycol (PEG), called PEG diacrylate (PEGDA) [8, 76]. PEGDA hydrogels are a suitable candidate material for the correction of soft tissue defects as they exhibited rheological properties that are qualitatively

superior to human adipose tissue and the shear thinning is explained by the partial elongation of the polymer chains with an increase in shear stress and orienting along the stream lines of the shear force [77].

2.4.2.2 Polyelectrolyte-based polymers

Polyelectrolyte-based hydrogels are three-dimensional polymeric networks formed by noncovalent association of amphiphilic polyelectrolytes, for example, by ionic or hydrophobic interaction. A blend of synthetic and natural polymers is developed consisting of hyaluronic acid (HA) crosslinked by well-defined block copolymers of the cationic poly(2-aminoethyl methacrylate) (PAEM) and polyethylene glycol (PEG) to generate an injectable hybrid polyelectrolyte hydrogel system. Robust, shear-thinning hybrid hydrogel was produced by mixing HA and 4-arm star PEG-PAEM block copolymer at 1:1 charge ratio. The encapsulation and release of highly viable human mesenchymal stem cells in physiological media was demonstrated. After subcutaneous injection of the hybrid gel in mice, mild but resolvable inflammatory response was observed. This hybrid gel could serve as a model system for studying structure-function relationship of polyelectrolyte hydrogels and as a practical injectable biomaterial for medical applications [78].

2.4.2.3 PolyHIPEs: Polymerization of High internal Phase Emulsions

Polymerization of high internal phase emulsions (polyHIPEs) have an internal droplet phase volume fraction greater than 74% and can be made of biodegradable monomers to form the emulsions, which when polymerized are at the gel point and have a viscosity that enables the injectability and with reaction thermodynamics that allow for polymerization at physiological conditions.

A biodegradable and injectable polyHIPE system based on propylene fumarate dimethacrylate (PFDMA) macromers is investigated for applications in bone grafting [79]. The thermodynamic properties of the polyHIPE are dictated by the interfacial energy of the different phase components, which are, in turn, brought together by the surfactants. The role of surfactants is to reduce the interfacial tension and form a barrier between the phase components. PFDMA macromers are hydrophobic and the surfactant is chosen to stabilize the hydrophilic-lipophilic balance and when mixed along with DI water, it should result in successful HIPE formation, characterized by opaque, white porous substance with a notable value of viscosity. The surfactant concentration also dictates the pore size and wall thickness between droplets [80]. The pore architecture is dependent on the mixing speed of the components along with the concentration of the surfactant. The end result is a biodegradable and biocompatible, porous, injectable scaffold, showing a great promise as a bone graft, allowing osteoconductivity *in vivo*. Poly HIPE made of the oil phase contained 78% Styrene, 8% DVB monomer (cross-linking agent) and 14% Span 80 surfactant, sorbitan monooleate and modified with Hydroxyapatite (HA) for the aqueous phase is used as a blend with the peptide RAD16-I with the sequence AcN-RADARADARADARADA-CNH₂ for scaffolds for osteoblast differentiation [81, 82]. But, the scaffold is not injectable as the constituents are not all biocompatible and needs to be eliminated to have the peptide-enhanced scaffold that supports cell culture.

A review of the existing literature for PolyHIPEs used in regenerative medicine and other biomedical applications has revealed a clear shortcoming of not addressing the shear-thinning exponent of the rheological analysis of the material [79, 82-85]. Most of the Poly HIPEs reviewed here have a continuous phase of an aqueous surfactant solution and this is usually a shear-thinning, lyotropic liquid crystalline phase. Under the influence of mechanical shear

forces, there is a potential rupture of the individual droplet/micelle after a state of elongation and the smaller droplets are theorized to organize themselves into lamellar structure to result in the lower viscosity material [86, 87]. None of the existing Non-Newtonian fluid models account for the role of surfactant in the shear-thinning exponent of the material.

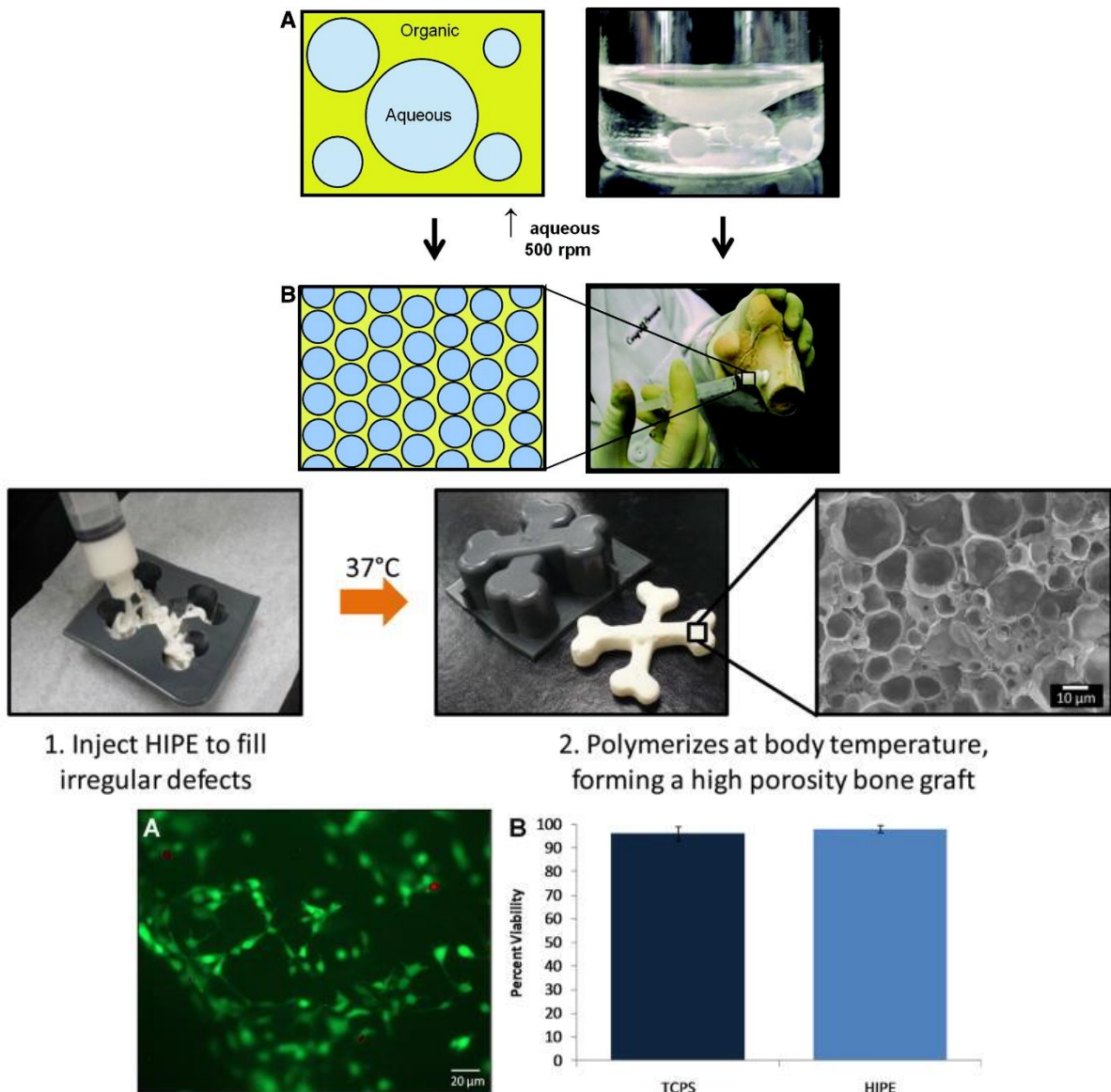


Figure 8: Schematic representation of the process to fabricate a polymerized high internal phase emulsion [84]. (A) The emulsion is composed of a hydrophobic organic phase and an

aqueous phase. **(B) High internal phase emulsion (HIPE) is defined by the aqueous volume phase greater than 74% and exhibits a whipped mayonnaise consistency before cure.**

b. Injectable PFDMA polyHIPEs can be used *in situ* to space fill complex defects [79]

c. 24 hour 3T3 Live/Dead analysis of 5 wt% PGPR polyHIPEs. A) Fluorescent image (green = live, red = dead) B) Comparison of viable cells on tissue culture polystyrene and HIPE (n=15). No significant difference was observed between the polystyrene ($96 \pm 3\%$) and HIPE ($95 \pm 6\%$).

2.4.2.4 Polymers as delivery vehicles for microsphere/nanoparticles

Hydroxyapatite microspheres were generated to be used for bone filling applications via an injectable medium of a shear-thinning fluid [88-90]. The viscosity of the vehicle solution is an important consideration as it is not favorable for the liquid to be too shear-thinning and lead to the leak from the desired site of delivery and form hazardous embolism in the circulatory system. Sodium alginate is chosen over two different forms of cellulose, hydroxypropylmethylcellulose (HPMC) and carboxymethylcellulose (NaCMC) as it allows the spheres to be injected with a higher extrusion force and is relatively physically stable at the physiological conditions upto 3 months of time.

In their recent work, Appel et. al. describe the preparation and application of shear-thinning and self-healing hydrogels in a mild, modular and scalable manner driven by non-covalent interactions between hydroxyl propyl methyl cellulose derivatives (HPMC-x) and core-shell NPs for biomedical applications [91]. The physical model they adapted takes advantage of the hydrophobic modification of HPMC (yielding HPMC-x) to increase the energy associated with

each PNP interaction ($\alpha k_{\beta}T$), thereby increasing the modulus of the gel given the same number of interactions per unit volume. This modification would facilitate favorable interactions between the hydrophobic moiety on the HPMC chain and the hydrophobic core of the PSNPs, thereby enhancing the adsorption energy of the HPMC to the NPs. A direct correlation between the NP size and the number of NPs, and the shear storage modulus has been established to understand the robustness of the hydrogel. Transient and reversible interactions between the NPs and HPMC chains govern polymer–NP (PNP) hydrogel self-assembly which are formulated with poly(ethylene glycol)-*block*-poly(lactic acid) (PEG-*b*-PLA) NPs to enable dual loading of a hydrophobic molecule into the PEG-*b*-PLA NPs and a second, hydrophilic molecule into the aqueous bulk of the gel, allowing for flow under applied stress and complete recovery of their structural properties when the stress is relaxed. PEG-*b*-PLA PNP hydrogels are biocompatible and allow the differential release of multiple compounds *in vivo* following subcutaneous implantation.

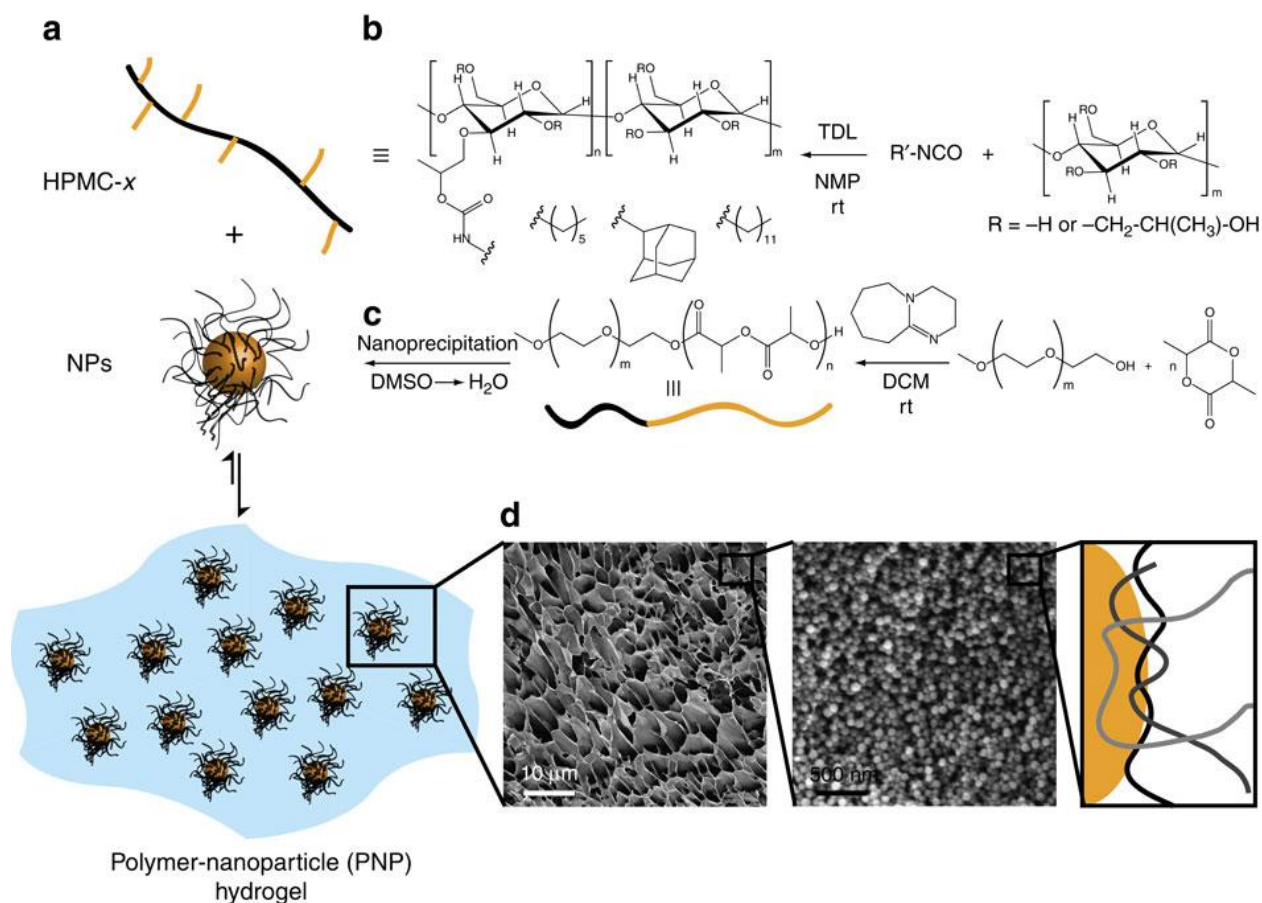


Figure 9: (a) Schematic representation of the preparation of polymer–nanoparticle (PNP) hydrogels utilizing non-covalent interactions between core-shell nanoparticles (NPs) and (b) hydrophobically modified hydroxypropylmethylcellulose. (c) The NPs can be composed of either poly(styrene) (PS; non-degradable) or poly(ethylene glycol)-*block*-poly(lactic acid) (PEG-*b*-PLA; biodegradable). (d) Cryogenic scanning electron microscopy images of PNP gels composed of PSNPs ($d \sim 50$ nm) demonstrate a homogeneous distribution of NPs within the gel structure, indicating that the network is held together by multivalent, dynamic polymer–nanoparticle interactions (as illustrated; polymer chains, grey scale; nanoparticle, orange). [92]

2.5 Conclusions

In summary, a wide range of shear-thinning systems are being developed that self-assemble to form network structures under physiological conditions, flow under moderate pressure (during injection), and self-heal (after injection). These systems are highly tunable and amenable to the incorporation of biological functionality, such as matrix degradation and adhesion sites. Although the use of these systems as injectable hydrogels in biomedicine is very recent and mostly limited to in vitro studies, the majority of these systems are potentially suitable for tissue engineering and molecule delivery applications.

However, there is a pressing requirement for the development of a standardized shear-thinning model that can have optimum shear-thinning and recovery kinetics to allow for the cell encapsulation and delivery when required and potentially allow for the entrapment of the growth factors and small molecules at the site of injury. Further improvements to the existing biomaterials, in the form of chemical modifications will allow for the development of the biomimetic ECM-like scaffold with tunable mechanical properties, with universal tissue engineering applications.

2.6 REFERENCES

1. Mori, H. and K. Esato, [*Hydrogel complexes as materials for artificial organs*]. Iyodenshi To Seitai Kogaku, 1985. **23**(3): p. 203-9.
2. Harris, M.G. and L.G. Mock, *The effect of saline solutions of various compositions on hydrogel lens dimensions*. Am J Optom Physiol Opt, 1974. **51**(7): p. 457-64.

3. Kolthammer, J., *The in vitro adsorption of drugs from horse serum onto carbon coated with an acrylic hydrogel*. J Pharm Pharmacol, 1975. **27**(11): p. 801-5.
4. Krohn, D.L. and J.M. Breiffeller, *Quantitation of pilocarpine delivery across isolated rabbit cornea by noncross-linked high viscosity polymer gel*. Invest Ophthalmol, 1976. **15**(4): p. 324-7.
5. Chepurov, A.K., et al., [*Thromboresistant properties of hydrophilic gels*]. Polim Med, 1980. **10**(3): p. 121-33.
6. Quinn, C.A., R.E. Connor, and A. Heller, *Biocompatible, glucose-permeable hydrogel for in situ coating of implantable biosensors*. Biomaterials, 1997. **18**(24): p. 1665-70.
7. Leaper, D.J., et al., *Experimental infection and hydrogel dressings*. J Hosp Infect, 1984. **5 Suppl A**: p. 69-73.
8. Li, X., et al., *Engineering in situ cross-linkable and neurocompatible hydrogels*. J Neurotrauma, 2014. **31**(16): p. 1431-8.
9. Sato, M., T.Z. Wong, and R.D. Allen, *Rheological properties of living cytoplasm: endoplasm of Physarum plasmodium*. J Cell Biol, 1983. **97**(4): p. 1089-97.
10. Rainer, F. and V. Ribitsch, [*Viscoelastic properties of normal human synovia and their relation to biomechanics*]. Z Rheumatol, 1985. **44**(3): p. 114-9.
11. Zahm, J.M., et al., *Role of simulated repetitive coughing in mucus clearance*. Eur Respir J, 1991. **4**(3): p. 311-5.
12. Tiffany, J.M., *The viscosity of human tears*. Int Ophthalmol, 1991. **15**(6): p. 371-6.

13. Buchsbaum, G., et al., *Dynamics of an oscillating viscoelastic sphere: a model of the vitreous humor of the eye*. Biorheology, 1984. **21**(1-2): p. 285-96.
14. Jackson, G.W. and D.F. James, *The hydrodynamic resistance of hyaluronic acid and its contribution to tissue permeability*. Biorheology, 1982. **19**(1/2): p. 317-30.
15. Dutta, A. and J.M. Tarbell, *Influence of non-Newtonian behavior of blood on flow in an elastic artery model*. J Biomech Eng, 1996. **118**(1): p. 111-9.
16. White, J.L. and A.B. Metzner, *Thermodynamic and Heat Transport Considerations for Viscoelastic Fluids*. Chemical Engineering Science, 1965. **20**(12): p. 1055-&.
17. Lacroix, C., M. Aressy, and P.J. Carreau, *Linear viscoelastic behavior of molten polymer blends: A comparative study of the Palierne and Lee and Park models*. Rheologica Acta, 1997. **36**(4): p. 416-428.
18. Brodkey, R.S., *Transport Phenomena .2. Areas of Specialization*. Chemical Engineering Progress, 1967. **63**(10): p. 21-&.
19. Cross, M.M., *Rheology of Non-Newtonian Fluids - a New Flow Equation for Pseudoplastic Systems*. Journal of Colloid Science, 1965. **20**(5): p. 417-&.
20. Tiu, C., T. Moussa, and P.J. Carreau, *Steady and dynamic shear properties of non-aqueous drag-reducing polymer solutions*. Rheologica Acta, 1995. **34**(6): p. 586-600.
21. Carreau, P.J., *Rheological Equations from Molecular Network Theories*. Transactions of the Society of Rheology, 1972. **16**(1): p. 99-&.
22. Pek, Y.S., et al., *A thixotropic nanocomposite gel for three-dimensional cell culture*. Nat Nanotechnol, 2008. **3**(11): p. 671-5.

23. Bodnar, T., A. Sequeira, and M. Prosi, *On the shear-thinning and viscoelastic effects of blood flow under various flow rates*. Applied Mathematics and Computation, 2011. **217**(11): p. 5055-5067.
24. Sarvestani, A.S. and E. Jabbari, *Modeling the viscoelastic response of suspension of particles in polymer solution: The effect of polymer-particle interactions*. Macromolecular Theory and Simulations, 2007. **16**(4): p. 378-385.
25. Chaffey, C.E., *Mechanisms and Equations for Shear Thinning and Thickening in Dispersions*. Colloid and Polymer Science, 1977. **255**(7): p. 691-698.
26. Milner, S.T., *Relating the shear-thinning curve to the molecular weight distribution in linear polymer melts*. Journal of Rheology, 1996. **40**(2): p. 303-315.
27. Colby, R.H., et al., *Shear thinning of unentangled flexible polymer liquids*. Rheologica Acta, 2007. **46**(5): p. 569-575.
28. Graessley, W.W., *Entangled Linear, Branched and Network Polymer Systems - Molecular Theories*. Advances in Polymer Science, 1982. **47**: p. 67-117.
29. Rouse, P.E., *A theory of the linear viscoelastic properties of dilute solutions of coiling polymers. II. A first-order mechanical thermodynamic property*. Journal of Chemical Physics, 1998. **108**(11): p. 4628-4633.
30. Chandrasekaran, R., *Cations, Water-Molecules and Gel-Forming Polysaccharides - 3-Dimensional Structures*. Biomedical and Biotechnological Advances in Industrial Polysaccharides, 1989: p. 423-434.
31. Chandrasekaran, R., et al., *Cation Interactions in Gellan - an X-Ray Study of the Potassium-Salt*. Carbohydrate Research, 1988. **181**: p. 23-40.

32. Chandrasekaran, R. and V.G. Thailambal, *The Influence of Calcium-Ions, Acetate and L-Glycerate Groups on the Gellan Double-Helix*. Carbohydrate Polymers, 1990. **12**(4): p. 431-442.
33. Kirchenbuechler, I., et al., *Direct visualization of flow-induced conformational transitions of single actin filaments in entangled solutions*. Nature Communications, 2014. **5**.
34. Chandrasekaran, R., *Interactions of Ordered Water and Cations in the Gel-Forming Polysaccharide Gellan Gum*. Water Relationships in Foods, 1991: p. 773-784.
35. Chandrasekaran, R., *Interactions of ordered water and cations in the gel-forming polysaccharide gellan gum*. Adv Exp Med Biol, 1991. **302**: p. 773-84.
36. Chandrasekaran, R., A. Radha, and V.G. Thailambal, *Roles of Potassium-Ions, Acetyl and L-Glyceryl Groups in Native Gellan Double Helix - an X-Ray Study*. Carbohydrate Research, 1992. **224**: p. 1-17.
37. Miyoshi, E., T. Takaya, and K. Nishinari, *Rheological and thermal studies of gel-sol transition in gellan gum aqueous solutions*. Carbohydrate Polymers, 1996. **30**(2-3): p. 109-119.
38. Nakajima, K., T. Ikehara, and T. Nishi, *Observation of gellan gum by scanning tunneling microscopy*. Carbohydrate Polymers, 1996. **30**(2-3): p. 77-81.
39. Ricardo, N.M., et al., *Effect of water-soluble polymers, polyethylene glycol and poly(vinylpyrrolidone), on the gelation of aqueous micellar solutions of Pluronic copolymer F127*. J Colloid Interface Sci, 2012. **368**(1): p. 336-41.

40. Lu, H.D., et al., *Injectable shear-thinning hydrogels engineered with a self-assembling Dock-and-Lock mechanism*. *Biomaterials*, 2012. **33**(7): p. 2145-53.
41. Hardingham, T.E., et al., *Viscoelastic Properties of Proteoglycan Solutions with Varying Proportions Present as Aggregates*. *Journal of Orthopaedic Research*, 1987. **5**(1): p. 36-46.
42. Soby, L., et al., *Viscoelastic and rheological properties of concentrated solutions of proteoglycan subunit and proteoglycan aggregate*. *Biopolymers*, 1990. **29**(12-13): p. 1587-92.
43. Tuinier, R., et al., *Concentration and shear-rate dependence of the viscosity of an extracellular polysaccharide*. *Biopolymers*, 1999. **50**(6): p. 641-6.
44. Jansson, P.E., B. Lindberg, and P.A. Sandford, *Structural Studies of Gellan Gum, an Extracellular Polysaccharide Elaborated by Pseudomonas-Elodea*. *Carbohydrate Research*, 1983. **124**(1): p. 135-139.
45. Cerqueira, M.T., et al., *Gellan gum-hyaluronic acid spongy-like hydrogels and cells from adipose tissue synergize promoting neoskin vascularization*. *ACS Appl Mater Interfaces*, 2014. **6**(22): p. 19668-79.
46. Campana, S., et al., *On the solution properties of bacterial polysaccharides of the gellan family*. *Carbohydr Res*, 1992. **231**: p. 31-8.
47. Wavikar, P.R. and P.R. Vavia, *Rivastigmine-loaded in situ gelling nanostructured lipid carriers for nose to brain delivery*. *J Liposome Res*, 2014: p. 1-9.
48. Zhong, L., et al., *Rheological behavior of xanthan gum solution related to shear thinning fluid delivery for subsurface remediation*. *J Hazard Mater*, 2013. **244-245**: p. 160-70.

49. Oviatt, H.W. and D.A. Brant, *Thermal-Treatment of Semidilute Aqueous Xanthan Solutions Yields Weak Gels with Properties Resembling Hyaluronic-Acid*. International Journal of Biological Macromolecules, 1993. **15**(1): p. 3-10.
50. Sandolo, C., et al., *Characterization of polysaccharide hydrogels for modified drug delivery*. European Biophysics Journal with Biophysics Letters, 2007. **36**(7): p. 693-700.
51. Richter, S., T. Brand, and S. Berger, *Comparative monitoring of the gelation process of a thermoreversible gelling system made of xanthan gum and locust bean gum by dynamic light scattering and H-1 NMR spectroscopy*. Macromolecular Rapid Communications, 2005. **26**(7): p. 548-553.
52. Xu, X., et al., *Hyaluronic Acid-Based Hydrogels: from a Natural Polysaccharide to Complex Networks*. Soft Matter, 2012. **8**(12): p. 3280-3294.
53. Kogan, G., et al., *Hyaluronic acid: a natural biopolymer with a broad range of biomedical and industrial applications*. Biotechnol Lett, 2007. **29**(1): p. 17-25.
54. Xiao, L., et al., *Hyaluronic acid-based hydrogels containing covalently integrated drug depots: implication for controlling inflammation in mechanically stressed tissues*. Biomacromolecules, 2013. **14**(11): p. 3808-19.
55. Liu, L.S., et al., *Hyaluronate-heparin conjugate gels for the delivery of basic fibroblast growth factor (FGF-2)*. J Biomed Mater Res, 2002. **62**(1): p. 128-35.
56. Prestwich, G.D., et al., *Controlled chemical modification of hyaluronic acid: synthesis, applications, and biodegradation of hydrazide derivatives*. Journal of Controlled Release, 1998. **53**(1-3): p. 93-103.

57. Pouyani, T. and G.D. Prestwich, *Functionalized derivatives of hyaluronic acid oligosaccharides: drug carriers and novel biomaterials*. *Bioconjug Chem*, 1994. **5**(4): p. 339-47.
58. Cai, S., et al., *Injectable glycosaminoglycan hydrogels for controlled release of human basic fibroblast growth factor*. *Biomaterials*, 2005. **26**(30): p. 6054-67.
59. Chen, Y., M. Wang, and L. Fang, *Biomaterials as novel penetration enhancers for transdermal and dermal drug delivery systems*. *Drug Deliv*, 2013. **20**(5): p. 199-209.
60. Cui, N., et al., *Functional hyaluronic acid hydrogels prepared by a novel method*. *Mater Sci Eng C Mater Biol Appl*, 2014. **45**: p. 573-7.
61. Baumann, M.D., et al., *Intrathecal delivery of a polymeric nanocomposite hydrogel after spinal cord injury*. *Biomaterials*, 2010. **31**(30): p. 7631-9.
62. Baumann, M.D., et al., *An injectable drug delivery platform for sustained combination therapy*. *Journal of Controlled Release*, 2009. **138**(3): p. 205-13.
63. Hu, X., et al., *Biomaterials from ultrasonication-induced silk fibroin-hyaluronic acid hydrogels*. *Biomacromolecules*, 2010. **11**(11): p. 3178-88.
64. Huin-Amargier, C., et al., *New physically and chemically crosslinked hyaluronate (HA)-based hydrogels for cartilage repair*. *J Biomed Mater Res A*, 2006. **76**(2): p. 416-24.
65. Becker, T.A. and D.R. Kipke, *Flow properties of liquid calcium alginate polymer injected through medical microcatheters for endovascular embolization*. *J Biomed Mater Res*, 2002. **61**(4): p. 533-40.

66. Leonard, M., et al., *Hydrophobically modified alginate hydrogels as protein carriers with specific controlled release properties*. J Control Release, 2004. **98**(3): p. 395-405.
67. Gupta, D., C.H. Tator, and M.S. Shoichet, *Fast-gelling injectable blend of hyaluronan and methylcellulose for intrathecal, localized delivery to the injured spinal cord*. Biomaterials, 2006. **27**(11): p. 2370-9.
68. Ramachandran, S., Y. Tseng, and Y.B. Yu, *Repeated rapid shear-responsiveness of peptide hydrogels with tunable shear modulus*. Biomacromolecules, 2005. **6**(3): p. 1316-21.
69. Schneider, J.P., et al., *Responsive hydrogels from the intramolecular folding and self-assembly of a designed peptide*. J Am Chem Soc, 2002. **124**(50): p. 15030-7.
70. Haines-Butterick, L., et al., *Controlling hydrogelation kinetics by peptide design for three-dimensional encapsulation and injectable delivery of cells*. Proc Natl Acad Sci U S A, 2007. **104**(19): p. 7791-6.
71. Huang, H., et al., *Peptide hydrogelation and cell encapsulation for 3D culture of MCF-7 breast cancer cells*. PLoS One, 2013. **8**(3): p. e59482.
72. Baldursdottir, S.G., et al., *Riboflavin-photosensitized changes in aqueous solutions of alginate. Rheological studies*. Biomacromolecules, 2003. **4**(2): p. 429-36.
73. Wang, S., et al., *Photo-crosslinked poly(epsilon-caprolactone fumarate) networks for guided peripheral nerve regeneration: material properties and preliminary biological evaluations*. Acta Biomater, 2009. **5**(5): p. 1531-42.

74. Rui, J., et al., *Controlled release of vascular endothelial growth factor using poly-lactic-co-glycolic acid microspheres: in vitro characterization and application in polycaprolactone fumarate nerve conduits*. *Acta Biomater*, 2012. **8**(2): p. 511-8.
75. Tong, Z. and X. Jia, *Biomaterials-Based Strategies for the Engineering of Mechanically Active Soft Tissues*. *MRS Commun*, 2012. **2**(2): p. 31-39.
76. Zhu, J., *Bioactive modification of poly(ethylene glycol) hydrogels for tissue engineering*. *Biomaterials*, 2010. **31**(17): p. 4639-56.
77. Patel, P.N., C.K. Smith, and C.W. Patrick, Jr., *Rheological and recovery properties of poly(ethylene glycol) diacrylate hydrogels and human adipose tissue*. *J Biomed Mater Res A*, 2005. **73**(3): p. 313-9.
78. Cross, D., et al., *Injectable Hybrid Hydrogels of Hyaluronic Acid Crosslinked by Well-Defined Synthetic Polycations: Preparation and Characterization In Vitro and In Vivo*. *Macromol Biosci*, 2015.
79. Moglia, R.S., et al., *Injectable polyHIPEs as high-porosity bone grafts*. *Biomacromolecules*, 2011. **12**(10): p. 3621-8.
80. Williams, J.M., A.J. Gray, and M.H. Wilkerson, *Emulsion stability and rigid foams from styrene or divinylbenzene water-in-oil emulsions*. *Langmuir*, 1990. **6**(2): p. 437-444.
81. Akay, G., M.A. Birch, and M.A. Bokhari, *Microcellular polyHIPE polymer supports osteoblast growth and bone formation in vitro*. *Biomaterials*, 2004. **25**(18): p. 3991-4000.

82. Bokhari, M.A., et al., *The enhancement of osteoblast growth and differentiation in vitro on a peptide hydrogel-polyHIPE polymer hybrid material*. *Biomaterials*, 2005. **26**(25): p. 5198-208.
83. Oh, B.H., A. Bismarck, and M.B. Chan-Park, *High internal phase emulsion templating with self-emulsifying and thermoresponsive chitosan-graft-PNIPAM-graft-oligoproline*. *Biomacromolecules*, 2014. **15**(5): p. 1777-87.
84. Robinson, J.L., et al., *Achieving interconnected pore architecture in injectable PolyHIPEs for bone tissue engineering*. *Tissue Eng Part A*, 2014. **20**(5-6): p. 1103-12.
85. Hayman, M.W., et al., *Growth of human stem cell-derived neurons on solid three-dimensional polymers*. *J Biochem Biophys Methods*, 2005. **62**(3): p. 231-40.
86. Welch, C.F., et al., *Rheology of high internal phase emulsions*. *Langmuir*, 2006. **22**(4): p. 1544-50.
87. Yaron, P.N., et al., *Nano- and microstructure of high-internal phase emulsions under shear*. *J Phys Chem B*, 2010. **114**(10): p. 3500-9.
88. Ribeiro, C.C., C.C. Barrias, and M.A. Barbosa, *Preparation and characterisation of calcium-phosphate porous microspheres with a uniform size for biomedical applications*. *J Mater Sci Mater Med*, 2006. **17**(5): p. 455-63.
89. Oliveira, S.M., et al., *Injectability of a bone filler system based on hydroxyapatite microspheres and a vehicle with in situ gel-forming ability*. *J Biomed Mater Res B Appl Biomater*, 2008. **87**(1): p. 49-58.

90. Oliveira, S.M., et al., *Characterization of polymeric solutions as injectable vehicles for hydroxyapatite microspheres*. AAPS PharmSciTech, 2010. **11**(2): p. 852-8.
91. Appel, E.A., et al., *Self-assembled hydrogels utilizing polymer-nanoparticle interactions*. Nature Communications, 2015. **6**: p. 6295.
92. Appel, E.A., et al., *Self-assembled hydrogels utilizing polymer-nanoparticle interactions*. Nat Commun, 2015. **6**: p. 6295.

3. PREPARATION AND CHARACTERIZATION OF GELLAN GUM-BASED SHEAR-THINNING HYDROGELS

3.1 INTRODUCTION

Shear-thinning hydrogels are quickly emerging to become beacons for next generation *in vitro* cell culture technology with their self-healing ability along with their capacity of providing a biomimetic model for three-dimensional cell culture [1]. The gels have wide varieties of biological and biomedical applications in the fields of tissue engineering, regenerative medicine, toxicology and drug delivery [2, 3]. Existing two-dimensional culture models have difficulty replicating the cell-scaffold interactions as seen in natural tissue conditions and since the cell proliferation, migration and growth are influenced by the cell-cell interactions along with the cell-scaffold interactions, they are unreliable and require modification. The native extracellular matrix (ECM) of the tissue microenvironment also acts as a reserve of the required growth factors and differentiating factors to elicit different cell behaviors and morphogenetic events [4]. The ECM also protects the bioactive small molecules from degradation and enables a sustainable exposure of cells to the necessary small molecules over a prolonged period of time [5].

Shear-thinning hydrogels are Non-Newtonian fluids that show a decrease in fluid viscosity with an increase in shear-stress and some possess self-healing properties by showing a recovery in the viscosity over a period of time[6]. The self-healing ability is due to the fluid property called thixotropy [7, 8]. These hydrogels are also referred to as “Smart hydrogels” as they respond to the external stimuli along with being reversible in the properties, retaining their original structure over a period of time or with the removal of external stimulus. Growth factors, drugs or cells can be mixed with the hydrogel before injection for the *in vivo* experiments [9]. Recent experiments

show shear-thinning hydrogels that resemble extracellular matrix in their chemical and mechanical properties, with their high permeability for metabolites, oxygen, nutrients and assist in intercellular chemical signaling [10, 11]. All hydrogels are basically visco-elastic materials. Shear-thinning hydrogels show varying levels of viscous and elastic components in response to external mechanical stimulus, shear stress. Oscillatory testing using dynamic oscillatory rheology is used to analyze the varying properties of these hydrogels. Storage modulus, loss modulus and phase angle are generally quantified to get a measure of the change in viscoelasticity of the shear-thinning hydrogels. Stress-relaxation tests are used to identify the time-dependency of the hydrogels, which in turn, are characterized as thixotropic. In the human body, some prime examples of shear-thinning fluids include the cytoplasm, blood, mucus, vitreous humor, tears, synovial fluid and ground substance of tissues, which adds to the increasing interest in the understanding and further development of shear-thinning hydrogels targeted towards biomedical applications [12-18]. The increasing knowledge on the physical and mechanical properties of the body fluids is enabling the development of improved solutions to the existing problems in the field of tissue engineering in the form of improved biomaterials.

The use of hydrogels to promote cell culture and proliferation is a better alternative to the outdated two-dimensional adhesive models by providing the cells with a complex three-dimensional native architecture [19]. An ideal three-dimensional *in vitro* cell culture model should allow for cell passaging, along with enabling cell adhesion over the scaffold backbone. Hydrogels with tunable biomechanical properties are an ideal choice for simulating local microenvironment experienced by cells in tissues. Another important criterion deciding the cell survival within the hydrogels is the porosity, which allows for the diffusion of gases and nutrients, as well as, growth factors to and from the cells [20]. This forms for a major condition

for the long term sustenance of the cells within the hydrogel, for either just the proliferation purposes or eventual differentiation studies. It is ideal to develop a hydrogel made of a biodegradable material, which will eliminate the issues pertaining to the removal of the scaffold or leaching out through connective tissue.

Polysaccharide based hydrogels are excellent candidates for biomedical applications, owing to the properties like higher polarity, varied chemical composition giving a stereological advantage, biocompatible and show minimum to no cytotoxicity . A major component of ECM is formed by chondroitin sulfate and hyaluoronan [21]. Gellan gum is an anionic polysaccharide produced by the fermentation of bacterium *Sphingomonas elodea*, and is commonly used in food and pharmaceutical industry[21]. It is easily dissolved in water when heated and forms a hydrogel on lowering of the temperature and has tunable gelation properties by modifying the concentration of gellan gum and also, by mixing with varying concentrations of mono or divalent cations [22]. It has structural similarities with ECM [23]. Gellan forms thermoresponsive hydrogels with varying structural conformation at different temperatures and in combination with different ions [24]. It is formed at higher temperatures, when initially it is in the coil form. Upon the reduction of temperature moving towards room temperature, the random coils assemble themselves towards anti-parallel double helices, enhancing the structural integrity of the gel at lower temperatures. The addition of cations further brings these double helices closer, rendering higher mechanical strength to the gels made in salt solutions or immersed in it [25-27]. Another advantage, establishing gellan gum as a favorable biomaterial for transplantation and regenerative medicine, is that it does not elicit immune response since it is a polysaccharide based gel and the structure of polysaccharide does not depend on any genetic code [28-30].

In this chapter, we focus on the preparation and characterization of the optimal concentrations of gellan gum for producing shear thinning hydrogels for applications in three dimensional cell culture. On looking at a range of concentrations of gellan gum and addition of cations through the DMEM-based cell culture medium and Phosphate Buffer Saline (PBS), we identify the range of concentrations that can be used for later cell studies. In particular, we focus on the rheological analysis of the gellan gum hydrogels to investigate the shear-thinning feature at different stages of hydrogel usage in cell culture.

3.2 MATERIALS AND METHODS

3.2.1 Materials

Gellan gum, under the trade name of Phytigel™, phosphate buffered saline (PBS), FITC-Dextran of different molecular weights (4, 70, 150, 500 kDa) were purchased from Sigma-Aldrich. Lysozyme, from egg white was purchased through VWR. Recombinant human Vascular Endothelial Growth Factor-A (VEGF) and VEGF DuoSet ELISA kit were purchased from R&D Systems. Ethanol, 200 Proof, was purchased from Fisher-Scientific.

3.2.2 Preparation of hydrogels

Gellan gum, supplied by Sigma-Aldrich under the trade name Phytigel™ was added slowly to the water at room temperature with rapid stirring to eliminate any lumps before heating. It was sterilized by means of autoclaving for about fifteen minutes before use for three-dimensional cell culture. Depending on the concentration, the congealing temperature varies, but generally, the congealing temperature is 27-32°C. Different concentrations (0.5-5.0%) were made using the

above described procedure. The gel morphology was observed at room temperature and the effect of cell culture medium was seen on the injectability of the hydrogels.

3.2.3 Aerogel synthesis and Scanning electron microscope

Gellan gum aerogels were generated using CO₂ as a volatile acidifying sol-gel accelerator. Gradual immersion of hydrogels in 100% ethanol was performed by incubating the hydrogels in 10%, 25%, 50%, 75% and 100% ethanol solutions made in 1X PBS in order to replace the water with alcohol, making them alcogels. These alcogels were then placed in a 300 mL stainless steel vessel, heated to 40 °C, and pressurized with CO₂ to 100 bar. The CO₂ was later vented to recover the aerogel to be used for imaging via scanning electron microscopy. Scanning electron microscopic images were obtained with a HITACHI SU-70 SEM with an accelerating voltage of 1 keV. The hydrogels were cut into fine sections and mounted on aluminum stubs. A 10 nm platinum coating was then applied to the sample via spin coating (Denton Vacuum, USA, Model: Desk V TSC).

3.2.4 Rheological characterization of hydrogels

For rheological study, hydrogel solutions of Phytigel™ at various concentrations and combinations with medium were mixed on the steel plate geometry and inspected by oscillatory shear rheometry immediately. A DHR3 rheometer (TA Instruments Inc.) with standard geometry of 8 mm diameter was used for the rheological characterization of all hydrogels samples. The test methods employed were oscillatory time sweep, frequency sweep and stress sweep. The time sweep was performed to monitor the *in situ* gelation of the hydrogel solutions at 37 °C. The test, which was operated at constant frequency (1 Hz) and strain (5%) and terminated after 600

seconds, recorded the temporal evolution of shear storage modulus (G') and the shear loss modulus (G''). The stress sweep was set up by holding the temperature $37\text{ }^{\circ}\text{C}$ and constant frequency (1 Hz) while increasing the stress level from 1 to 10 Pa. The applied range of 1-10 Pa was found to be safe-for-use from a prior experiment where we determined the linear viscoelastic region (LVR) profiles of the hydrogels by shearing them until structure breakdown. We also subjected hydrogels to a frequency sweep at 50% of their respective ultimate stress levels. At this fixed shear stress and temperature ($37\text{ }^{\circ}\text{C}$), the oscillatory frequency was increased from 0.1 to 100 Hz and the G' was recorded. The change in phase angle was observed to indicate the sol-gel transition and the transition time point.

Young's modulus, E , can be evaluated by $E = 2G(1+\gamma)$. When a material can be assumed to be incompressible, its Poisson's ratio, γ , approaches 0.5 and this relationship approaches $E = 3G$. This assumption for hydrogels is supported by a research showing that n for polyacrylamide hydrogels is nearly 0.5, and these hydrogels typically used under very low strain. This relationship between E and G then provides a useful tool for comparing mechanical properties of substrates and tissues that have been determined using other methods of measurement.

A combination of oscillatory time sweep and flow sweep was used to calculate the time course of gelation of the hydrogel. The oscillatory time sweep was performed under constant stress for 360 seconds to get the G' at equilibrium conditions, followed by an intermittent period of 60 seconds of high shear strain rate of 1500 s^{-1} to incorporate the shear thinning step, immediately followed by the oscillatory time sweep under constant stress to calculate the time taken for the storage modulus to reach the pre-shear G' .

The shear stress creep and recovery was observed by an application of stress for a time period followed by an immediate recovery stage with no stress applied. This was continued for five

cycles to record the change in viscosity with the application of shear stress and the recovery stages.

3.2.5 Swelling of hydrogels

Hydrogels of different concentrations were used to determine the swelling properties of hydrogels in cell culture medium and PBS. To characterize the swelling behavior of the hydrogels, they were weighed immediately after preparation. Hydrogels were placed in 2 mL of PBS solution at 37 °C and allowed to swell. Weights were taken every 24 hours for the next 21 days. Fresh PBS and cell culture medium, previously equilibrated at 37 °C, was replaced every 24 hours at the time of measurement. The swelling ratio was calculated by the ratio of the change in weight of the hydrogels at equilibrium swelling over the initial weight of hydrogel after gelation. Deionized water was used as a control condition for the swelling studies. Each time point was taken for three different gel samples and the weight of gel at each time point was reported as the mean of the triplicate.

3.2.6 Degradation studies

To analyze the potential *in vivo* degradation, the hydrogels were incubated in serum concentration of lysozyme, 1.5 µg/ml. The experiments were performed along the same lines as swelling studies and the hydrogels were incubated in lysozyme solution, made in 1X PBS. The hydrogel weights were taken at each time point and the replaced lysozyme buffer was replaced with the same volume after each time point. The degradation ratio was calculated by dividing the change in weight of hydrogel at each time point over the hydrogel initial weight after gelation.

Each time point was taken for three different gel samples and the weight of gel at each time point was reported as the mean of the triplicate.

3.2.7 In vitro growth factor release studies

The VEGF of known concentration was used loaded to the hydrogels along with cell culture medium to get a 1:1 ratio of hydrogel to cell culture medium with VEGF solution to make the loaded hydrogels. These were incubated in a release buffer made up of 1X PBS with 1% BSA and 10 µg/ml heparin sodium salt. The hydrogel of 300 µl volume was added to form a gel layer of less than 1mm thickness in a 12-well culture plate and incubated in 1ml of release buffer. At each time point, 500 µl of release buffer was removed to be used for an ELISA later and replaced with 500 µl of fresh release buffer equilibrated to 37°C. For the first 12 hours, the readings were performed for every two hours, i.e., 0hr, 2hr, 4hr, 6hr, 8hr, 10hr, 12hr. The next time points were at 24hr, 48hr, 72hr, 96hr, and 168hr. All the release buffer vials corresponding to each time point were stored at -80°C until the ELISA was performed to quantify the concentration of VEGF in the release buffer at each time point. Each gel condition was incubated in 1 ml of release buffer in an incubator at 37 °C and 5% CO₂. Each release condition was performed in triplicates. The kit protocol was followed to perform ELISA. The total accumulated release of VEGF was calculated by the integration of individual measurements over a cumulative time of the experiment. The cumulative release percentage was given by the ratio of the cumulative release concentration at each time point and the theoretical loading concentration of VEGF.

3.2.8 Fluorescence Recovery after Photobleaching (FRAP)

To calculate the value of diffusion coefficient of medium components or cells in the hydrogel, FITC-conjugated Dextran of different molecular weights (4, 70, 150 and 500 kD) were used. Hydrogel samples of a total volume of 200 μ l were made by mixing equal volumes of hydrogel and FITC-Dextran solutions made in 1X PBS to get an end concentration of 1 mg/ml of the FITC-Dextran. Zeiss LSM-710 confocal microscope was used to perform the experiments. A 488 nm Argon laser was used for FITC excitation. The regions intended to be bleached were selected by drawing the region of interest, in this case, a circle. Pre-FRAP and post-FRAP recovery images were taken at 512 x 512 pixels using a 10x objective, with the bleaching step performed at slowest scanning speed and 100% laser power. Three separate FRAP experiments were performed on each sample of three independently prepared samples for each condition. The $\tau_{1/2}$ was calculated from the plot of normalized intensity vs time as the time point corresponding to the intensity level which is a half of the recovered intensity plateau. The diffusion coefficient, D was given by the formula:

$$D = \frac{0.88w^2}{4\tau_{1/2}}$$

Where w is the radius of the region of interest.

3.3 RESULTS

3.3.1 Hydrogel formation and gel morphology

Gellan gum hydrogels were easily formed at various concentrations (0.5-5.0%) by dissolving in water (Figure 1). They were thermo-reversible and also prone to shear-thinning over the application of shearing mechanical forces. The readily forming hydrogels were highly favorable

for potential cell culture by being highly transparent with and without the addition of cell culture medium (Figure 3.1A). The gel in a particular range of concentrations (0.9-1.5%) was easily extruded by simple pipetting into desired shapes and features (Figure 3.1B).

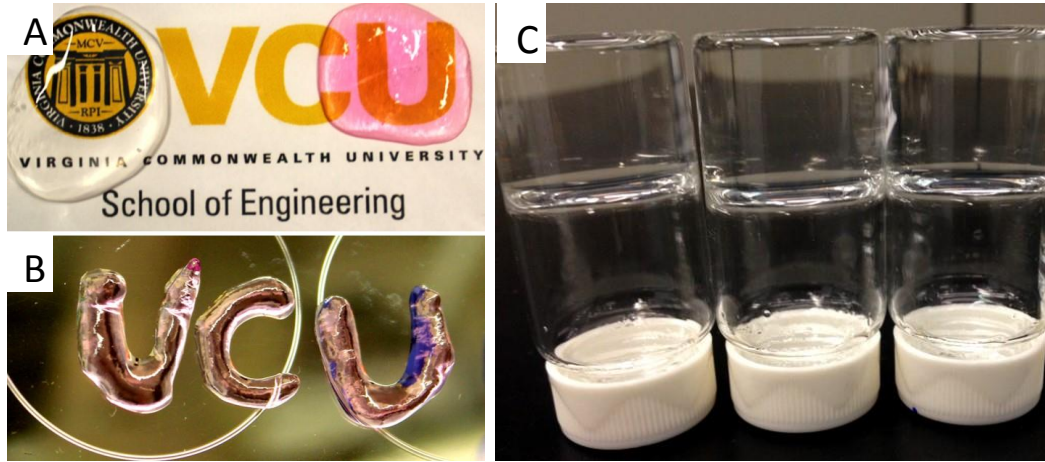


Figure 3.1: Hydrogel morphology A. Gellan gum with and without cell culture medium, B. Hydrogel can be injected into the desired shapes or patterns, C. The gellan gum sets into gels which can be reversed into a solution with the application of shear forces

3.3.2 Scanning electron microscopy for porosity

The hydrogels were converted to aerogels via the intermediate stage of alcogel by a gradual immersion of the sample in 100% ethyl alcohol, going through different concentrations of ethyl alcohol made in 1X PBS, in order to protect the structural integrity of the hydrogel. Using supercritical CO₂, the aerogels were made and used for the scanning electron microscopy to observe the porous structures. The aerogels revealed a microporous structure suitable for the cell culture along with the nanofibrillar back bone of the scaffolding (Figure 3.2).

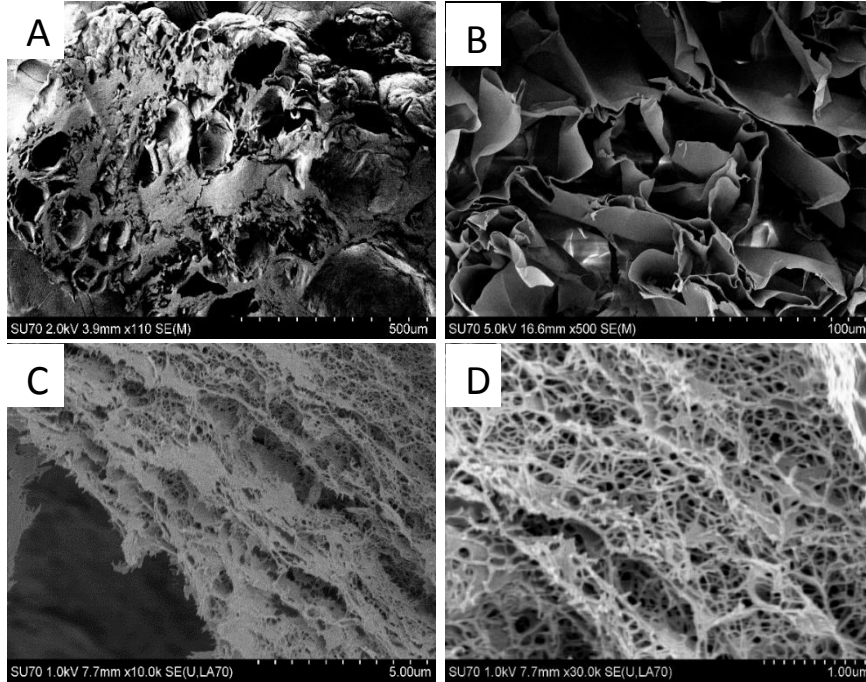


Figure 3.2: The porosity and textural properties were studied by observing the microscale features using the scanning electron microscopy of supercritical CO₂ dried hydrogels at different scales

3.3.3 Rheological characterization of the hydrogels

Hydrogels of different concentrations corresponded to different mechanical properties as explained by their rheological analysis. After identifying the LVR of the hydrogels using the oscillatory amplitude sweep, the storage modulus (G') and loss modulus (G'') were identified using the oscillatory frequency sweep and the sol-gel transitions were observed under the application of constant stress using the oscillatory time sweep (Figure 3.3). The gel phase was identified as the region with higher value for G' than G'' and the solution phase was the one with

G'' greater than G' . The time point of gelation was identified as the time point at which the curves for G' and G'' intersect and at this point, the phase angle (δ) is 45° .

Table 3.1: The G' values of the different concentrations of gellan gum hydrogels were evaluated from the oscillatory time sweep studies

Hydrogel Condition	Storage Modulus (Pa)
1.4%	191.029
1.1%+Medium	472.127
1.4%+Medium	2251.33
1.7%+Medium	10344.5

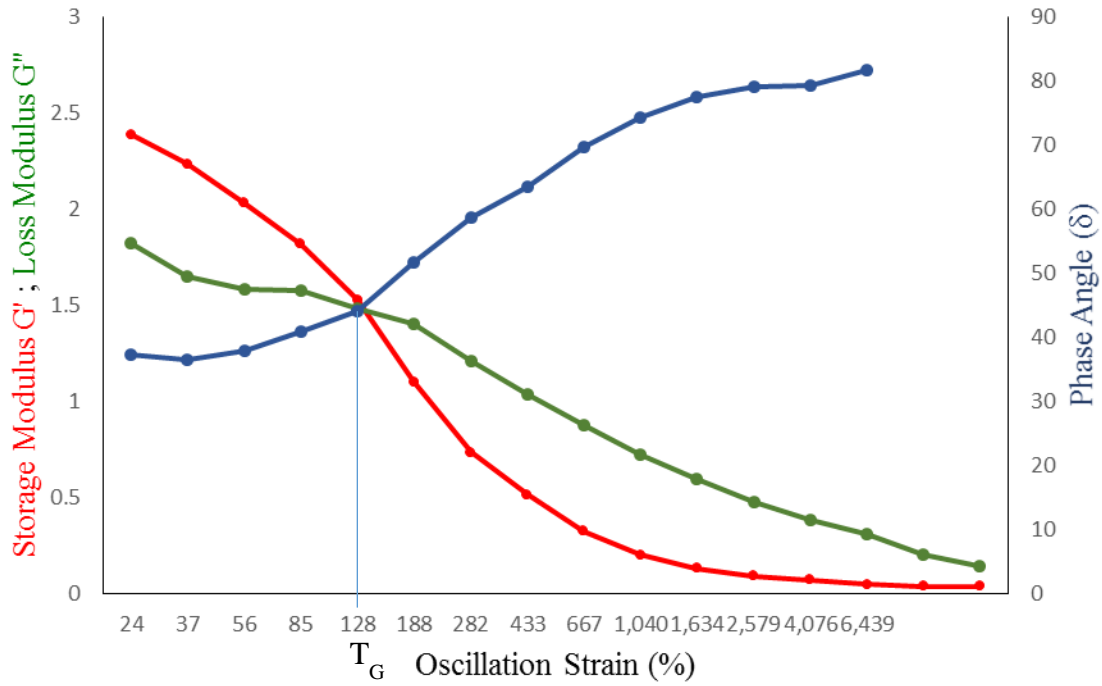


Figure 3.3: The sol-gel transition was observed by the changes in the storage and loss moduli (G' and G'') and phase angle (δ)

The addition of cell culture medium or 1X PBS to the gellan gum hydrogel showed an increase in the gel stiffness as observed by the almost ten-fold increase in the storage modulus of the hydrogel with the addition of cell culture medium (Figure 3.4).

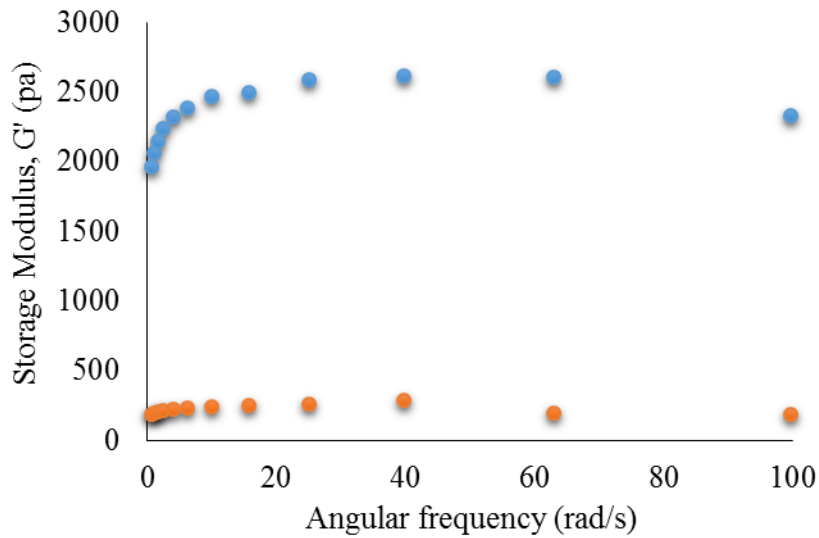


Figure 3.4: The addition of cell culture medium added the cationic interactions which made the gellan gum gels stronger as observed by the difference in the storage modulus (G') with red data points for gellan gum only (1.4%) and blue data points for gellan gum (1.4%) with cell culture medium

Also, when the hydrogels mixed with the cell suspension in the culture medium were incubated at 37°C and 5% CO₂, the gel showed a gradual increase in stiffness as observed by the increase in the value of G' (Figure 3.5).

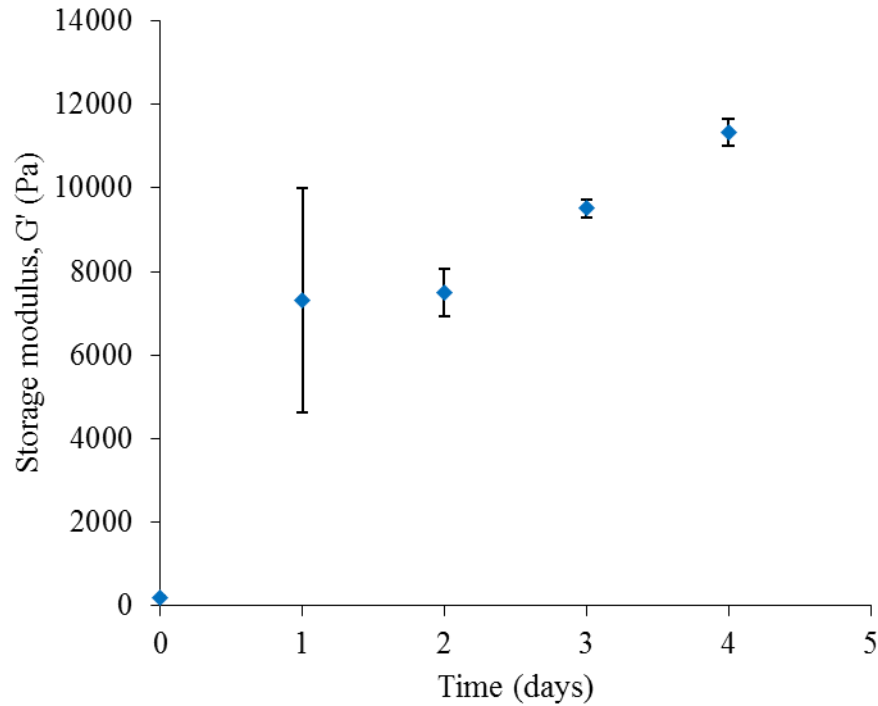


Figure 3.5: The storage modulus (G') increased with an increase in the number of days of incubation in the cell culture medium when loaded with cells (Mean \pm Std. Dev)

The shear-thinning ability of the hydrogels at various concentrations (Figure 3.6A) and in combination with medium (Figure 3.6B) was concluded from the decrease in the viscosity of the hydrogel with an increase in the shear-strain rate. This is a classic feature for any shear-thinning fluids. The zero-rate viscosity values give a measure of the viscosity when no shear-stress is applied and the values are tabulated in Table 3.2.

Table 3.2: The zero-rate viscosity increased with an increase in gellan gum concentration

Hydrogel Conc. (%)	Zero Rate Viscosity (Pa.s)
1.1%	6.474
1.2%	6.839
1.3%	36.678
1.4%	74.156
2.0%	318.9
4.0%	427896

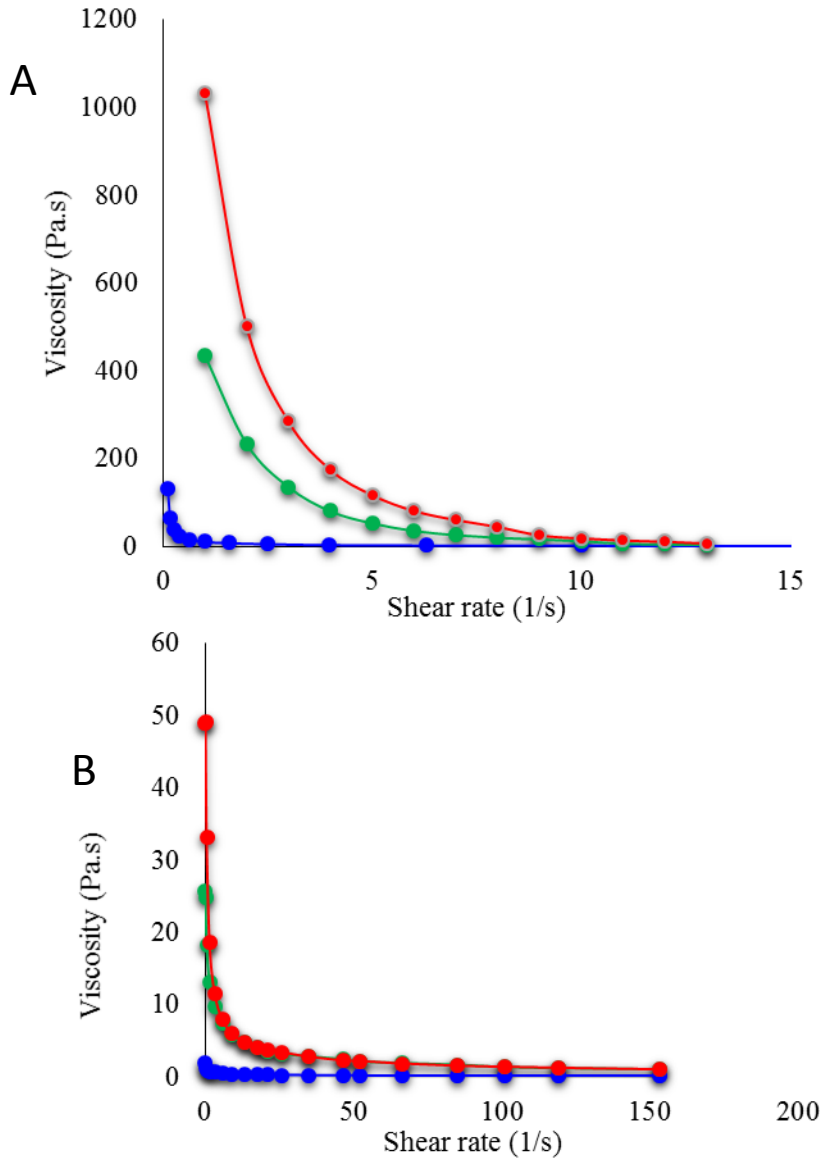


Figure 3.6: Shear thinning effect of the hydrogels was measured by the change in the viscosity with an increase in shear rate and the similar trend was recorded in the gels with (A) and without (B) cell culture medium (Blue: 1.1%, Green: 1.4%, Red: 1.7% of Gellan gum)

To calculate the time taken for the gelation following a period of shear thinning, a user-defined program was designed on the rheometer to first quantify the storage modulus of the gel over a period of time with no apparent stress on the hydrogel by means of oscillatory time sweep and

interrupted with a high stress to induce the shear-thinning as recorded with the drop of the values of viscosity for a time period of 60 seconds (Figure 3.7). This was followed by the measurement of G' after the removal of the shear stress using the oscillatory time sweep again and the time taken for the G' to get back to the initial value is taken as the time needed for the gelation after shear thinning.

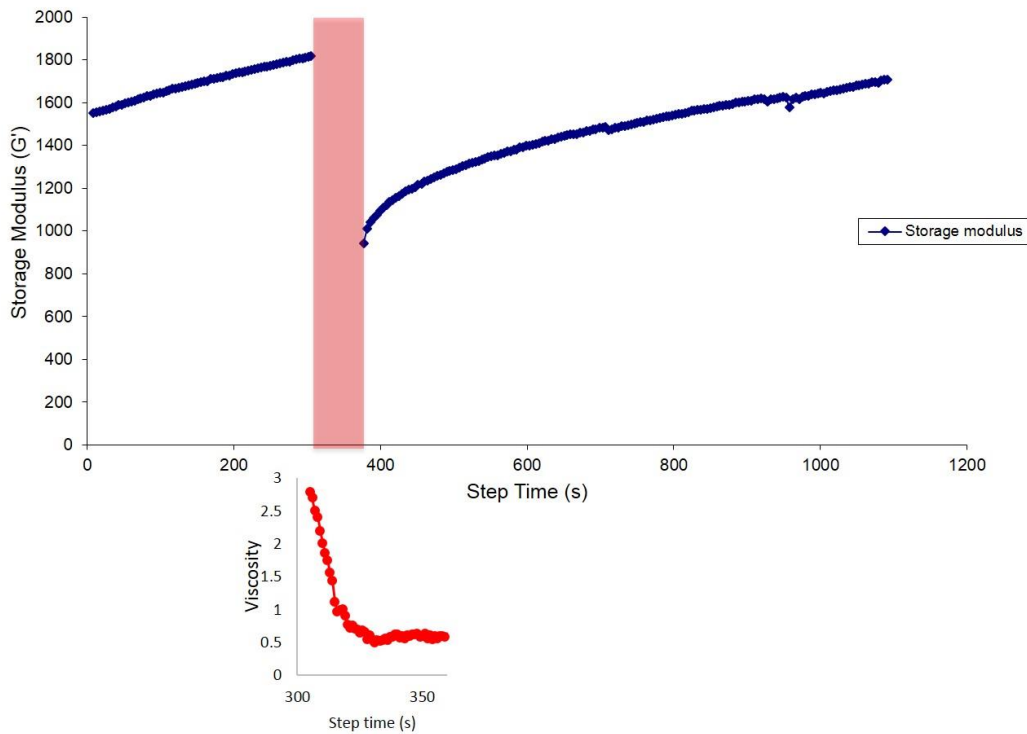


Figure 3.7: Oscillatory time sweep and flow sweep were used in combination to get the time needed for the gelation proceeding shear thinning, inset: the viscosity reading of the intermittent high shear stress period of 60 sec

The shear-thinning property of the hydrogel was retained even after a period of incubation of the hydrogel with cells in the culture medium with different cations and at 37°C and at 5% CO₂ (Figure 3.8). This was evident from the transient cycles of shear-stress and recovery. With an

application of shear stress at 20 N.m for 10 seconds, the hydrogels undergo shear thinning as observed from the pattern of the viscosity drop and following a 30 second period for recovery, the viscosity levels were within the range of the pre-shear viscosity. This was performed for five cycles to understand the effect of repeated shear stress application on the hydrogels with the cells.

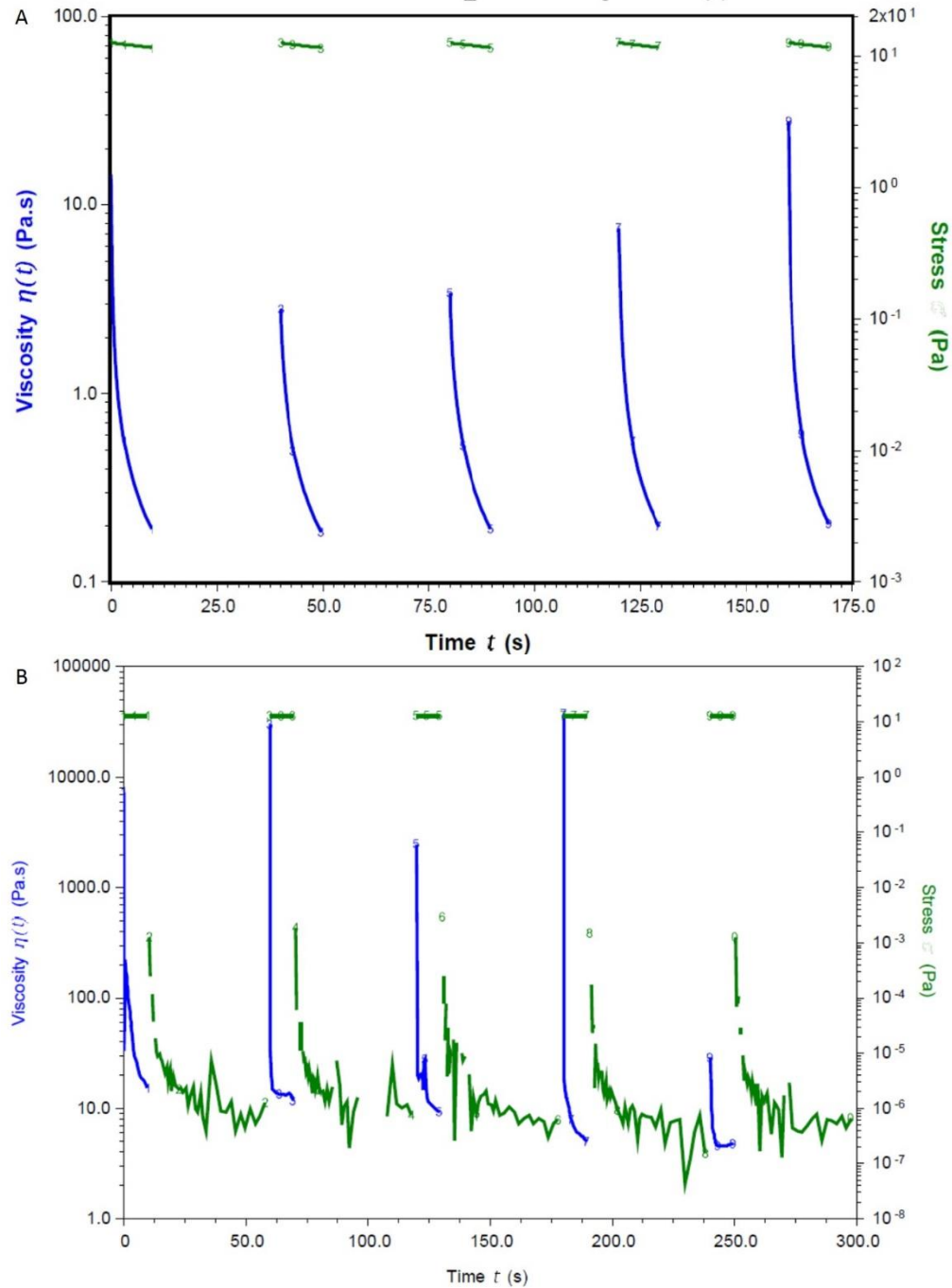


Figure 3.8: Shear stress and relaxation test was used to observe the effect of shear-thinning and consequent thixotropic recovery of the initial state with the removal of the shear stress after 3 days (A) and 7 days (B) in cell culture

3.3.4 Swelling studies

The swelling studies, performed in both 1X PBS and cell culture medium revealed no significant change in the weight corresponding to swelling of the hydrogels (Figure 3.9 A, B and D). The net weight increase was less than 10% in both the conditions for over a period of 21 days. The negative control was de-ionized water, in which, the lower concentrations of the hydrogels underwent hydrolysis within 24 hours of incubation of the hydrogels at 37°C and at 5% CO₂. The higher concentrations of hydrogel at 3% and 4% gellan gum did not undergo 100% hydrolysis but showed significant reduction in the weight as quantified from the initial pre-incubation weight of the hydrogels.

3.3.5 Degradation studies

Degradation studies were performed on the lower concentrations of the hydrogel at 1.5 µg/ml concentration of lysozyme (Figure 3.9C). At this concentration, for over a period of 7 days, the hydrogels underwent minimum gel lysis with a net weight loss of 5%.

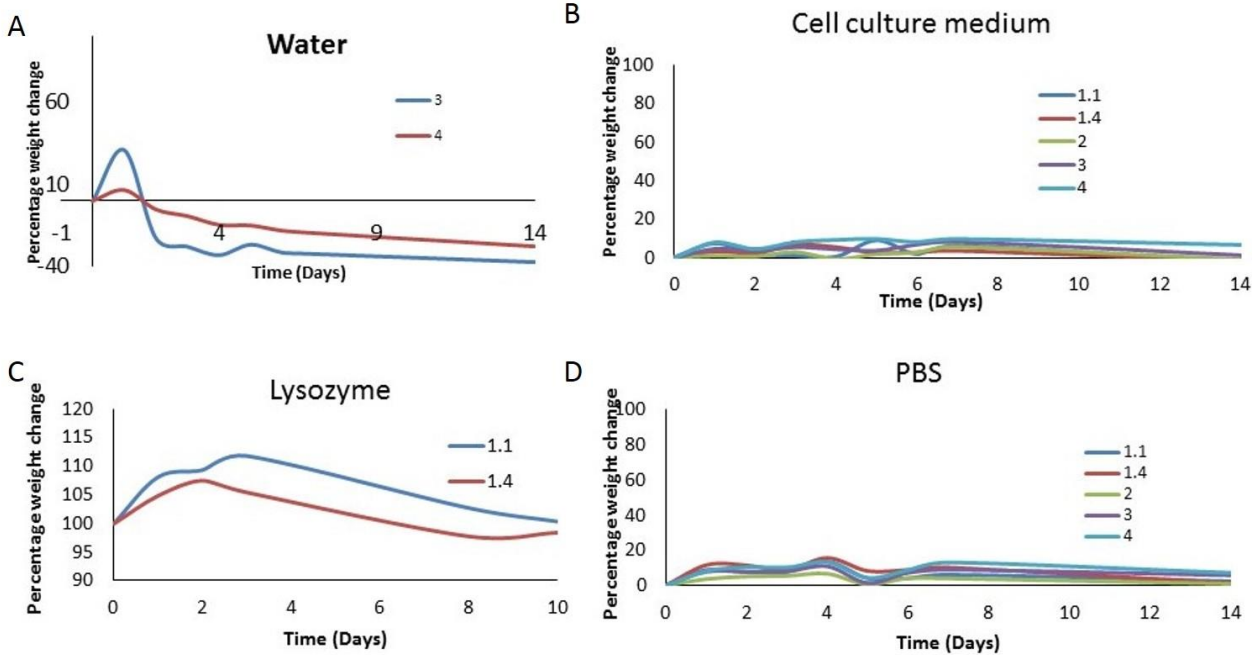


Figure 3.9: Swelling studies were performed in cell culture medium and PBS in the lower to high gel stiffness range as quantified from the prior rheology experiments and the gel samples in DI water were used as control. A. DI water, B. Cell culture medium, D. PBS. The degradation studies were performed for the lower stiffness gels in serum concentrations of the enzyme lysozyme.

3.3.6 In vitro release of VEGF

With the nanofibrillar and porous microstructures, it was proposed to understand the potential entrapment and sustained release of the vascular endothelial growth factor (VEGF) which was later quantified by means of ELISA. In the first release study, VEGF at 100 ng/ml final concentration was made in the endothelial cell medium before mixing it with equal volumes of the 1.1% and 1.4% gellan gum hydrogels to get a crosslinked and loaded hydrogel, which

showed a sustained release of the VEGF for 14 days, in a similar fashion, from both the concentrations of the hydrogel (Figure 3.10).

In the next experiment, the VEGF at two loading concentrations, 500 ng/ml (Condition 1) and 100 ng/ml (Condition 2) were made in endothelial cell culture medium, which was added to equal volumes of gellan gum hydrogel at the medium gel stiffness, corresponding to the concentration of 1.4% gellan gum (Figure 3.11). The VEGF release from the hydrogel was quantified by measuring the concentration of VEGF in the release buffer for a time period of 7 days. The cumulative release percentage showed that gellan gum released less than 1% of the loading concentration of VEGF.

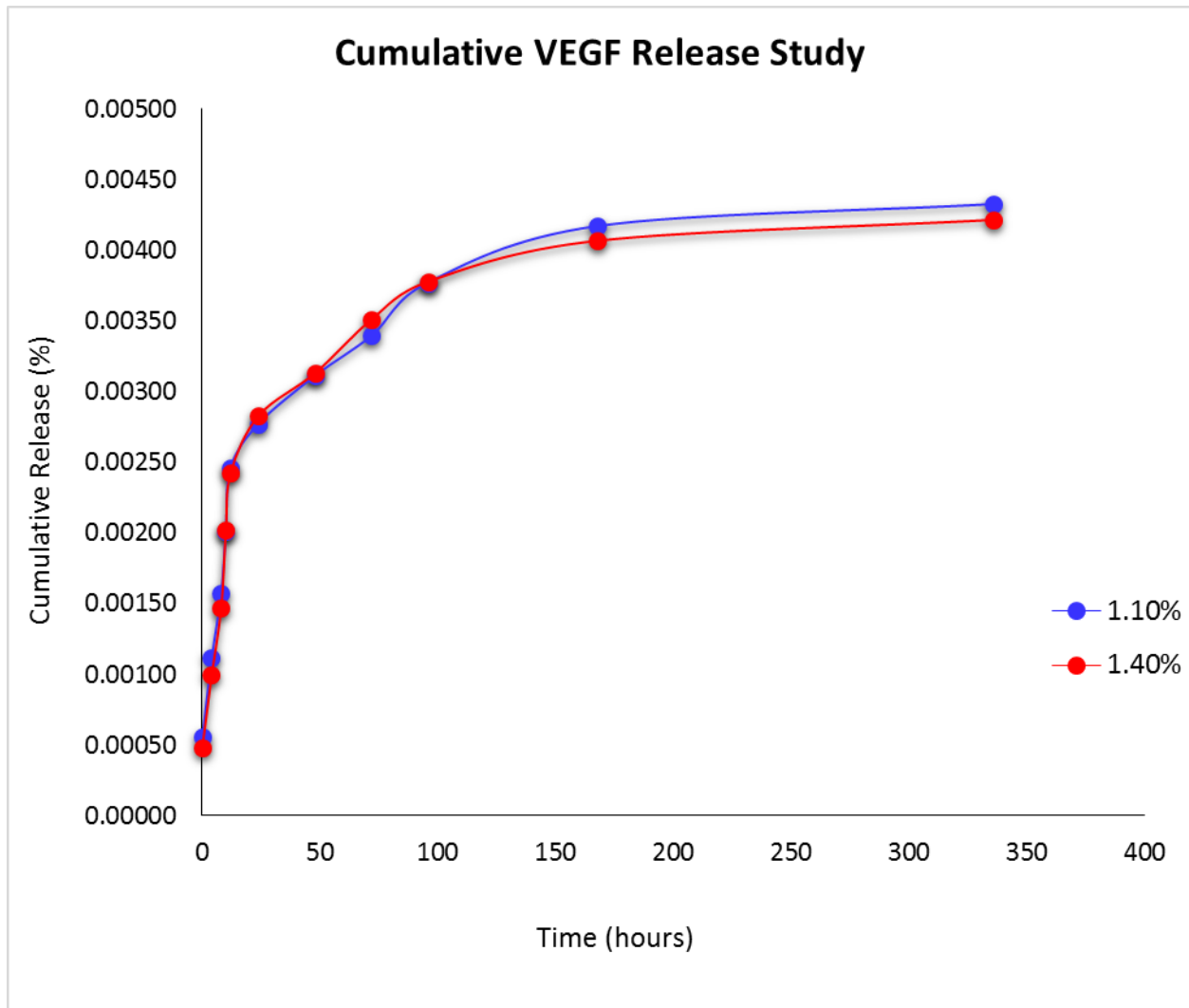


Figure 3.10: Cumulative release of the VEGF was recorded over a period of two weeks in two different concentrations of gellan gum, one representing the lower limit of the stiffness range to be used for cell studies, 1.1% and the other being the mid-range, 1.4%

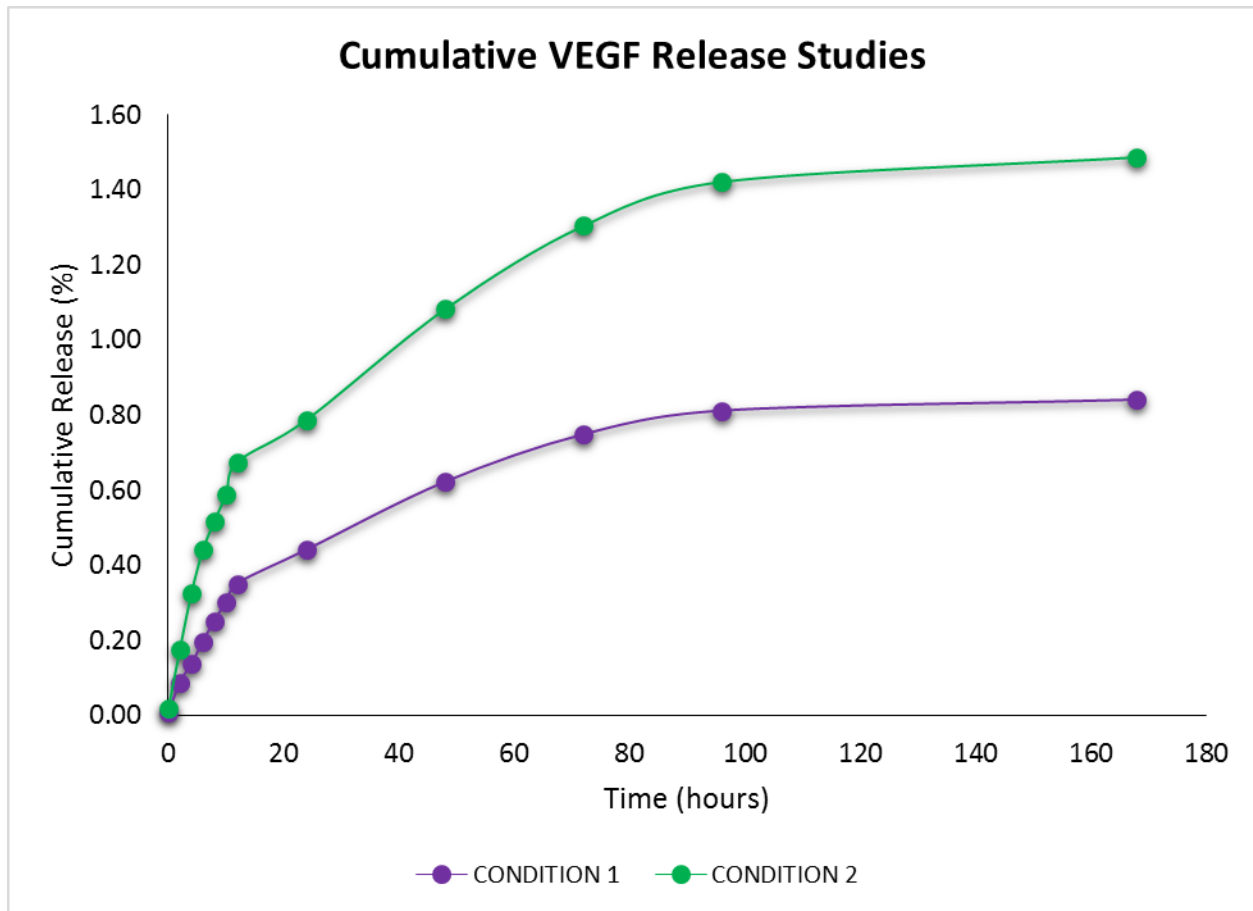
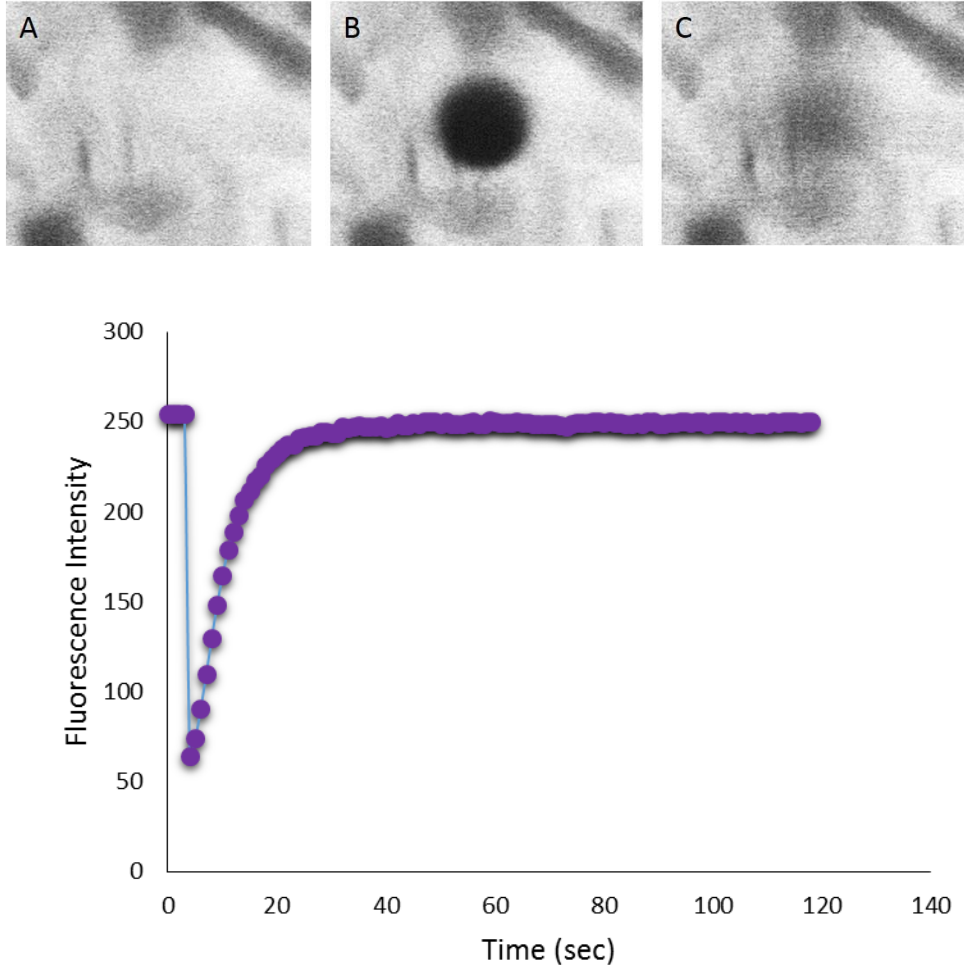


Figure 3.11: The cumulative release trend of the VEGF was confirmed by the release of VEGF from two different loading concentrations of condition 1, 500 ng/ml and condition 2, 100 ng/ml in the 1.4% gellan gum concentration of hydrogel over a period of seven days

3.3.7 Fluorescence Recovery After Photobleaching for Diffusion Coefficient

Fluorescence recovery after photobleaching was performed on the gellan gum at different concentrations by using FITC-conjugated Dextran of different molecular weights to get an idea of the property of diffusion of different model proteins within the hydrogel which are essential

for cell propagation, adhesion and differentiation. The diffusion coefficient, D was calculated from the $\tau_{1/2}$ and the radius of the region of interest.



D

Figure 3.12: Fluorescence recovery after photobleaching was used to get the values of D , diffusion coefficient of the different molecular weights of FITC-dextran in the gellan gum hydrogels to get an idea of the range of the sizes of proteins and cells to be housed in the hydrogels. A-C are the images corresponding to pre-FRAP (A), bleached region of interest (B), recovery or the post-FRAP image (C). The data of fluorescence intensity of pre-FRAP to the final recovery image is quantified in relation to the time taken for the recovery (D).

3.4 DISCUSSION

We have developed a gellan gum based hydrogel system in combination with the cations of the cell culture medium in volumes that are generally used in the *in vitro* cell culture models to give rise to a shear-thinning hydrogel model that can be adapted into an *in vitro* three-dimensional cell propagation system. The hydrogels are readily formed at various concentrations, both in water and in PBS. The advantage of making the gel model in water is to have them thermo-reversible and readily prone to the liquefaction by means of shear forces. These hydrogels can, in turn, interact with equal volumes of cation-rich cell culture medium and form reversible shear thinning hydrogels. The ability to control the gelation mechanics and physical properties are essential to enable cell encapsulation and potential therapeutic delivery model development.

Scanning electron microscopy images revealed the microporous and nanofibrillar structure of the gellan gum based hydrogels. This is an interesting observation to see the potential of the hydrogel to be used beyond the role of a generic scaffold for cell encapsulation. It mimics the complex extra cellular matrix of the tissues, which, apart from acting as a supporting backbone to the cells, also act as a reservoir for a multitude of growth factors and small molecules, all of which are stored in the polysaccharide pockets within the body to have a sustained release of the small molecules over a long period of time. Pores, both micro and macro, provide the necessary diffusivity to the scaffold. Irregular porosity makes the scaffold closer to the natural organization of the cells within the tissues. The microporosity plays an important role in the nutrient and oxygen transport to the cells.

A thorough rheological analysis was performed on the different hydrogel concentrations to get a range of biocompatible hydrogels which can be, later, used to study the interactions with different lineages of cells, each of which might respond differently to the different

microrheological environment. The LVR gives a working range of stress for the hydrogels. The gellan gum concentration from 0.9% (w/v) onward, readily formed gels at room temperature. At 37°C, gellan gum concentration of 1.1% was the starting point to show hydrogels at the physiological conditions. The gelation properties were also tested in combination with cell culture medium, which will be the potential application for the shear-thinning hydrogels that are being developed in the current study. The working range of concentrations up to 1.7% were practical to study for cell studies as the concentrations above 1.7% of hydrogel undergo gelation within the injecting source at room temperature and require higher shearing forces in order to undergo liquefaction. So, the concentration of 1.7% was considered as the upper limit for the rheological analysis. The oscillatory time sweep and oscillatory frequency sweep reveal that the gellan gum hydrogels formed in combination with the equal volume of cation-rich cell culture medium represent a range of 0.5-10 kPa of storage moduli and the values are still tunable depending on the increase or decrease of the interacting cations. The higher the cations, the higher the storage modulus of the gel.

The hydrogels, with and without cationic interaction, show the classic representation of a shear-thinning fluid model by showing a drop in the viscosity levels with an increase in the shear forces application. The zero-rate viscosity of the hydrogels increase with an increasing concentration of the gellan gum. Also, when the gels incubated with cells in cell culture medium were examined for their mechanical properties, the gels showed a gradual increase in the storage modulus over a course of seven days. This is potentially due to the interactions of the cells with the scaffold and the development of extra cellular matrix build up around the existing scaffold making it a stronger gel. It is interesting to note that the scaffold still remains shear-thinning despite the increase in G' . This is evident from the transient shear stress and recovery studies

performed for five cycles on the hydrogels which were incubated in cell culture up to seven days in incubation at 37°C.

The stability of hydrogels was determined by the water uptake and resulting weight change after incubation in physiological conditions for 21 days. It can be concluded from the 10% net weight change that the hydrogel is relatively stable without undergoing apparent physical changes under the incubation in cell culture medium and PBS. On the similar note, the gel does not undergo immediate drastic lysis in the presence of enzymatic concentrations of lysozyme in seven days. This is important for the potential *in vivo* studies for applications of the gellan gum based hydrogels for cell delivery or drug delivery applications.

The *in vitro* release studies of VEGF as quantified by ELISA show that the gellan gum hydrogel is an excellent storehouse of growth factors with a sustained release of around 1 ng per day, providing the cells with a growth factor- rich microenvironment. The release trends were similar for the two concentrations of gellan gum studied and the release showed an initial burst of release within the first 24 hours. The VEGF has been shown to interact electrostatically with the glycosaminoglycan based materials. This is highly favorable to make the hydrogel a pro-angiogenic biomaterial, which has profound applications in the regenerative medicine models and cancer research studies, which require, angiogenesis in the three-dimensional *in vitro* models.

3.5 CONCLUSIONS

In this study, we have prepared and characterized gellan-gum based hydrogels that are shear-thinning and showed that with their high rates of growth-factor entrapment and diffusivity of

molecules of different size ranges, they form excellent scaffolding materials for the adhesion and propagation of different cell types. The rheological analysis on the scaffolds have shown the shear thinning and recovery abilities of the hydrogel. These hydrogels will now be used for the applications in the development of a three-dimensional *in vitro* passaging model for the cells, providing a much closer microenvironment as the extracellular matrix of the natural tissues.

3.6 REFERENCES

1. Bajaj, P., et al., *3D biofabrication strategies for tissue engineering and regenerative medicine*. Annu Rev Biomed Eng, 2014. **16**: p. 247-76.
2. Lu, H.D., et al., *Secondary photocrosslinking of injectable shear-thinning dock-and-lock hydrogels*. Adv Healthc Mater, 2013. **2**(7): p. 1028-36.
3. Lozoya, O.A., et al., *Regulation of hepatic stem/progenitor phenotype by microenvironment stiffness in hydrogel models of the human liver stem cell niche*. Biomaterials, 2011. **32**(30): p. 7389-402.
4. Prokoph, S., et al., *Sustained delivery of SDF-1alpha from heparin-based hydrogels to attract circulating pro-angiogenic cells*. Biomaterials, 2012. **33**(19): p. 4792-800.
5. Zieris, A., et al., *FGF-2 and VEGF functionalization of starPEG-heparin hydrogels to modulate biomolecular and physical cues of angiogenesis*. Biomaterials, 2010. **31**(31): p. 7985-94.
6. Barbucci, R., G. Leone, and S. Lamponi, *Thixotropy property of hydrogels to evaluate the cell growing on the inside of the material bulk (Amber effect)*. J Biomed Mater Res B Appl Biomater, 2006. **76**(1): p. 33-40.

7. Pek, Y.S., et al., *A thixotropic nanocomposite gel for three-dimensional cell culture*. Nat Nanotechnol, 2008. **3**(11): p. 671-5.
8. Barbucci, R., et al., *A thixotropic hydrogel from chemically cross-linked guar gum: synthesis, characterization and rheological behaviour*. Carbohydr Res, 2008. **343**(18): p. 3058-65.
9. Bakota, E.L., et al., *Injectable multidomain peptide nanofiber hydrogel as a delivery agent for stem cell secretome*. Biomacromolecules, 2011. **12**(5): p. 1651-7.
10. Cross, D., et al., *Injectable Hybrid Hydrogels of Hyaluronic Acid Crosslinked by Well-Defined Synthetic Polycations: Preparation and Characterization In Vitro and In Vivo*. Macromol Biosci, 2015.
11. Guvendiren, M. and J.A. Burdick, *Engineering synthetic hydrogel microenvironments to instruct stem cells*. Curr Opin Biotechnol, 2013. **24**(5): p. 841-6.
12. Sato, M., T.Z. Wong, and R.D. Allen, *Rheological properties of living cytoplasm: endoplasm of Physarum plasmodium*. J Cell Biol, 1983. **97**(4): p. 1089-97.
13. Rainer, F. and V. Ribitsch, *[Viscoelastic properties of normal human synovia and their relation to biomechanics]*. Z Rheumatol, 1985. **44**(3): p. 114-9.
14. Zahm, J.M., et al., *Role of simulated repetitive coughing in mucus clearance*. Eur Respir J, 1991. **4**(3): p. 311-5.
15. Tiffany, J.M., *The viscosity of human tears*. Int Ophthalmol, 1991. **15**(6): p. 371-6.
16. Buchsbaum, G., et al., *Dynamics of an oscillating viscoelastic sphere: a model of the vitreous humor of the eye*. Biorheology, 1984. **21**(1-2): p. 285-96.
17. Jackson, G.W. and D.F. James, *The hydrodynamic resistance of hyaluronic acid and its contribution to tissue permeability*. Biorheology, 1982. **19**(1/2): p. 317-30.

18. Dutta, A. and J.M. Tarbell, *Influence of non-Newtonian behavior of blood on flow in an elastic artery model*. J Biomech Eng, 1996. **118**(1): p. 111-9.
19. Chwalek, K., et al., *Glycosaminoglycan-based hydrogels to modulate heterocellular communication in in vitro angiogenesis models*. Sci Rep, 2014. **4**: p. 4414.
20. Phull, M.K., et al., *Novel macro-microporous gelatin scaffold fabricated by particulate leaching for soft tissue reconstruction with adipose-derived stem cells*. J Mater Sci Mater Med, 2013. **24**(2): p. 461-7.
21. Prestwich, G.D., *Hyaluronic acid-based clinical biomaterials derived for cell and molecule delivery in regenerative medicine*. J Control Release, 2011. **155**(2): p. 193-9.
22. Chandrasekaran, R., *Cations, Water-Molecules and Gel-Forming Polysaccharides - 3-Dimensional Structures*. Biomedical and Biotechnological Advances in Industrial Polysaccharides, 1989: p. 423-434.
23. Oliveira, J.T., et al., *Gellan gum injectable hydrogels for cartilage tissue engineering applications: in vitro studies and preliminary in vivo evaluation*. Tissue Eng Part A, 2010. **16**(1): p. 343-53.
24. Silva-Correia, J., et al., *Rheological and mechanical properties of acellular and cell-laden methacrylated gellan gum hydrogels*. J Biomed Mater Res A, 2013. **101**(12): p. 3438-46.
25. Chandrasekaran, R., A. Radha, and V.G. Thailambal, *Roles of Potassium-Ions, Acetyl and L-Glycerol Groups in Native Gellan Double Helix - an X-Ray Study*. Carbohydrate Research, 1992. **224**: p. 1-17.
26. Chandrasekaran, R., *Interactions of Ordered Water and Cations in the Gel-Forming Polysaccharide Gellan Gum*. Water Relationships in Foods, 1991: p. 773-784.

27. Chandrasekaran, R., *Interactions of ordered water and cations in the gel-forming polysaccharide gellan gum*. Adv Exp Med Biol, 1991. **302**: p. 773-84.
28. Bacon, A., et al., *Carbohydrate biopolymers enhance antibody responses to mucosally delivered vaccine antigens*. Infect Immun, 2000. **68**(10): p. 5764-70.
29. Silva-Correia, J., et al., *Biocompatibility evaluation of ionic- and photo-crosslinked methacrylated gellan gum hydrogels: in vitro and in vivo study*. Adv Healthc Mater, 2013. **2**(4): p. 568-75.
30. Silva-Correia, J., et al., *Gellan gum-based hydrogels for intervertebral disc tissue-engineering applications*. J Tissue Eng Regen Med, 2011. **5**(6): p. e97-107.

4. APPLICATION OF GELLAN GUM-BASED SHEAR THINNING HYDROGELS FOR THREE-DIMENSIONAL CELL CULTURE

4.1 INTRODUCTION

Despite the advances in the fields of tissue engineering and regenerative medicine, the problem of increasing demand for organs and replacement tissue is yet to be solved [1]. The gap between the patients waiting for organs and those that actually get the replacement is widening by the day [2]. Mammalian tissue has cells growing in a complex, intricate scaffold of extracellular matrix which is not available to the current *in vitro* culture models. Therefore, the physiological behavior of the cells in *in vitro* models of cell culture is much different from their natural biochemical and mechanical response. Three-dimensional hydrogels are becoming a popular approach towards reducing this gap as a novel organ replacement technique [3-6]. Hydrogels hold promising potential as scaffolds for different biomedical applications such as regenerative medicine, drug discovery and biosensors [7-12]. They offer a microenvironment to the cells that provides physiological and biomechanical advantages of high water content, porosity and mechanical support [13]. Hydrogels have been used for tissue engineering applications for different tissue types such as brain, cartilage, bone and others [14-17].

Shear-thinning hydrogels add an interesting dimension to the biomimetic scaffolds by responding to the external stimuli along with being reversible in the properties retaining their original structure over a period of time or with the removal of external stimulus. Growth factors, drugs or cells can be mixed with the hydrogel before injection for the *in vivo* experiments. There are studies to develop shear-thinning hydrogels that resemble extracellular matrix in its chemical and mechanical properties, with their high permeability for metabolites, oxygen, nutrients and their ability to assist in intercellular chemical signaling [18, 19].

Polysaccharide based hydrogels are excellent candidates for biomedical applications, owing to the properties like higher polarity, varied chemical composition giving a stereological advantage, biocompatible and showing minimum to no cytotoxicity [13]. A major component of ECM is formed by chondroitin sulfate and hyaluoronan. Gellan gum (GG), a linear anionic extracellular bacterial polysaccharide hydrogel, has shown to be advantageous due to its gelation and rheological properties [16]. GG's excellent ability to form self-supporting structures combined with its resistance of unwanted dissolution due to ionic exchange proves beneficial for tissue engineering and long term cell culture in standard cell media[20]. Due to its ability to undergo easy gelation at even low concentrations, it is commonly used in food and pharmaceutical industry. It is easily dissolved in water when heated and forms a hydrogel on lowering of the temperature. I also has tunable gelation properties by modifying the concentration of gellan gum, and also, by mixing with varying concentrations of mono or divalent cations [21, 22]. Another advantageous characteristic is that it has structural similarities with the ECM [23]. Gellan gum forms thermoresponsive hydrogels with varying structural conformation at different temperatures and in combination with different ions [22]. It is formed at higher temperatures, when initially it is in the coil form. Upon the reduction of temperature moving towards room temperature, the random coils assemble themselves towards anti-parallel double helices, giving the gels great structural integrity at lower temperatures. The addition of cations further brings these double helices closer, rendering higher mechanical strength to the gels made in salt solutions or immersed in it [24]. One of the advantages of using gellan gum as a biomaterial for transplantation and regenerative medicine is that it does not elicit immune response since it is polysaccharide-based and the structure of polysaccharide does not depend on any genetic code [25-27]. GG also possesses mechanical similarity to the elastic moduli of common tissue,

making it a suitable scaffold for load-bearing applications [28-30]. GG has proven itself as a versatile encapsulating agent in numerous drug delivery systems for nasal, ocular, gastric and colonic applications, as implants for insulin delivery, and for wound healing applications due to its rapid gelation time near body temperature.

In our previous study, we have shown that gellan gum forms shear-thinning hydrogels at physiological conditions, both with, and without cell culture medium. The shear-thinning ability of the gels was retained even after an extended culture period with cells in the hydrogel. The gels are highly porous and show growth-factor retaining ability and excellent diffusivity, making it an ideal biomimetic model to develop a three-dimensional *in vitro* propagation model. In this study, we show the application of the shear-thinning GG hydrogels to show adhesion and propagation of cells from different lineages, including human pluripotent stem cells. We also look at the effect of gel stiffness on the cell morphology to identify the optimum growth conditions of the cells in the GG hydrogels. Also, to add further similarities to the physiological conditions, we added a source of polypeptides to the hydrogel in the form of silk fibroin. Silk fibroin provides peptide sequences that are essential to promote cell adhesion due to the higher RGD sequences and potentially improves cell viability. The addition of the SF polypeptide to the polysaccharide hydrogels provides with a well-rounded scaffold which is closer to the natural ECM conditions.

4.2 MATERIALS AND METHODS

4.2.1 Materials

Feeder-layer-free human induced pluripotent stem (hiPS) cell line derived from foreskin fibroblasts were obtained from WiCell (WiCell Research Institute – WB0002). Human neural stem cells (hNSCs) were obtained from Millipore (Billerica, MA). Growth Factor Reduced

Matrigel, was from BD Biosciences. ReNcell Neural Stem Cell Medium was from Millipore. mTeSR1 medium (mTeSR1 Basal Medium with mTeSR1 5X supplement) was from Stem Cell Technologies. Human brain microvascular endothelial cells were obtained from ScienCell Research Laboratories. Human endothelial cell medium was supplemented with 5% fetal bovine serum (FBS) and 1% Pencillin-Streptomycin and 1% endothelial cell growth supplement (ECGS) (ScienCell™). Murine β cell line, β TC-3 cell line was obtained from American *Type Culture* Collection (ATCC) and expanded in DMEM/High glucose with 4,500mg/L Glucose, 4.0mM L-Glutamine and 110mg/L Sodium Pyruvate and supplemented with 10% FBS (Life Technologies). Lithium bromide was purchased from Sigma-Aldrich. Snakeskin Dialysis Tubing was from Thermo Scientific, USA, MWCO 3,500. Dulbecco's Modified Eagle Medium culture medium, glucose, glutamine, penicillin/streptomycin, fetal bovine serum, AlexaFluor 488/546 phalloidin, para formaldehyde, AlamarBlue, Live-Dead assay and 4',6-Diamidino-2-Phenylindole are purchased from Life Technologies, USA. Vascular Endothelial Growth Factor-A was from R&D systems.

4.2.2 Cell culture

Human neural stem cells (hNSCs) were obtained from Millipore (Billerica, MA). The stem cell is an immortalized human neural progenitor cell line derived from the ventral mesencephalon region of human fetal brain and immortalized by retroviral transduction with the v-myc oncogene. Matrigel- coated culture plates (Growth Factor Reduced Matrigel, BD Biosciences) were used for hNSCs seeding. hNSCs were maintained in ReNcell Neural Stem Cell Medium (Millipore) with FGF-2 (20 ng/mL) and EGF (20 ng/mL). The cells were passaged using accutase.

Feeder-layer-free human induced pluripotent stem (hiPS) cell line derived from foreskin fibroblasts (WiCell Research Institute – WB0002) were expanded in accordance with supplier recommended protocols. Briefly, hiPSCs were grown on matrigel- coated culture plates (Growth Factor Reduced Matrigel, BD Biosciences) and expanded in chemically defined mTeSR1 medium (mTeSR1 Basal Medium with mTeSR1 5X supplement; Stem Cell Technologies). ROCK inhibitor (10 μ M) was added to the maintenance medium. Human brain microvascular endothelial cells were obtained from ScienCell Research Laboratories and expanded in human endothelial cell medium supplemented with 5% fetal bovine serum (FBS) and 1% Penicillin-Streptomycin and 1% endothelial cell growth supplement (ECGS) (ScienCell™). They were expanded by enzymatic passaging using 0.05% trypsin-EDTA.

Murine β cell line, β TC-3 cell line was obtained from American *Type Culture* Collection (ATCC) and expanded in DMEM/High glucose with 4,500mg/L Glucose, 4.0mM L-Glutamine and 110mg/L Sodium Pyruvate and supplemented with 10% FBS. These were expanded by enzymatic passaging in 0.25% trypsin-EDTA.

For the three-dimensional cell culture in the hydrogel, the hydrogel equilibrated at 37 °C was mixed with an equal volume of cell suspension by means of pipetting and added onto the bottom of the cell culture dish without exceeding the general thickness of 1-2 mm. Cell culture medium was added on the surface of the hydrogel as per the volume requirements of the cell culture dish being used. The medium change was performed with the frequency dependent on the cell type.

All the cells were incubated at 37 °C under 5% CO₂.

4.2.3 Silk fibroin extraction

Bombyx mori cocoons were heated in an aqueous solution of 0.02 M NaHCO₃ (1% w/v) at 90 °C for 60 minutes. Degummed fiber was recovered and washed with boiling water to remove the sericin that coats SF. The SF fiber was dried overnight in an oven at 40 °C. Dried silk fibroin fiber was dissolved in 9.3 M aqueous LiBr solution (10% w/v) at 65 °C for four hours. The solution was cooled to 25 °C and then dialyzed (Snakeskin Dialysis Tubing, Thermo Scientific, USA, MWCO 3,500) against distilled water for three days (2.5% v/v), with periodic water replacement. The concentration of aqueous silk fibroin solution was measured by determining the dry weight of SF after evaporating the water at 80 °C from one gram of sample. A final concentration of 0.08% was used all over the study.

4.2.4 Cell viability

After the generation of spheroids and their subsequent suspension culture, the viability of cells within the spheroids was examined using LIVE/DEAD Viability Kit, which is a two color fluorescent assay based on differential permeability of live and dead cells and allows preservation of the distinctive staining pattern for a couple of hours post fixation using 4% glutaraldehyde. Live cells were stained with green fluorescent SYTO 10; and dead cells with compromised cell membranes were stained with red fluorescent ethidium homodimer-2. The Olympus IX81 laser scanning confocal microscope was used to capture the images of the LIVE/DEAD cell staining patterns at the excitation wavelengths of roughly 488 and 595 nm.

4.2.5 Cellular actin cytoskeleton organization

Morphological change of the cells was inspected by immunostaining of actin. The cells were fixed with 4% paraformaldehyde for 30 minutes, permeabilized with 0.5% Triton X-100, and stained with Alexa Fluor-546 or 488 phalloidin (Molecular Probes, Eugene, OR) for 30 minutes followed by nuclei staining with 1 $\mu\text{g}/\text{mL}$ DAPI for 30 minutes. The cells were imaged using an Olympus IX81 laser scanning confocal microscope.

4.2.6 Rheological characterization of hydrogels

For rheological study, hydrogel solutions of Phytigel™ with cells growing in them were subjected to oscillatory shear rheometry on a daily basis to investigate the effects of cell growth and medium on the storage modulus of the hydrogels. A DHR3 rheometer (TA Instruments Inc.) with standard geometry of 8 mm diameter was used for the rheological characterization of all hydrogels samples. The test methods employed were oscillatory time sweep, frequency sweep and stress sweep. The time sweep was performed to monitor the *in situ* gelation of the hydrogel solutions at 37 °C. The test, which was operated at constant frequency (1 Hz) and strain (5%) and terminated after 600 seconds, recorded the temporal evolution of shear storage modulus (G') and the shear loss modulus (G''). The stress sweep was set up by holding the temperature 37 °C and constant frequency (1 Hz) while increasing the stress level from 1 to 10 Pa. The applied range of 1-10 Pa was found to be safe-for-use from a prior experiment where we determined the linear viscoelastic region (LVR) profiles of the hydrogels by shearing them until structure breakdown. We also subjected hydrogels to a frequency sweep at 50% of their respective ultimate stress levels. At this fixed shear stress and temperature (37 °C), the oscillatory frequency was increased from 0.1 to 100 Hz and the G' was recorded.

4.2.7 Statistical analysis

Data are shown as mean \pm S.D. Statistical analyses were performed using one way ANOVA (analysis of variance) followed by the paired t-test where appropriate. A probability (p) value of <0.05 was considered statistically significant.

4.3 RESULTS AND DISCUSSION

In this study, we demonstrate using human induced pluripotent cells, human neural stem cells, human endothelial cells and mouse beta cells, that cells from all three germ layers and pluripotent cells can be successfully cultivated three-dimensionally in different concentrations of gellan-gum based hydrogels. Different concentrations were analyzed before selecting a range of gellan gum concentrations suitable for cell studies, based on the temperature of gelation, time required for gelation, storage modulus at 37°C, and ability to be injected or extruded at room temperature. This work has been described and discussed in the previous chapter. Within the selected range of concentrations, we have chosen the lower limit, mid-range and the upper limit to show the effect of mechanical properties in the form of storage modulus of the gel on the cell survival, proliferation and morphology and further, assembly of the cells into organoid-like structures. Additionally, silk fibroin was chosen to add the complexity of polypeptide-based microarchitecture to the gellan gum hydrogel, in order to simulate the combination of polypeptide and polysaccharide based ECM of the tissues. Silk fibroin (SF) from *Bombyx mori* silkworm cocoons has been a widely investigated natural polymer for biomedical applications.

4.3.1 General cell culture model and material characterization with cells

The cell culture model in this study is described schematically in Figure 4.1. We are proposing a three dimensional shear-thinning hydrogel to be used as the scaffold for the cell studies, following which, it can undergo mechanical stress in the form of centrifugal forces to get the cells separated to be passaged further. The silk fibroin extraction protocol is described in Figure 4.2.

The three concentrations of hydrogels will be represented by using the initial concentration of gellan gum used to make the hydrogel before mixing it with equal volumes of cell culture medium.

To understand the change in the mechanical properties of the hydrogel with the cell growth, oscillatory frequency sweep was performed on the 1.4% GG with β TC-3 cells growing them. With the time points of day 0, 1, 2, 3, 4, and 7, the hydrogels showed an increase in their storage modulus, G' , denoting an increase in the hydrogel stiffness with an increase in the duration of the cell culture (Figure 4.3). There is a larger increase in the first 24 hours due to the added crosslinking as a result of the incubation in the cell culture medium. The rest of the intervals had an increase but it was around 1kPa per day. Mostly, the increase in gel stiffness is observed though the equilibrium crosslinking is attained in the first 24 hours is due to the potential extra cellular matrix generation by the cells.

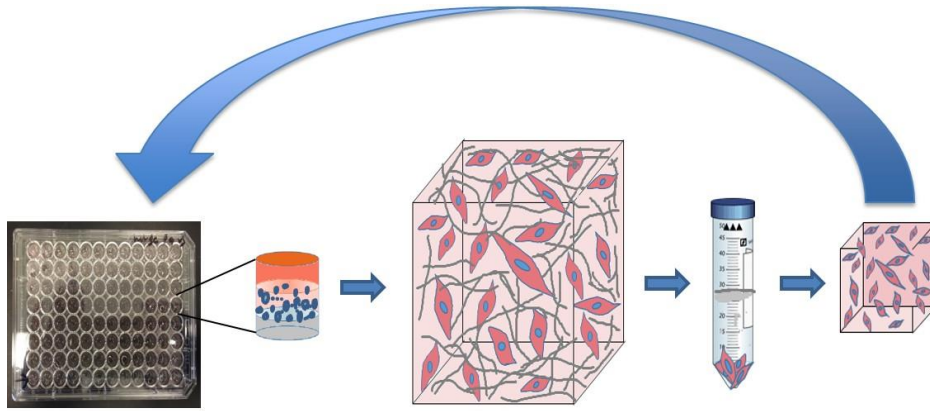


Figure 4.1: Schematic for the development of the *in-vitro* gellan-gum based three-dimensional cell propagation model

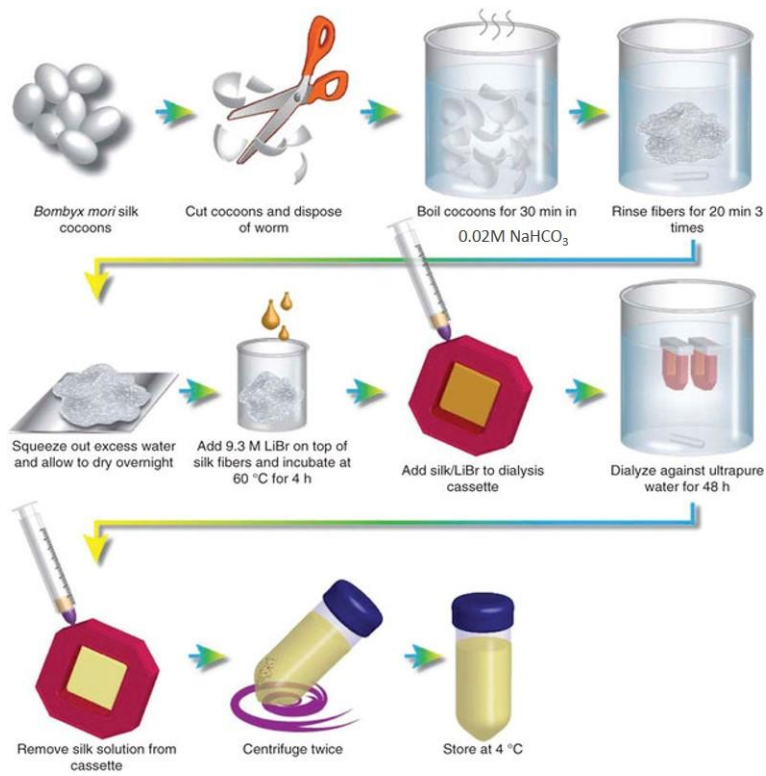


Figure 4.2: Schematic for the silk fibroin extraction from silk worm cocoons[31]

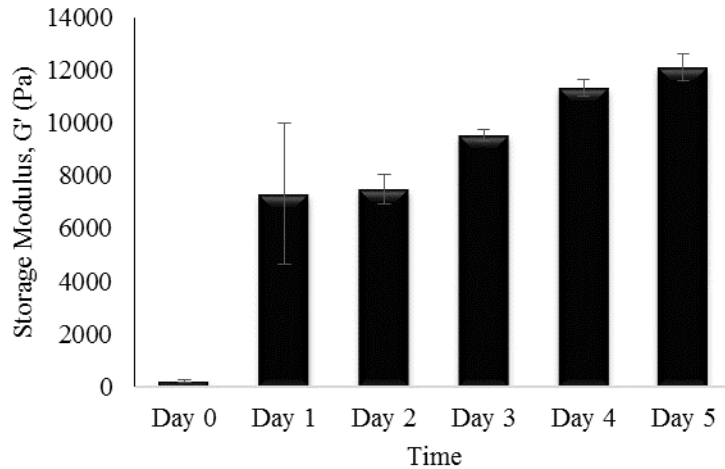


Figure 4.3: The rheological analysis showed a gradual increase in the storage modulus of the hydrogels with the β TC-3 cells being cultured in them for a time period of 7 days (Mean \pm Std. Dev.)

Scanning electron microscopy confirms the presence of extracellular matrix build-up by the cells with the passage of time (Figure 4.4). In the previous chapter, we had seen the micro and macro porosity of the hydrogels and in this figure, we have observed the saturated pores of the hydrogel which have cell growth and the residual ECM around the scaffold. This is important in changing the mechanical properties of the hydrogel. The phase contrast images for the four cell types were taken to show the cell assembly towards three dimensional features for all the cell types (Figure 4.5).

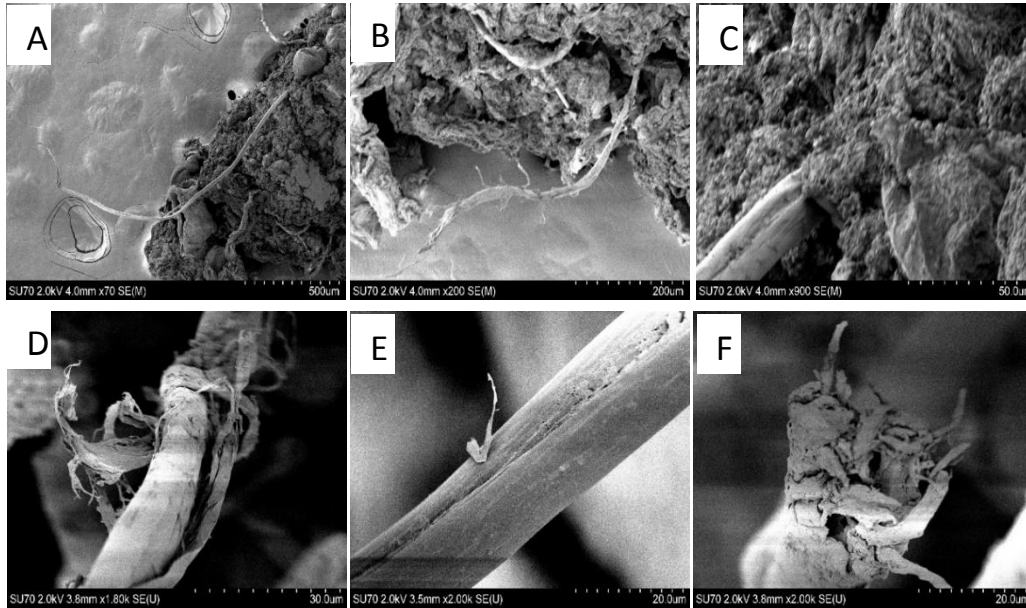


Figure 4.4: Scanning electron microscopic images of the supercritical dried hydrogel samples with day 5 human endothelial cells, the images show various magnifications of the scaffold and potential extracellular matrix generated by the cells within the scaffold

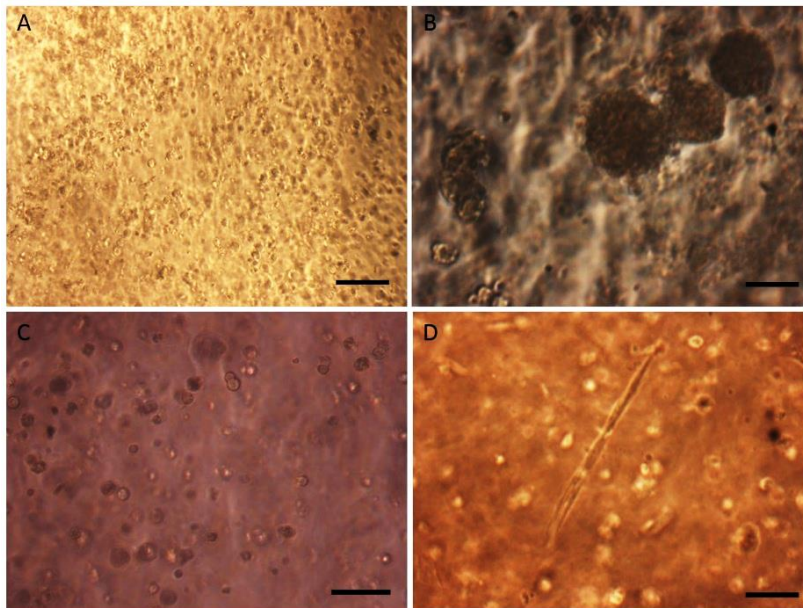


Figure 4.5: Phase contrast microscopic images of the three-dimensional culture of the different cell types in the gellan-gum hydrogels with A. hiPSC B. hNSCs C. β TC-3 D. hECs (Scale bar: 100 μ m)

4.3.2 β TC-3 cell culture

For the β TC-3 culture, the effect of gel's stiffness was examined by seeding the cells at same seeding density in 1.1%, 1.4% and 1.7% gellan gum. In the lower stiffness hydrogel, the cells formed small clusters (Figure 4.6 A-C). The number and size of the clusters formed is lower than those seen in the 1.4% gellan gum hydrogel. In the hydrogel with the highest stiffness amongst those that were examined, the cells did not multiply beyond the single cell seeding, nor did they show any assembly into the cluster-like structures. The gel stiffness plays a role in the cell proliferation as well as potential migration towards each other to develop the cluster-like structures.

The next study was to investigate the effect of silk fibroin in the development of cluster-like structures and cell proliferation (Figure 4.6). In this, we have observed that for both 1.1% and 1.4%, the size and number of the cluster-like structures is much higher for the hydrogel with 0.08% SF than for those without any silk fibroin. Also, an important point to note is the 1.7% hydrogel did not show any difference in the cell morphology or the number with or without silk fibroin. This is because of the higher gel stiffness which is not a favorable environment for the cell proliferation or migration. A closer look at the individual islet structure as seen using a 40X objective showed the well-organized cell structure (Figure 4.7).

The optimal seeding density was identified by seeding different cell numbers to the hydrogels and identifying the condition that allowed for a higher proliferation rate. Cell proliferation rate

was observed by using AlamarBlue™ dye to calculate the percent reduction of the dye from day 0 to day 4 and the cell number was correlated with the difference in the reduction in the dye (Figure 4.8). From this experiment, it was concluded that the hydrogel allowed for β TC-3 cell proliferation. The cell viability within the hydrogel was confirmed via Live-Dead assay (Figure 4.9).

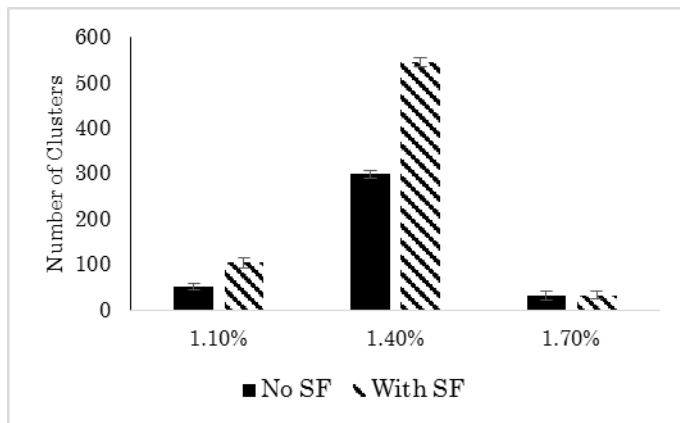
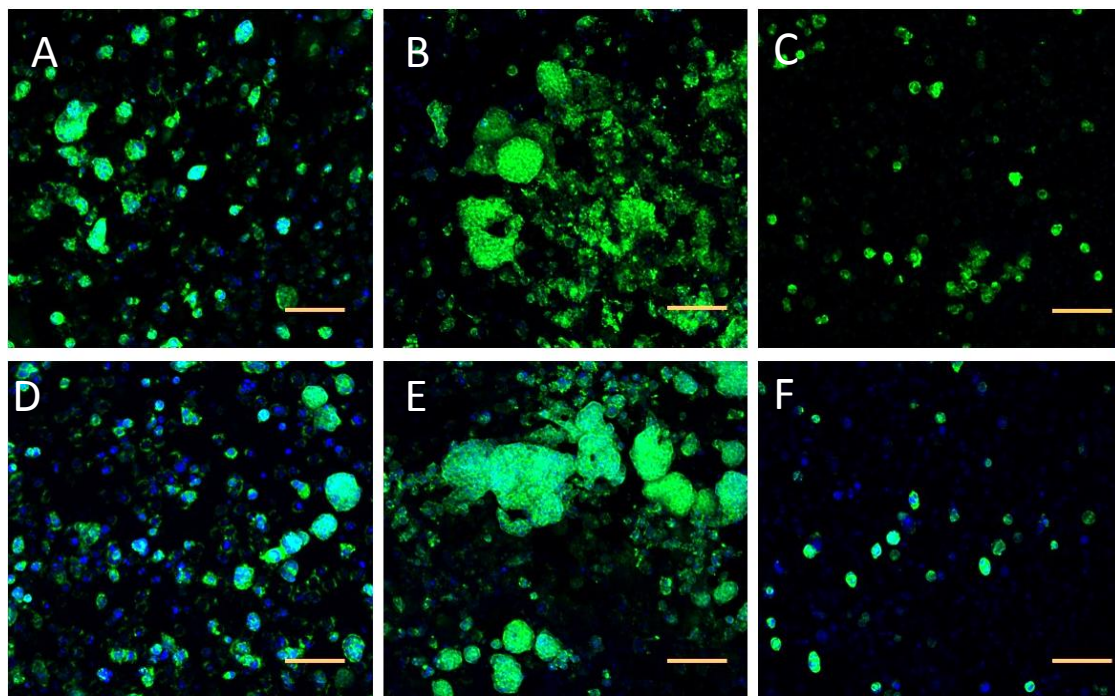


Figure 4.6: The effect of gel stiffness and cell seeding density were observed for the β TC3 cells seeded at 500k/100 μ l seeding density. Conditions: Hydrogels without Silk Fibroin (A-C), with Silk Fibroin (D-F), initial gellan gum concentrations of gellan gum, 1.1% (A, D), 1.4% (B, E), 1.7% (C, F) (Scale bar: 100 μ m) The numbers are quantified based on the number of clusters with size larger than 50 μ m diameter per unit area pf image (n=3)

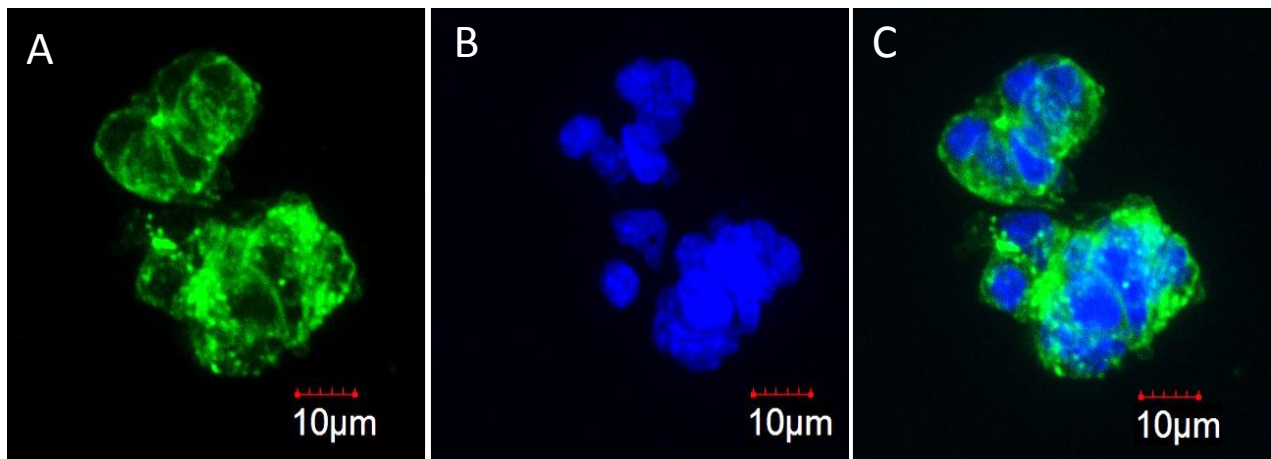


Figure 4.7: The individual islet-like structures seen at close using a 40X objective with AlexaFluor 488 staining for Actin and DAPI for cell nuclei (Scale bar: 10 μ m)

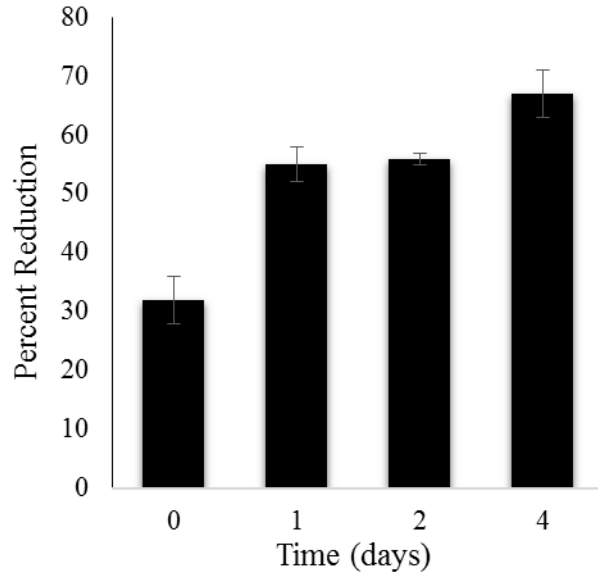


Figure 4.8: Cell proliferation was observed for a time period of four days by using AlamarBlue™ to correlate the percent reduction of the dye as the cell number per time point (Mean ± Std. Dev.)

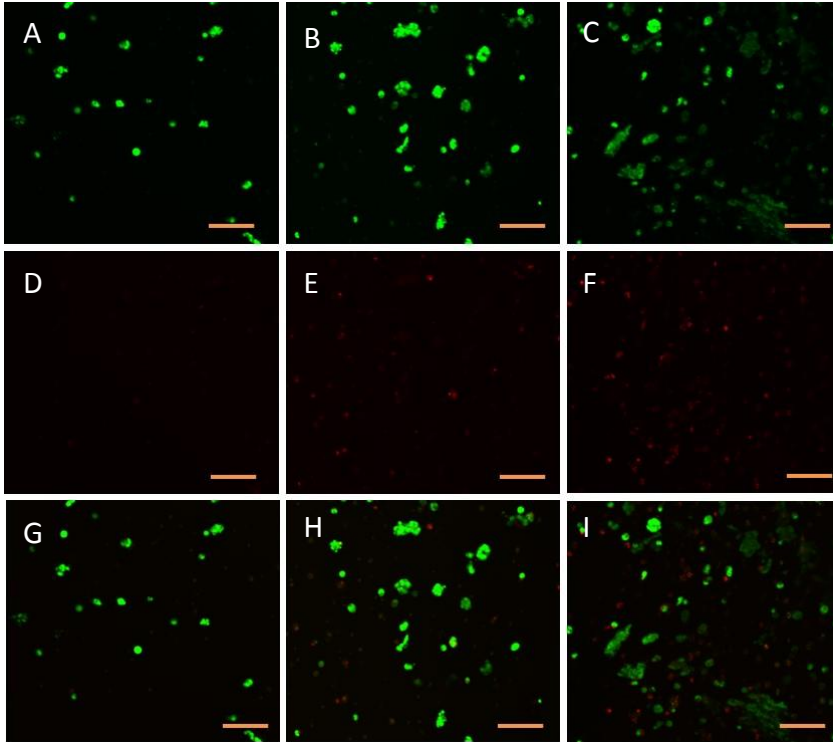


Figure 4.9: Cell viability assay was used to conclude that the hydrogel showed negligible number of dead cells at the cell seeding densities of 50k (A, D, G), 100k (B, E, H) and 500k (C, F, I) per 100 μl with the viable live cells seen A-C; dead cells seen in D-F; Merge (G-I) (Scale bar: 100 μm)

4.3.3 Human Endothelial Cell Culture

Angiogenesis is the outgrowth of blood vessels and plays an important role in tissue engineering and regenerative medicine. In this study, *de-novo* assembly of human endothelial cells (hECs) to form blood vessel-like structures has been observed. Multiple factors play important roles in this process. In our experiments, the role of cell seeding density, hydrogel concentration, effect of silk fibroin and the role of the growth factors like vascular endothelial growth factor- A (VEGF) have been investigated.

Out of the three hydrogel concentrations being studied, we have observed that the 1.1% with 0.08% silk fibroin has been favorable for the hEC proliferation (Figure 4.10). Also in the same experiment, it is observed that the lower cell seeding densities are favorable for the assembly of the hECs into the tubular vessel-like structure (Figure 4.10A). The assembly is due to the cell growth, proliferation and migration as the regions around the vessel-like structure do not have as many cells in them as the other conditions. Also, the actin morphology reveals the well-organized tubular vessel like structure that spans the three axes of the hydrogel (Figure 4.11). The cross-section of the tubular assembly, performed by using the software of the Olympus IX81 confocal microscope confirmed that the tubular structure included a well-formed lumen, mostly made up of single cells, as seen with the DAPI staining of the nuclei and is not a structure made up of cell clumping (Figure 4.12).

The role of VEGF in the cell proliferation and angiogenesis was investigated in two ways: one by supplementing the hydrogels with the VEGF by means of the cell culture medium which was changed, once in two days. The second method was by mixing it directly into the hydrogel during the cell seeding into the scaffold. In the first method, prominent and larger vessel-like assembly was noticed in comparison to the hydrogel without the VEGF (Figure 4.13). The cell number around the tubular assembly was less, and it can be hypothesized that there was a potential cell migration towards the assembly of the tubular vessel. In the second method, the VEGF mixed in the hydrogel directly promoted cell proliferation along with cell assembly towards tubular structures (Figure 4.14). This data is in line with the growth factor release studies performed in the previous chapter, where in, it was observed that the hydrogel showed extraordinary capability of retaining the loaded growth factor releasing it at the rate of 1 ng/day.

The cell data confirms that the hydrogel retains the VEGF in a way that does not alter the bioavailability of the VEGF.

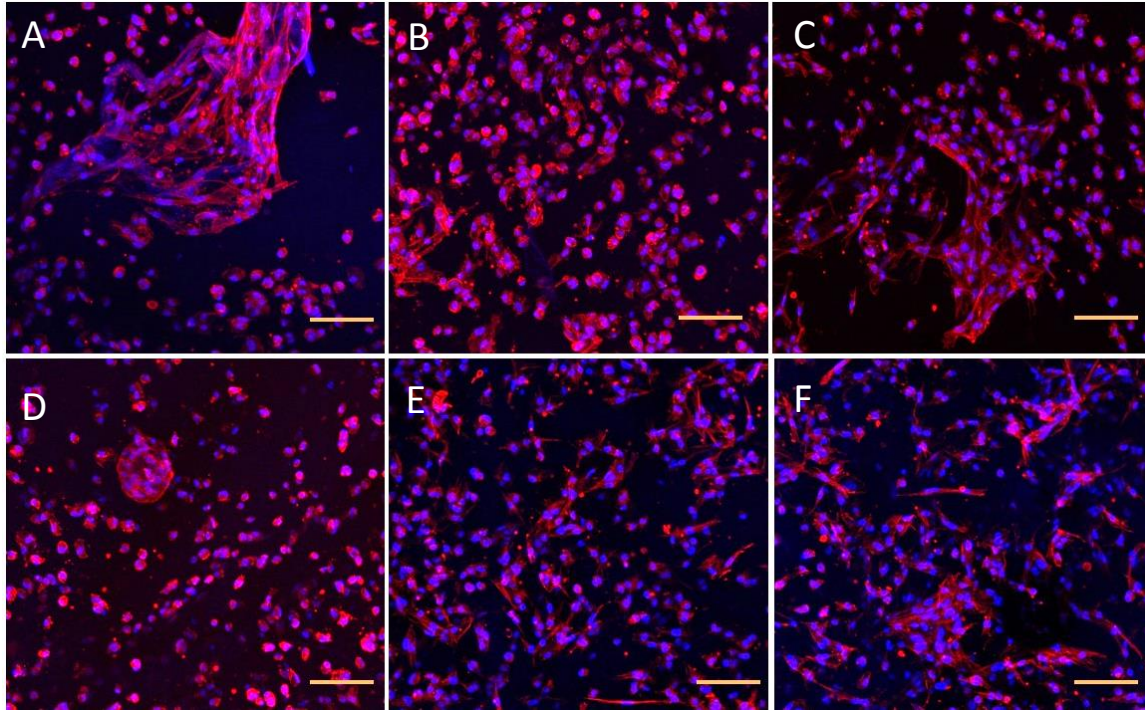


Figure 4.10: The effect of cell seeding density is observed by staining for actin using AlexaFluor 546 and DAPI for cell nuclei for two different hydrogels with initial gellan gum concentration of 1.1% (A-C) and 1.4% (D-F). The cell seeding densities were 125k/100 μ l (A,D); 500k/ μ l (B,E); 1000k/100 μ l (C,F) (Scale bar: 100 μ m)

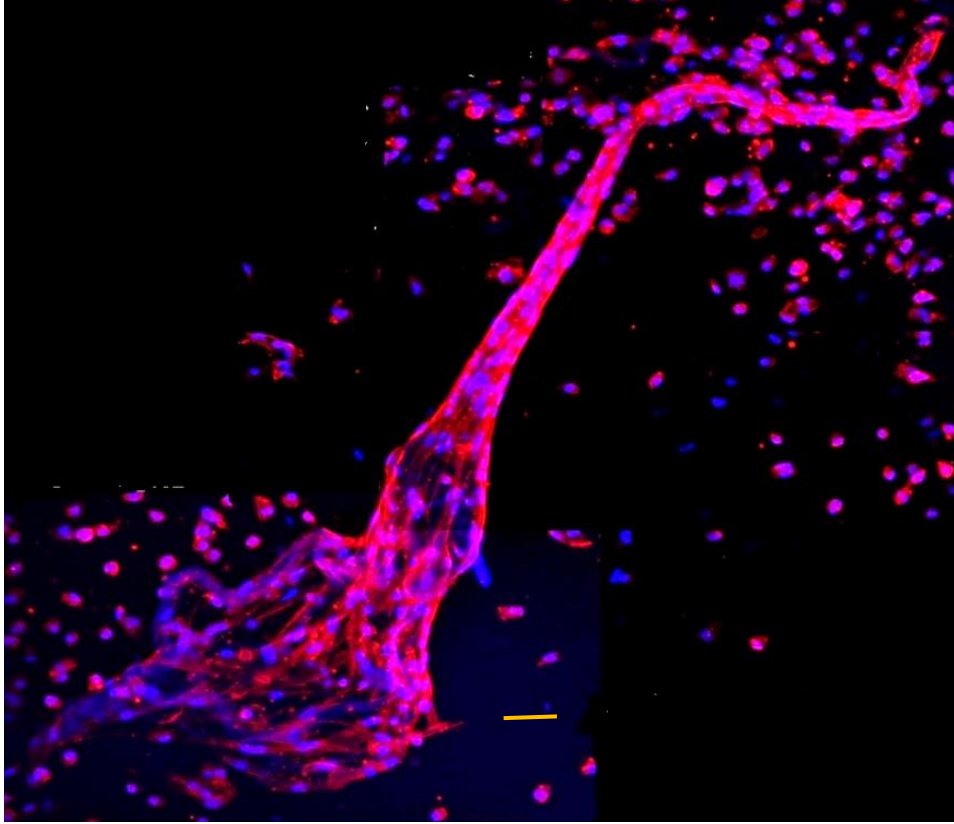


Figure 4.11: The actin morphology of the cells shows the tubular assembly of the cells within the 1.1% initial concentration of gellan gum and silk fibroin added hydrogel (Scale bar: 100 μm)

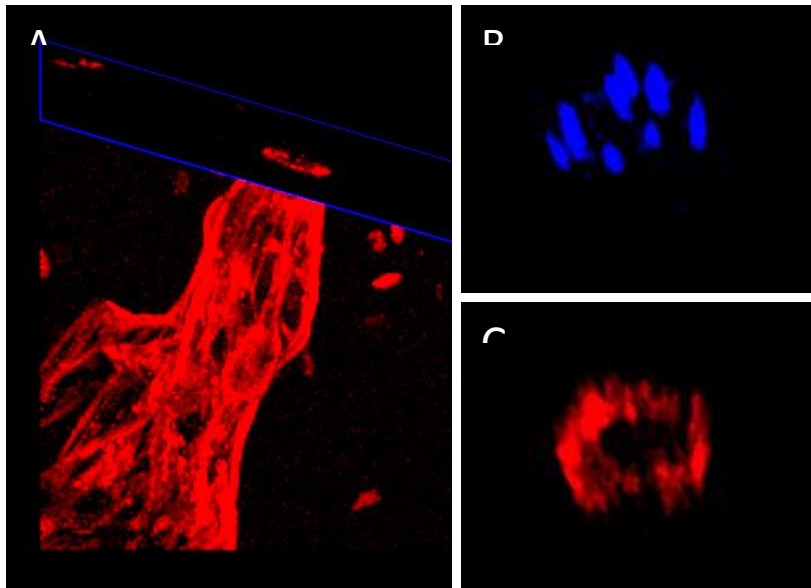


Figure 4.12: Orthogonal sectioning confirmed the hollow tubular structure of the formed vessel-like cell assembly with A. The cross section of the tubular structure, B. DAPI, C. AlexaFluor 546 Phalloidin

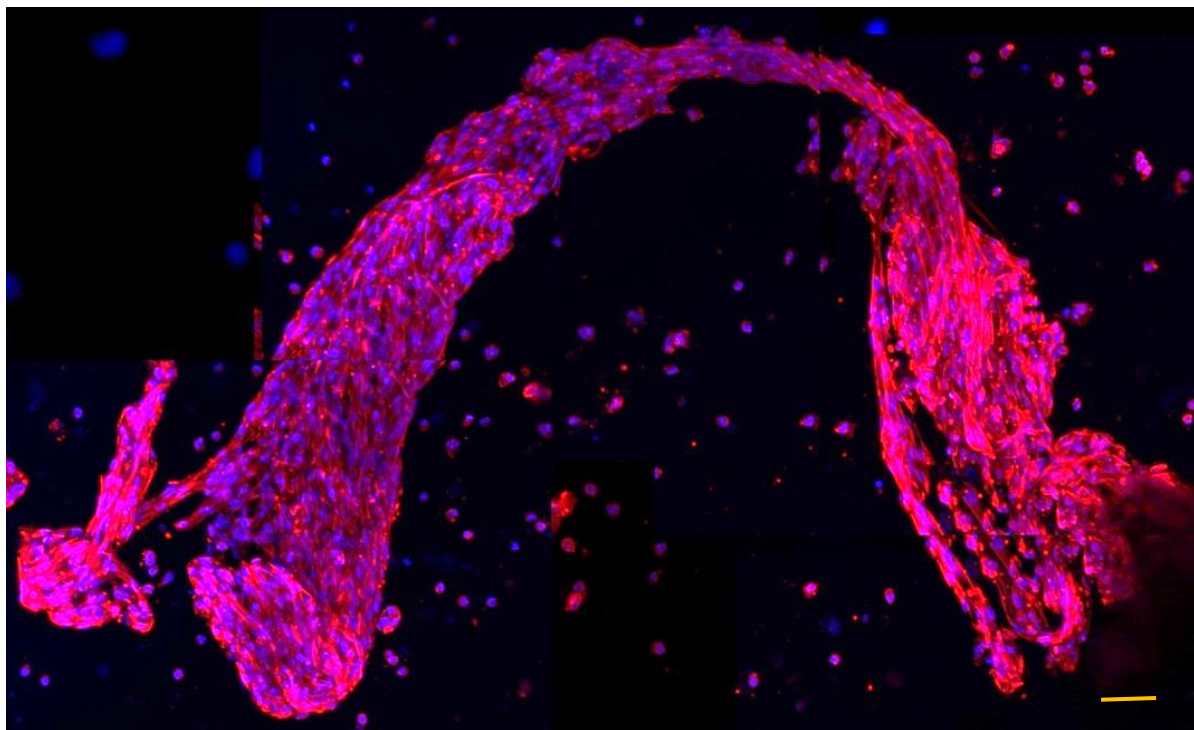


Figure 4.13: The tubular assembly was further enhanced with the addition of VEGF to the cell culture medium in which the hydrogel was incubated (Scale bar: 100 μ m)

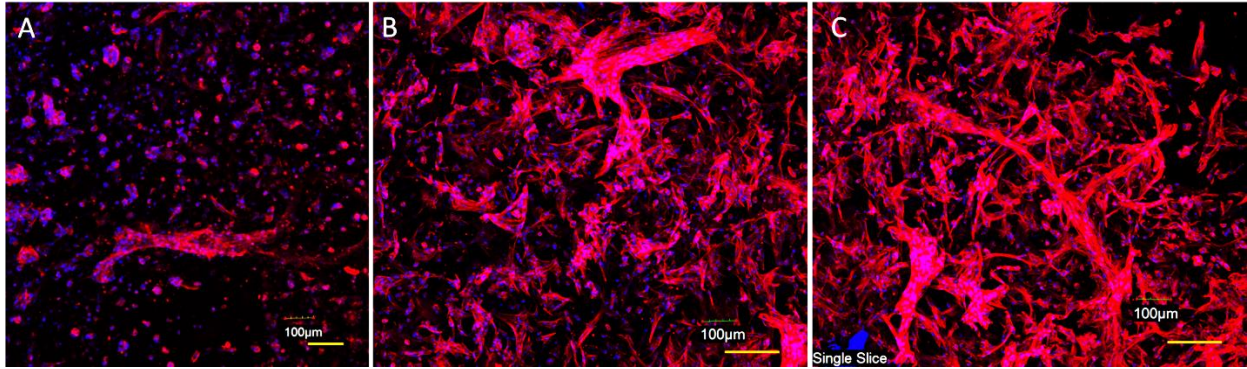


Figure 4.14: The role of VEGF in the cell adhesion and proliferation is proven with the incorporation of VEGF in the hydrogel directly. A. hECs growing in the hydrogel with no VEGF and B, C. Hydrogel with VEGF added to the hydrogel directly to get a final concentration of 100 ng/ml. (Scale bar: 100 μ m)

4.3.4 Human induced pluripotent stem cells

The cell viability of the hiPSCs in the gellan gum was confirmed via Live-Dead assay in the different hydrogel concentrations and also, the role of silk fibroin to improve the cell viability was observed by the same assay (Figure 4.15). From this assay, it was observed that silk fibroin did not have a favorable effect on the cell viability as evident from the number of dead cells in the conditions with the silk fibroin added to the hydrogel (Figure 4.15H). Also, the gellan gum concentration of the 1.4% showed the higher cell number and a higher green-red cell staining ratio (Figure 4.15G).

The actin morphology was difficult to observe due to the smaller cell size of the hiPSC which are in the single cell suspension (Figure 4.16).

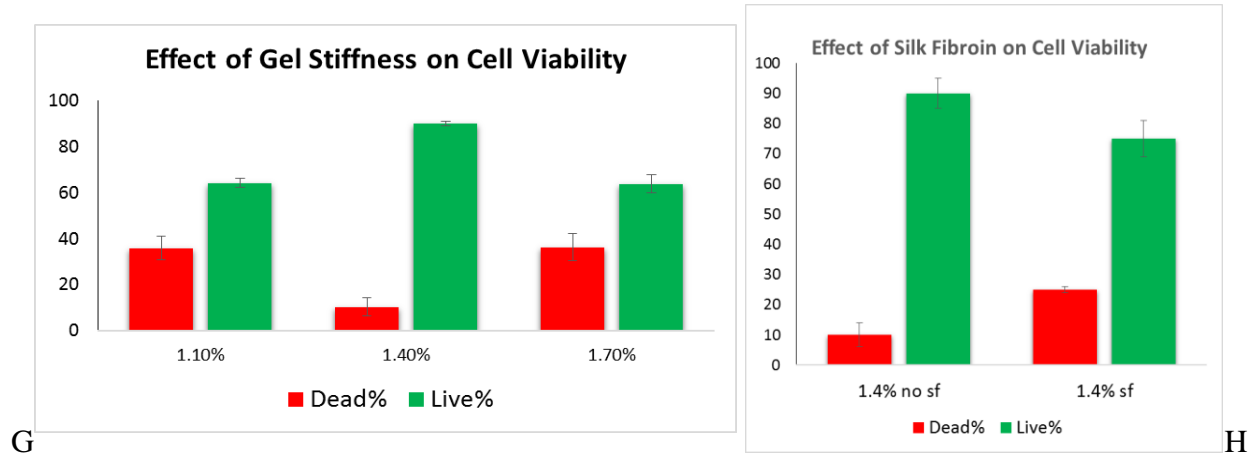
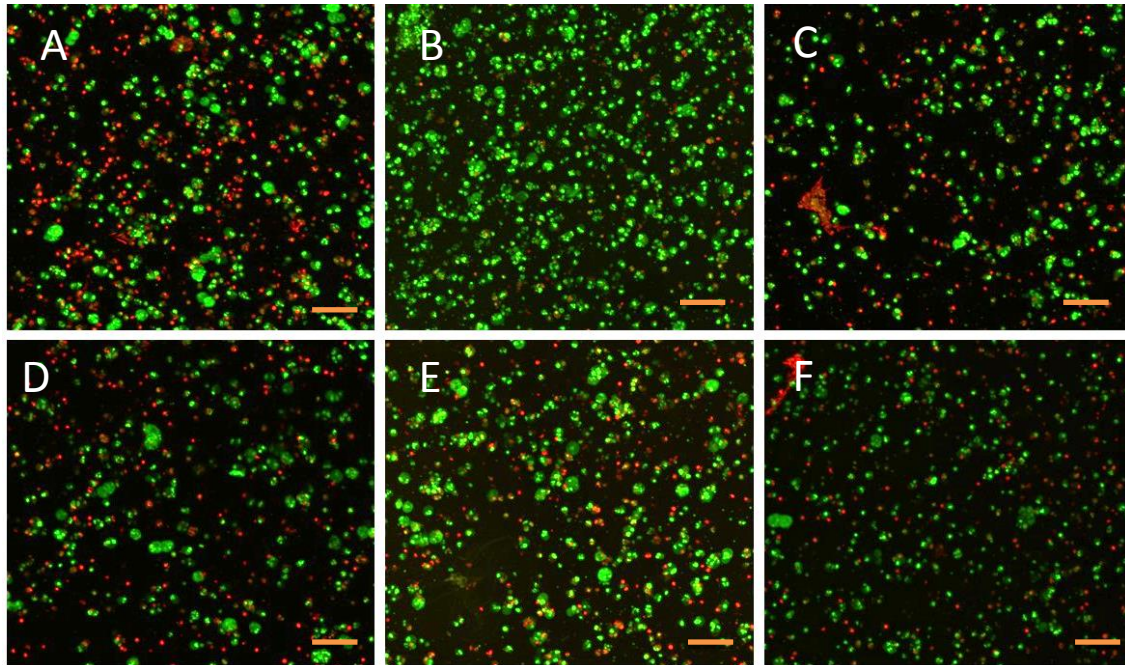


Figure 4.15: Live-Dead assay was performed to identify the hydrogel concentration favorable to the hiPSC survival. Also the effect silk fibroin was observed in the different hydrogel stiffness as well. Conditions without silk fibroin (A-C), conditions with silk fibroin (D-F). The starting concentration of gellan gum used is 1.1% (A, D), 1.4% (B, E) and 1.7%

(C, F) (Scale bar: 100 μm) G. The live and dead cell count is quantified per unit area of the image (n=3) and the live to dead cell ratio is the highest for the gellan gum concentration 1.4% at 9:1. H. The addition of silk fibroin was observed to be unfavorable for the cell viability with the reduction in the live to dead cell ratio.

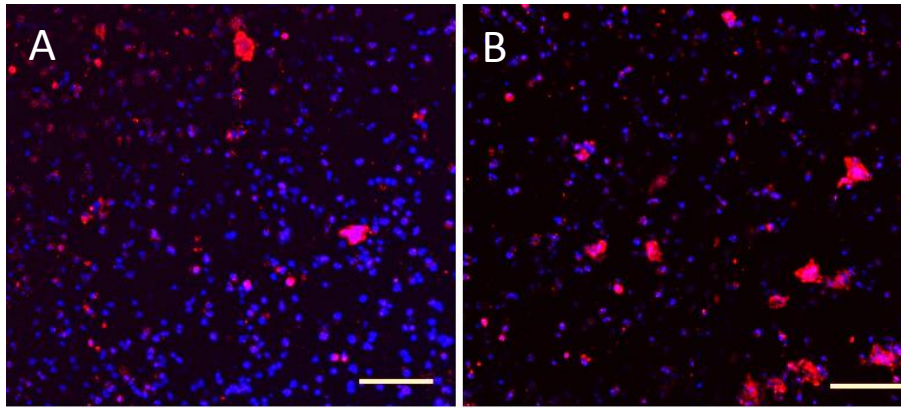


Figure 4.16: The cell morphology of the hiPSCs was observed by staining for actin and DAPI for nuclei in two different cell seeding densities, A. 50k cells/100 μl and B. 100k cells/100 μl (Scale bar: 100 μm)

4.3.5 Human neural stem cells

Human neural stem cells (hNSC) were cultured in the hydrogels of different stiffness, in different seeding densities, with and without silk fibroin and studies over different time points for up to ten days to determine the favorable conditions for the cell adhesion, proliferation and assembly towards neurospheres. The effect of seeding densities (Figure 4.17) showed that the higher seeding density promoted the assembly into spheroids. A closer look at the human neurosphere can be seen in Figure 4.18 with the well-defined cell assembly. The moderate hydrogel stiffness of the 1.4% gellan gum concentration was observed to be favorable to allow

the cell proliferation in comparison to the 1.1% and 1.7% (Figure 4.19). Silk fibroin does not show prominent effect on cell morphology, assembly or proliferation (Figure 4.20). The human neurosphere development was observed from day 5 (Figure 4.21). The neurospheres showed nestin protein expression which confirmed the stemness of the neurospheres formed (Figure 4.22).

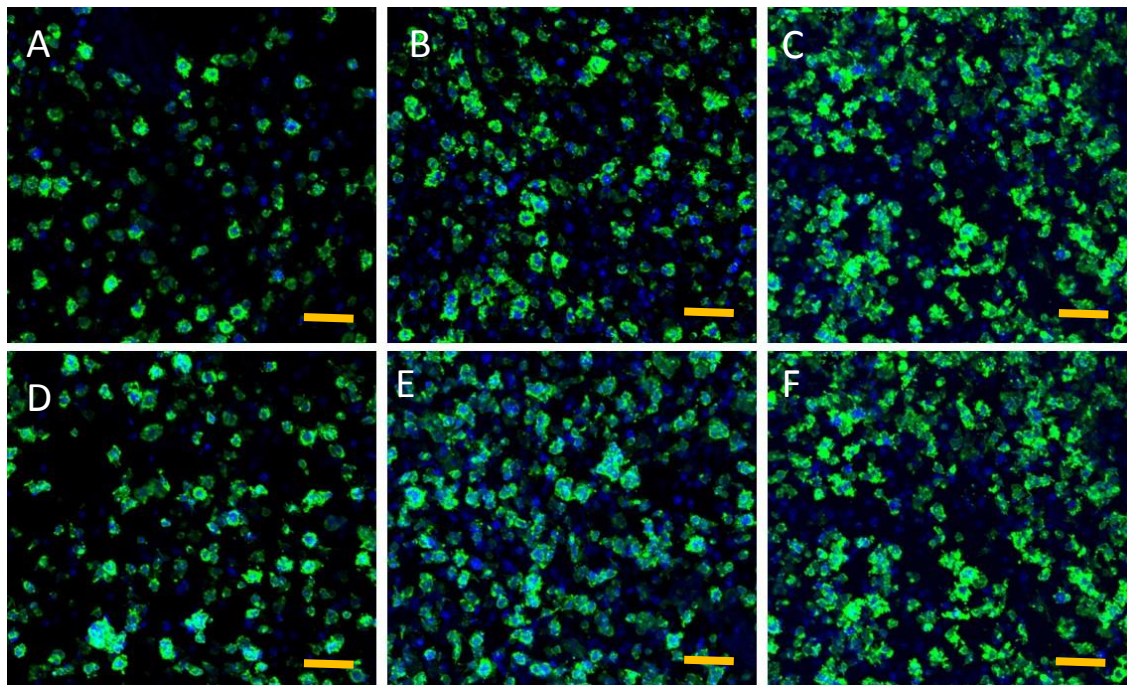


Figure 4.17: The effect of cell seeding density is observed by staining for actin using AlexaFluor 488 and DAPI for cell nuclei for two different hydrogels with initial gellan gum concentration of 1.1% (A-C) and 1.4% (D-F). The cell seeding densities were 125k/100 μ l (A,D); 500k/ μ l (B,E); 1000k/100 μ l (C,F) (Scale bar: 100 μ m)

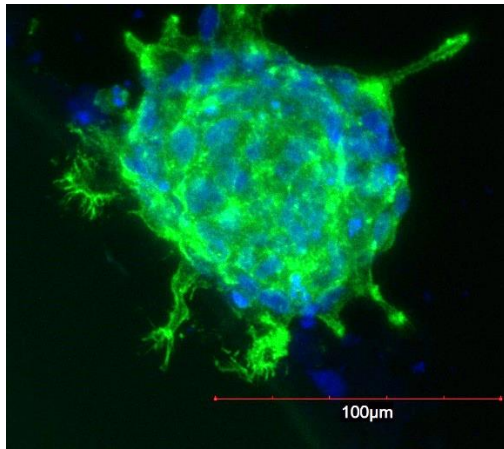


Figure 4.18: A closer look at the human neurosphere as seen using a 40X objective

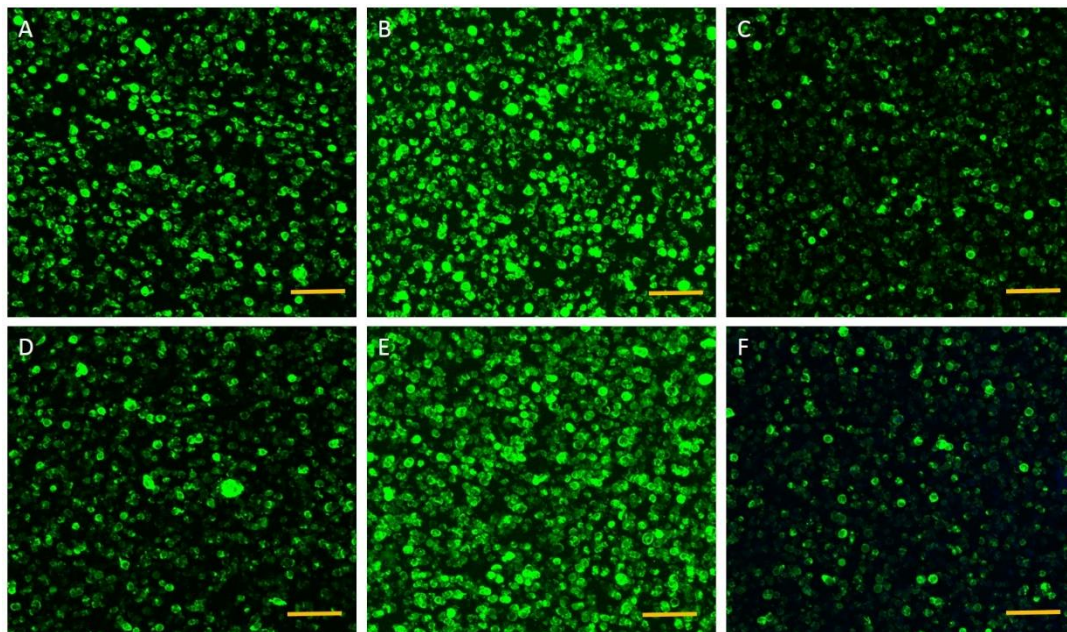


Figure 4.19: The effect of gel stiffness and cell seeding density were observed for the hNSCs seeded at 200k/100 μ l (A-C), 500k/100 μ l (D-F) seeding density, initial gellan gum concentrations of gellan gum, 1.1% (A, D), 1.4% (B, E), 1.7% (C, F) (Scale bar: 100 μ m)

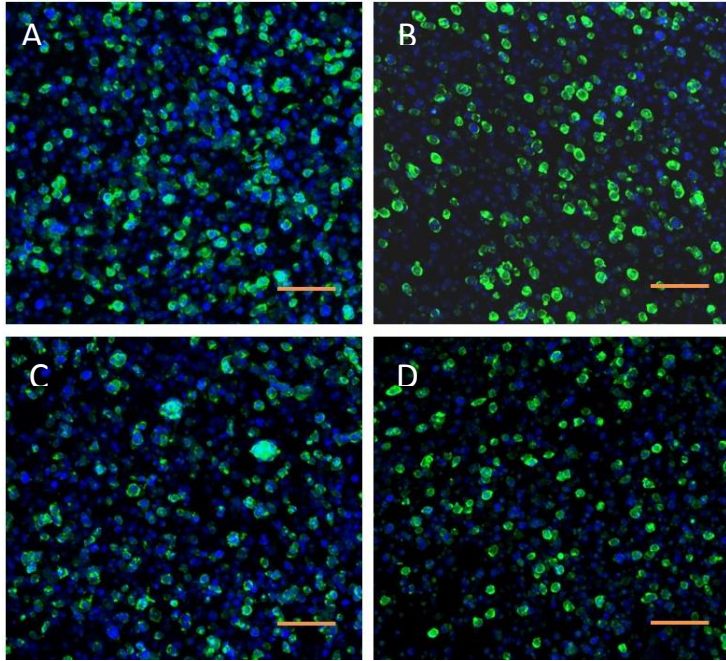


Figure 4.20: The effect of adding silk fibroin to the hNSCs was observed in 1.4% (A, C) and 1.7% (B, D) was observed with the conditions A, B without silk fibroin and B, D with silk fibroin added (Scale bar: 100 μm)

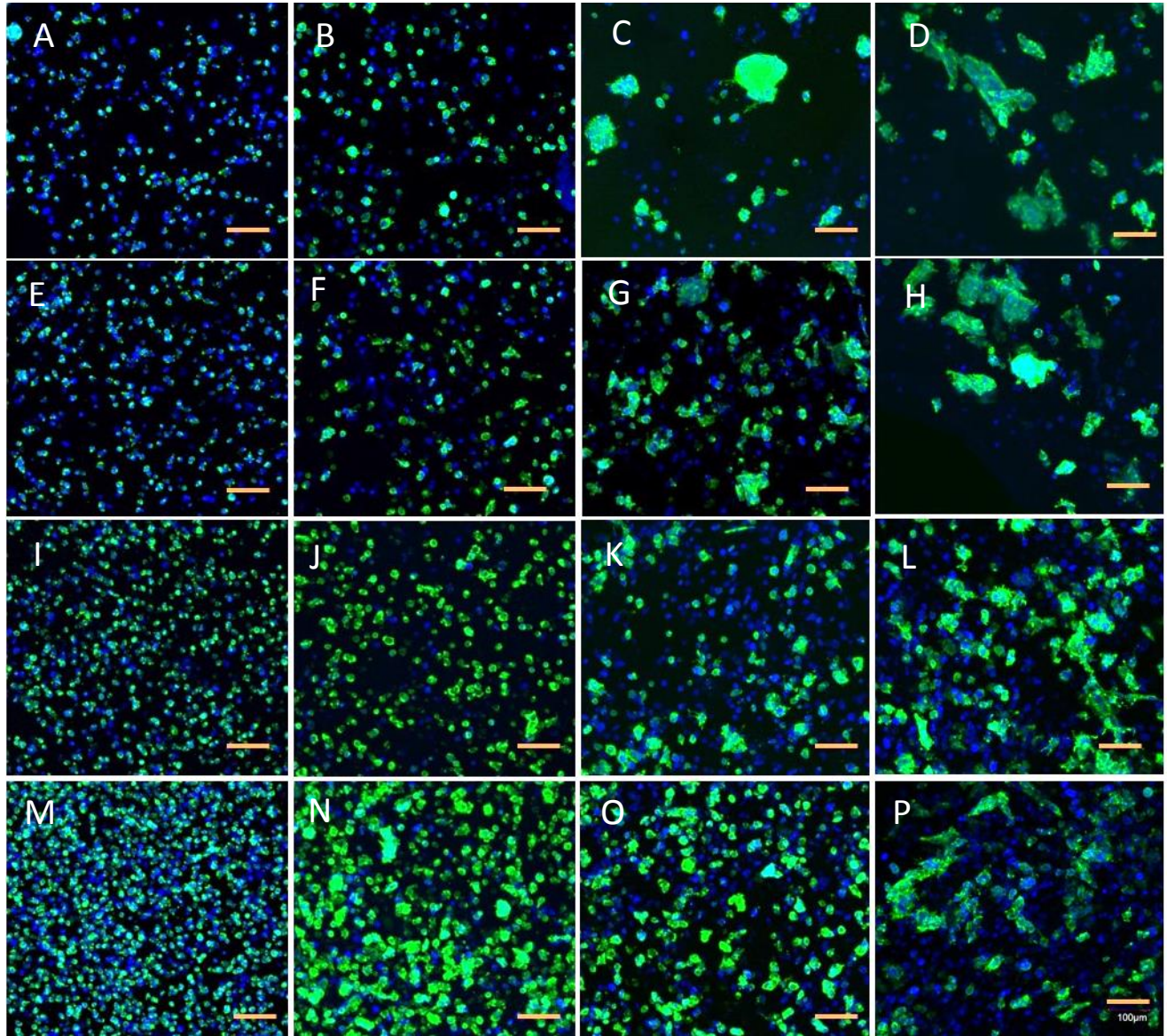


Figure 4.21: An extensive study on the effect of cell seeding density was performed on hNSCs with cell morphology observed by AlexaFluor 488 staining for actin and DAPI for cell nuclei during different time points: day 1 (A, E, I, M), day 3 (B, F, J, N), day 5 (C, G, K, O), day 10 (D, H, L, P) with cell densities being 125k (A-D), 250k (E-H), 500k (I-L), 1000k (M-P) per 100µl (Scale bar: 100 µm)

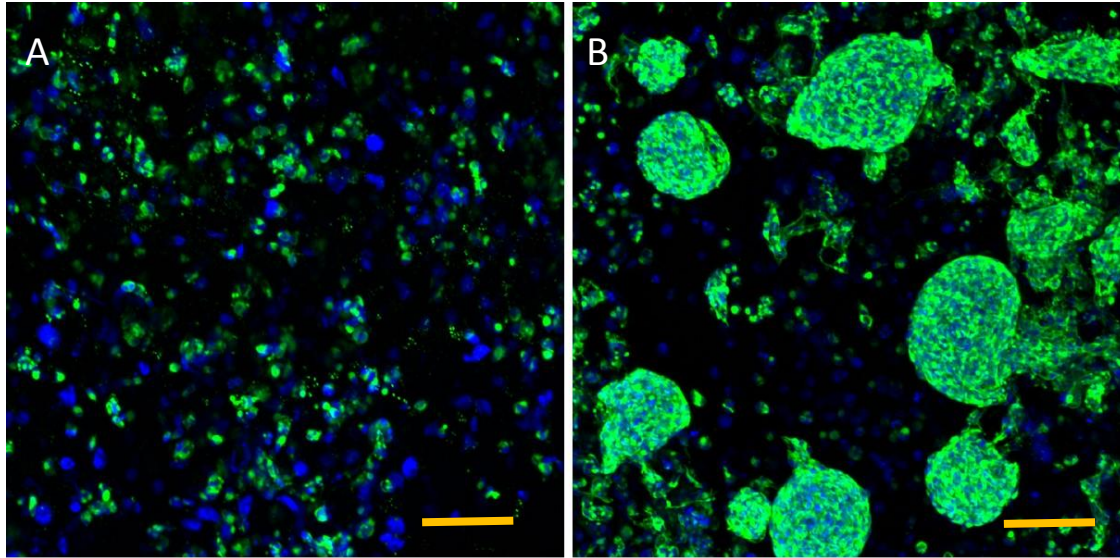


Figure 4.22: Nestin marker expression was observed to confirm the stemness of the hNSCs seeded in the 1.4% initial concentration of gellan gum hydrogels for two different seeding densities of 250k (A) and 500k (B) per 100 µl with silk fibroin (Scale bar: 100 µm)

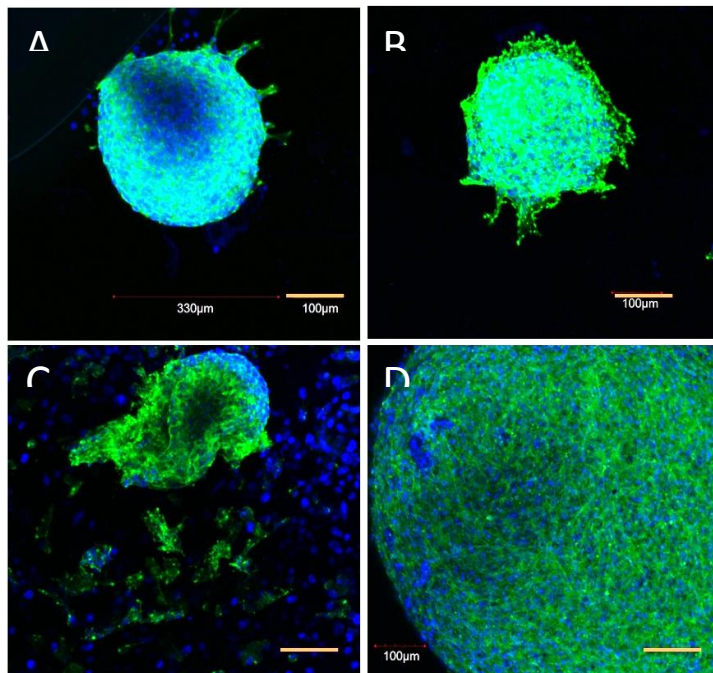


Figure 4.23: A closer look at the spheroid structures formed within the 1.4% gellan gum hydrogels with different initial seeding densities 250k (A, B) and 500k (C, D) per 100 μ l (Scale bar: 100 μ m)

4.4 CONCLUSIONS

In this study, the ability of the gellan gum based shear-thinning hydrogels to allow for cell adhesion, proliferation, and viability was tested with four different cell types, human induced pluripotent stem cells, human neural stem cells, primary cell line of human endothelial cells and the mouse insulinoma line for the pancreatic β -cells. In all the cell types investigated, it was observed that the cells could successfully assemble into organoid structures, i.e. hollow tubules for the hECs, neurospheres for the hNSCs and islet-like structures for the β -cells. The cell viability of the human induced pluripotent stem cells can be considered as the indicator for the biocompatibility of the material to majority of the cell types, as the hIPSCs are counted amongst the difficult cells to propagate on novel substrates. In the future studies, the hydrogels with the cells are used for the further development into the organoids to be used for tissue engineering and regenerative medicine applications.

4.5 REFERENCES

1. Lei, Y. and D.V. Schaffer, *A fully defined and scalable 3D culture system for human pluripotent stem cell expansion and differentiation*. Proc Natl Acad Sci U S A, 2013. **110**(52): p. E5039-48.
2. Atala, A., *Advances in tissue and organ replacement*. Curr Stem Cell Res Ther, 2008. **3**(1): p. 21-31.

3. Lu, H.D., et al., *Secondary photocrosslinking of injectable shear-thinning dock-and-lock hydrogels*. Adv Healthc Mater, 2013. **2**(7): p. 1028-36.
4. Lozoya, O.A., et al., *Regulation of hepatic stem/progenitor phenotype by microenvironment stiffness in hydrogel models of the human liver stem cell niche*. Biomaterials, 2011. **32**(30): p. 7389-402.
5. Lee, J., M.J. Cuddihy, and N.A. Kotov, *Three-dimensional cell culture matrices: state of the art*. Tissue Eng Part B Rev, 2008. **14**(1): p. 61-86.
6. Pampaloni, F., E.G. Reynaud, and E.H. Stelzer, *The third dimension bridges the gap between cell culture and live tissue*. Nat Rev Mol Cell Biol, 2007. **8**(10): p. 839-45.
7. Harris, M.G. and L.G. Mock, *The effect of saline solutions of various compositions on hydrogel lens dimensions*. Am J Optom Physiol Opt, 1974. **51**(7): p. 457-64.
8. Kolthammer, J., *The in vitro adsorption of drugs from horse serum onto carbon coated with an acrylic hydrogel*. J Pharm Pharmacol, 1975. **27**(11): p. 801-5.
9. Krohn, D.L. and J.M. Breidfeller, *Quantitation of pilocarpine delivery across isolated rabbit cornea by noncross-linked high viscosity polymer gel*. Invest Ophthalmol, 1976. **15**(4): p. 324-7.
10. Chepurov, A.K., et al., *[Thromboresistant properties of hydrophilic gels]*. Polim Med, 1980. **10**(3): p. 121-33.
11. Quinn, C.A., R.E. Connor, and A. Heller, *Biocompatible, glucose-permeable hydrogel for in situ coating of implantable biosensors*. Biomaterials, 1997. **18**(24): p. 1665-70.
12. Leaper, D.J., et al., *Experimental infection and hydrogel dressings*. J Hosp Infect, 1984. **5 Suppl A**: p. 69-73.

13. Chwalek, K., et al., *Glycosaminoglycan-based hydrogels to modulate heterocellular communication in in vitro angiogenesis models*. Sci Rep, 2014. **4**: p. 4414.
14. Li, X., et al., *Engineering in situ cross-linkable and neurocompatible hydrogels*. J Neurotrauma, 2014. **31**(16): p. 1431-8.
15. Pan, Y.S., G.X. Ding, and J. Wang, [*Research on repair strategies for articular cartilage defects*]. Zhongguo Gu Shang, 2013. **26**(2): p. 175-8.
16. Prestwich, G.D., *Hyaluronic acid-based clinical biomaterials derived for cell and molecule delivery in regenerative medicine*. J Control Release, 2011. **155**(2): p. 193-9.
17. Li, X., et al., *Engineering an in situ crosslinkable hydrogel for enhanced remyelination*. FASEB J, 2013. **27**(3): p. 1127-36.
18. Yan, C., et al., *Injectable solid hydrogel: mechanism of shear-thinning and immediate recovery of injectable beta-hairpin peptide hydrogels*. Soft Matter, 2010. **6**(20): p. 5143-5156.
19. Rodell, C.B., A.L. Kaminski, and J.A. Burdick, *Rational design of network properties in guest-host assembled and shear-thinning hyaluronic acid hydrogels*. Biomacromolecules, 2013. **14**(11): p. 4125-34.
20. Smith, A.M., et al., *An initial evaluation of gellan gum as a material for tissue engineering applications*. J Biomater Appl, 2007. **22**(3): p. 241-54.
21. Ferris, C.J., et al., *Modified gellan gum hydrogels for tissue engineering applications*. Soft Matter. **9**(14): p. 3705-3711.
22. Oliveira, J.T., et al., *Gellan gum injectable hydrogels for cartilage tissue engineering applications: in vitro studies and preliminary in vivo evaluation*. Tissue Eng Part A, 2010. **16**(1): p. 343-53.

23. Chandrasekaran, R., *Cations, Water-Molecules and Gel-Forming Polysaccharides - 3-Dimensional Structures*. Biomedical and Biotechnological Advances in Industrial Polysaccharides, 1989: p. 423-434.
24. Silva-Correia, J., et al., *Rheological and mechanical properties of acellular and cell-laden methacrylated gellan gum hydrogels*. J Biomed Mater Res A, 2013. **101**(12): p. 3438-46.
25. Chandrasekaran, R., A. Radha, and V.G. Thailambal, *Roles of Potassium-Ions, Acetyl and L-Glyceryl Groups in Native Gellan Double Helix - an X-Ray Study*. Carbohydrate Research, 1992. **224**: p. 1-17.
26. Chandrasekaran, R., *Interactions of Ordered Water and Cations in the Gel-Forming Polysaccharide Gellan Gum*. Water Relationships in Foods, 1991: p. 773-784.
27. Chandrasekaran, R., *Interactions of ordered water and cations in the gel-forming polysaccharide gellan gum*. Adv Exp Med Biol, 1991. **302**: p. 773-84.
28. Bacon, A., et al., *Carbohydrate biopolymers enhance antibody responses to mucosally delivered vaccine antigens*. Infect Immun, 2000. **68**(10): p. 5764-70.
29. Silva-Correia, J., et al., *Biocompatibility evaluation of ionic- and photo-crosslinked methacrylated gellan gum hydrogels: in vitro and in vivo study*. Adv Healthc Mater, 2013. **2**(4): p. 568-75.
30. Silva-Correia, J., et al., *Gellan gum-based hydrogels for intervertebral disc tissue-engineering applications*. J Tissue Eng Regen Med, 2011. **5**(6): p. e97-107.
31. Rockwood, D.N., et al., *Materials fabrication from Bombyx mori silk fibroin*. Nat Protoc, 2011. **6**(10): p. 1612-31.

5. GELLAN GUM-BASED SHEAR-THINNING HYDROGELS AS SUBSTRATES IN SCALABLE ROBOTIC FABRICATION OF IDENTICAL CELL SPHEROIDS FOR TISSUE ENGINEERING

5.1 INTRODUCTION

The conventional methods incorporated as a part of *in vitro* studies generally use two-dimensional cell culture methods, which do not mirror the natural environment of the tissues[1]. In the quest for the best *in vitro* model that mimics the unique three- dimensionality of the cells, researchers are thinking beyond the scope of the generic tissue culture models[2, 3]. The complex three-dimensional microenvironment of the natural tissue involves cell-cell interactions along with the extracellular matrix (ECM) generated by the neighboring cells [4]. The ECM provides the physical stability and regulates the cells by influencing their survival, development, migration, proliferation, shape, and function [5]. The cell-cell and cell-ECM interactions are very critical for normal cell physiology and as a result, the loss of tissue-specific properties for cells in 2D cultures is common [4, 6].

In an attempt to alleviate the problems associated with 2D culture, new models incorporating three-dimensionality are being developed [7]. This will enable the *in vitro* data to be closer to the *in vivo* studies, thereby, providing an easier transition at various stages of the research leading towards regenerative medicine or potential novel drug discovery [4, 8]. Cell spheroids are one of the popular forms of three dimensional cell culture due to the natural tendency of cell aggregation into a sphere.

Controlling the adhesive properties of cell surfaces or engineering cellular interactions enable the patterning of cell spheroids in myriad ways. A possible approach to further promote the aggregation of non-adhesive cells and the formation of multicellular assemblies could be to

chemically modify the cell surface molecules, although, the effects of modifications on cell biology are unknown. Another method could be to use biomaterials as a scaffold for the entrapment of cell spheroids, regulating the assembly of the spheroids based on the chemical and physical properties of the biomaterial. A potential concern is whether the cell encapsulation will hinder cell functions by inhibiting cellular interactions. [9]

Engineering tissue *in vitro* involves two steps: 1) Placing cells into a biomaterial scaffold, which provides the structural and logistic template for tissue formation. 2) Culturing in a bioreactor which provides microenvironmental control and necessary molecular and physical regulatory signals. The engineered tissue is implanted into the host once a sought after developmental stage is attained. [10]

The technology of cell printing has taken enormous strides from two-dimensional (2D) culture of cells on modified material surfaces to three-dimensional (3D) printing by means of additive manufacturing of single cell suspension along with pre-formed three-dimensional cell structures [11]. From a medical perspective, 3D printing (bioprinting) is significant since it can be used to provide human-like tissues and organs for the repair, regeneration and replacement of damaged or injured organs [12]. The fabrication of living structures involves the combination of cell spheroids and hydrogels in layer-by-layer addition (see figure 1a). Bioprinting also plays a significant role in drug discovery, analysis of chemical, biological and toxicological agents, and basic research [11]. Multiple conditions of drug dosage, along with various time points can be simultaneously tested on uniform cell spheroids to get statistically significant and more consistent data (see figure 1b).

Bioprinting technology can be categorized into three types: 1) Jetting-based bioprinting, a non-contact technique involving structures being printed by layering bio-ink droplets on a substrate.

2) Extrusion based bioprinting, a method comprised of dispensing cells mixed with a hydrogel through a micro-nozzle to print 2D or 3D structures. 3) Integrated bioprinting, a hybrid system that has the ability to print a synthetic biopolymer and cell-laden hydrogel enabling the generation of tissue constructs with high mechanical strength.[13, 14]

Currently, researchers have provided proof of concept of bioprinting by fabricating a knee meniscus, heart valve, spinal disk and an artificial ear [15]. Researchers at Organovo are fabricating strips of liver tissue to use for screening of new drug treatments and are also working on growing complete human organs for drug discovery possibly eliminating the use of animals in future studies[16, 17]. Although the proof of concept studies have been tested, the organs and tissues that have been fabricated are relatively simple in that they are avascular, aneural, alymphatic, thin or hollow[16]. When thickness of the fabricated tissue surpasses 150-200 micro meters, oxygen diffusion between host and transplanted tissue is limited, leading to a loss of metabolic functions for cells. As a result, 3D bioprinting requires the use of a porous, biocompatible 3D scaffold enabling the transport of nutrients and promoting metabolic function of cells.

Gellan gum (GG), a linear anionic extracellular bacterial polysaccharide hydrogel, has shown to be advantageous due to its gelation and rheological properties [18]. GG's excellent ability to form self-supporting structures combined with its resistance of unwanted dissolution due to ionic exchange proves beneficial for tissue engineering and long term cell culture in standard cell media[19, 20]. Another important characteristic of GG also possess mechanical similarity to the elastic moduli of common tissue, making it a suitable scaffold for load-bearing applications [21]. GG has proven itself as a versatile encapsulating agent in numerous drug delivery systems for

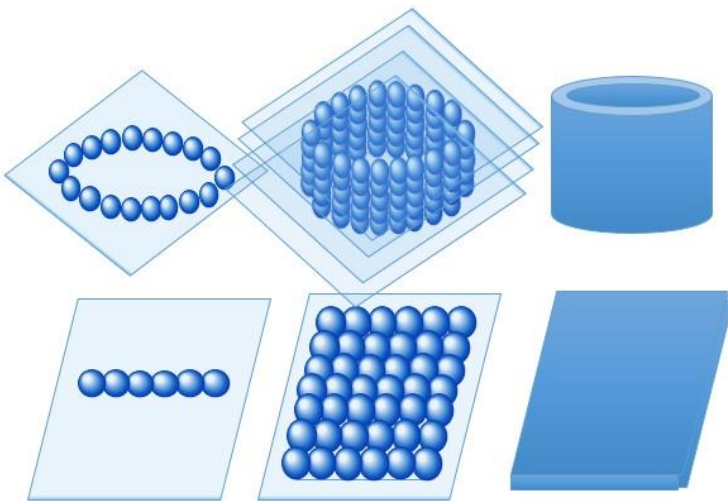
nasal, ocular, gastric and colonic applications, as implants for insulin delivery, and for wound healing applications due to its rapid gelation time near body temperature. [20].

In our study, we are using the human stem cells, human induced pluripotent stem cells and human neural stem cells to test the spheroid formation using the gellan gum based microwells generated by means of the computer controlled high-throughput robotics. These cell types are picked because of their significance for the clinical applications of cell transplantation and cell-based therapies. Human neural stem cells are a candidate cell type in studying the central nervous system disorders like traumatic brain injury and the neurodegenerative disorders like Parkinson's disease, Alzheimer's disease and subsequent cell therapy in order to generate the appropriate neuronal lineage. A major drawback involving cell survival after transplantation currently exists due to acute inflammation/immune response, trophic factor withdrawal, oxidative stress, excitotoxicity, hypoxia, or anoikis[22]. Anoikis, a form of programmed cell death, occurs due to the detaching of anchorage-dependent cells from the surrounding ECM and neighboring cells[22]. In order to prevent anoikis, appropriate and identically size neurospheres, rather than individual cell suspension, may be used. Neurospheres have shown to proliferate faster than cells in monolayer cultures with their differentiation mimicking that seen *in vivo*[22].

The second cell type being tested in the current study is the human pluripotent stem cells, Embryonic-like stem cells, including induced pluripotent cells (iPS) have a limitless capability for expansion *in vitro* and differentiation in multiple cell lineages. [10] In order to promote survival of dissociated hESCs after passage and assist the EB formation from dissociated single-cell suspension of hESCs, the p160 Rho-associated coiled-coil kinase inhibitor (ROCKi) has been used [23]. Although the exact mechanism of how ROCKi promotes survival of hESCs and assists hEB formation is unknown, evidence suggests ROCKi may prevent anoikis.[24] Using

our technology, we are able to successfully form the hEBs which do not use any xenofactor, like ROCKi or centrifugation which have a higher probability of inducing mechanical stress to the cell spheroids.

a.



b.

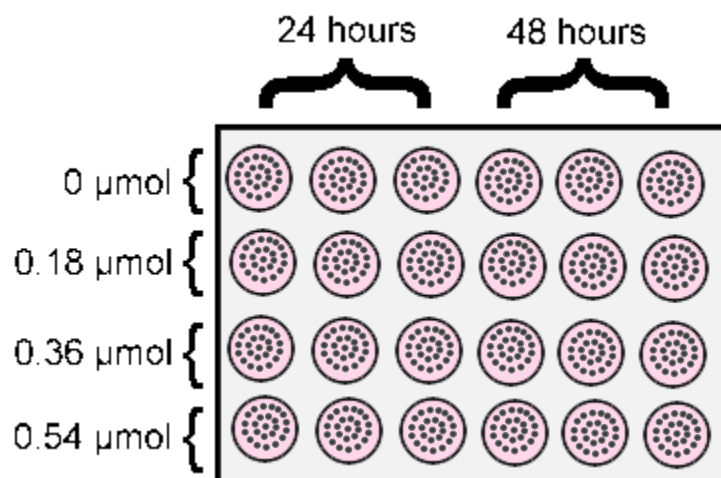


Figure 5.1: (a) Layer by layer fabrication of cell sheets with embedded spheroids as building blocks. (b) Toxicology testing of multiple drug concentrations and time points simultaneously performed on multiple spheroids per condition

5.2 MATERIALS AND METHODS

5.2.1 Materials

Phytigel™ was purchased from Sigma (St. Louis, MO). Recombinant fibroblast growth factor-2 (FGF-2) and epidermal growth factor (EGF) were purchased from Peprotech (Rocky Hill, NJ). Accutase was purchased from Innovative Cell Technologies (San Diego, CA). LIVE/DEAD viability kit was purchased from Molecular Probes (Eugene, OR). 4', 6-Diamidino-2-Phenylindole, Dihydrochloride (DAPI) was obtained from Molecular Probes (Eugene, OR). Rabbit anti- β III tubulin was purchased from Sigma Aldrich (St. Louis, MO). Mouse anti-CD68 antibody was obtained from Abcam (Cambridge, MA). Mouse anti-mitochondria antibody was purchased from Millipore (Billerica, MA). Mouse anti-GFP was obtained from Invitrogen (Carlsbad, CA). Fluorophore-conjugated secondary antibodies were purchased from Jackson ImmunoResearch (West Grove, PA). Live-Dead assay was purchased from Life Technologies. Human neural stem cells (hNSCs) were obtained from Millipore (Billerica, MA). Growth Factor Reduced Matrigel, was from BD Biosciences. ReNcell Neural Stem Cell Medium was from Millipore. mTeSR1 medium (mTeSR1 Basal Medium with mTeSR1 5X supplement) was from Stem Cell Technologies. Feeder-layer-free human induced pluripotent stem (hiPS) cell line derived from foreskin fibroblasts were obtained from WiCell (WiCell Research Institute – WB0002).

5.2.2 Preparation of hydrogels

Gellan gum, supplied by Sigma-Aldrich under the trade name Phytigel™ was added slowly to the water at room temperature with rapid stirring to eliminate any lumps before heating. It was sterilized by means of autoclaving before use for three-dimensional cell culture. Depending on the concentration, the congealing temperature varies, but generally, the congealing temperature is 27-32°C. Different concentrations (0.5-5.0%) were made using the above described procedure.

5.2.3 Rheological characterization of hydrogels

For rheological study, hydrogel solutions of Phytigel™ at various concentrations and combinations with medium were mixed on the steel plate geometry and inspected by oscillatory shear rheometry immediately. A DHR3 rheometer (TA Instruments Inc.) with standard geometry of 8 mm diameter was used for the rheological characterization of all hydrogels samples. The test methods employed were oscillatory time sweep, frequency sweep and stress sweep. The time sweep was performed to monitor the *in situ* gelation of the hydrogel solutions at 37 °C. The test, which was operated at constant frequency (1 Hz) and strain (5%) and terminated after 600 seconds, recorded the temporal evolution of shear storage modulus (G') and the shear loss modulus (G''). The stress sweep was set up by holding the temperature 37 °C and constant frequency (1 Hz) while increasing the stress level from 0.1 to 100 Pa. The range of safe-for-use stress levels are fixed by shearing them until structure breakdown and this is labelled as linear viscoelastic region (LVR) profiles of the hydrogels. We also subjected hydrogels to a frequency

sweep at 50% of their respective ultimate stress levels. At this fixed shear stress and temperature (37 °C), the oscillatory frequency was increased from 0.1 to 100 Hz and the G' was recorded.

Young's modulus, E , can be evaluated by $E = 2G(1+\gamma)$. When a material can be assumed to be incompressible, its Poisson's ratio, γ , approaches 0.5 and this relationship approaches $E = 3G$. This assumption for hydrogels is supported by a research showing that ν for polyacrylamide hydrogels is nearly 0.5, and these hydrogels typically used under very low strain. This relationship between E and G then provides a useful tool for comparing mechanical properties of substrates and tissues that have been determined using other methods of measurement.

5.2.4 Swelling of hydrogels

Hydrogels of different concentrations were used to determine the swelling properties of hydrogels in cell culture medium and PBS. To characterize the swelling behavior of the hydrogels, they were weighed immediately after preparation. Hydrogels were placed in 2 mL of PBS solution at 37 °C and allowed to swell. Weights were taken every 24 hours for the next 21 days. Fresh PBS and cell culture medium, previously equilibrated at 37 °C, was replaced every 24 hours at the time of measurement. The swelling ratio was calculated by dividing the change in weight of the hydrogels at equilibrium swelling by their weight after gelation. Deionized water was used as a control condition for the swelling studies.

5.2.5 Human neural stem cell culture

Human neural stem cells (hNSCs) were obtained from Millipore (Billerica, MA). The stem cell is an immortalized human neural progenitor cell line derived from the ventral mesencephalon region of human fetal brain and immortalized by retroviral transduction with the v-myc oncogene. Matrigel- coated culture plates (Growth Factor Reduced Matrigel, BD Biosciences) were used for hNSCs seeding. hNSCs were maintained in ReNcell Neural Stem Cell Medium (Millipore) with FGF-2 (20 ng/mL) and EGF (20 ng/mL). Human NSCs were incubated at 37 °C under 5% CO₂ and used before passage 10 in this study.

5.2.6 Human induced pluripotent stem cell maintenance culture

Feeder-layer-free human induced pluripotent stem (hiPS) cell line derived from foreskin fibroblasts (WiCell Research Institute – WB0002) were expanded in accordance with supplier recommended protocols. Briefly, hiPSCs were grown on matrigel- coated culture plates (Growth Factor Reduced Matrigel, BD Biosciences) and expanded in chemically defined mTeSR1 medium (mTeSR1 Basal Medium with mTeSR1 5X supplement; Stem Cell Technologies). For the human embryoid body formation, parallel experiments were performed using cells cultured under all the culture medium conditions.

5.2.7 Cell viability

After the generation of spheroids and their subsequent suspension culture, the viability of cells within the spheroids was examined using LIVE/DEAD Viability Kit, which is a two color fluorescent assay based on differential permeability of live and dead cells and allows preservation of the distinctive staining pattern for a couple of hours post fixation using 4%

glutaraldehyde. Live cells were stained with green fluorescent SYTO 10; and dead cells with compromised cell membranes were stained with red fluorescent ethidium homodimer-2. The Olympus IX81 laser scanning confocal microscope was used to capture the images of the LIVE/DEAD cell staining patterns at the excitation wavelengths of roughly 488 and 595 nm.

5.2.8 Embryoid body formation

Gellan gum based microwell arrays were made using in-house developed Teflon stamps. Briefly, the stamps with micropillar array (Supplement Figure 4A) were first designed using SolidWorks (Waltham, MA) and exported into STL file format. The STL file was then transferred to computer numerical controlled (CNC) ultra-high precision lathe (Siemens) to fabricate the micropillars on the Teflon stamp surface. Each micropillar was highly polished. Phytigel™ (Sigma Aldrich) was used to fabricate microwells and form embryoid bodies (EBs) in large quantity from dissociated hiPSCs. The automatic spheroid fabricator was built on a TT-C3-4040 robot (IAI Corporation, Shizuoka, Japan) with an electric triggered gripper to pick up the stamp and pipette tip uptake and ejection actuator to handle liquid. The Phytigel™ at 3.5% was dissolved in deionized water and sterilized by autoclaving. The sterilized Phytigel™, maintained on the built-in heating elements on the robotic platform was pipetted into the culture ware. The Teflon stamps were pressed into the Phytigel™ by the robotic arm for approximately 5 min. The Phytigel™ gelled in about 2 minutes, the stamps were withdrawn, and microwell array was formed into the gel substrate. The microwell arrays were stored at 37°C in PBS for a prolonged period of time (up to 2 months). No signs of contamination or other stability issues were observed at any time during the storage. The hiPSC colonies were incubated with Accutase (Innovative Cell Technologies) for 5 min at 37°C to form a single-cell suspension. The cell

suspensions were centrifuged and counted using a hemocytometer-based trypan blue dye exclusion for cell quantification method. Using this method, it was possible to obtain an accurate count of the cells, obtaining the different percentages of live and dead cells that allowed us to plate the desired number of cells into each mold. For EB formation by hiPSCs, 50 ml of cell suspension containing a total of 5,000 to 45,000 cells per well was pipetted into the hydrogel micro-well array. The cell suspension was allowed 10 minutes to settle into the microwells before more maintenance medium was added.

5.2.9 Embryonic body suspension culture and growth evaluation

After a 24-hr incubation in the hydrogel microwell array, the hiPSC EBs were pipetted from the wells and placed in suspension culture with the same maintenance medium that was used during EB formation. The iPS EBs were cultured at 37°C and 5% CO₂ under gentle agitation using a shaker. The images of the iPS EBs were acquired for diameter measurement using Image Pro Plus (Media Cybernetics, version 4.0). The size was reported as the mean and standard deviation for the batch.

5.2.10 Human Neurosphere Formation

Different cell seeding densities of 125,000 cells/microwell to upto 3x10⁶ cells/microwell were suspended in 1ml of medium and added dropwise onto the surface of the microwells robotically. After letting the cells settle down into the microwells for over a period of ten minutes, the cell culture medium for maintaining the hNSCs was added onto the surface of the microwells. The cells in the microwells were incubated at 37°C and 5% CO₂ for three days for neurosphere

formation. The formed neurospheres were transferred to a suspension culture at 37°C and 5% CO₂ under gentle agitation using a shaker for the long term culture of the neurospheres.

5.2.11 Immunofluorescence

For immunolocalization, differentiated EBs were fixed with 4% (wt/vol) paraformaldehyde for 15 min, permeabilized with 0.3% (vol/vol) Triton-X 100 in PBS for 10 min and blocked with 0.5% (vol/vol) goat serum in PBS for 1 hr. The samples were incubated with the primary antibody at 4°C overnight and then with the secondary antibody at room temperature for 1 hr. The nuclei were stained with 4',6-diamidino-2-phenylindole (DAPI) in PBS for 5 min. The following primary antibodies were used for the three germ layers for the hEBs: mouse anti-alpha 1 fetoprotein (abcam, ab3980, 5 mg/ml), rabbit anti-SOX1 (abcam, ab22572, 4 mg/ml), and goat anti-brachyury (Santa Cruz, as-17743, 1550). The secondary antibodies were Cy2-AffiniPure goat anti-mouse IgG, Fc Subclass 1 Specific (Jackson ImmunoResearch, 15100), Cy3-AffiniPure goat anti-rabbit IgG (H1L) (Jackson ImmunoResearch, 15100), Cy5-conjugated AffiniPure rabbit anti-goat IgG (Jackson ImmunoResearch, 15100). Fluorescent images of the stained EBs and neurospheres were acquired with an Olympus IX81 confocal microscope.

For the human neurospheres, nestin colocalization within the hNSCs was confirmed by using primary antibody for nestin, Mouse Anti-Nestin Antibody, clone 10C2 (Millipore, MAB5326, 1:100) and Cy2-conjugated Affinipure secondary antibody, goat anti-mouse IgG/FCγ1 (Jackson ImmunoResearch, 15100).

5.2.12 Statistical analysis

Data are shown as mean \pm S.D. Statistical analyses were performed using one way ANOVA (analysis of variance) followed by Tukey's post tests and the paired t-test where appropriate. A probability (p) value of <0.05 was considered statistically significant.

5.3 RESULTS

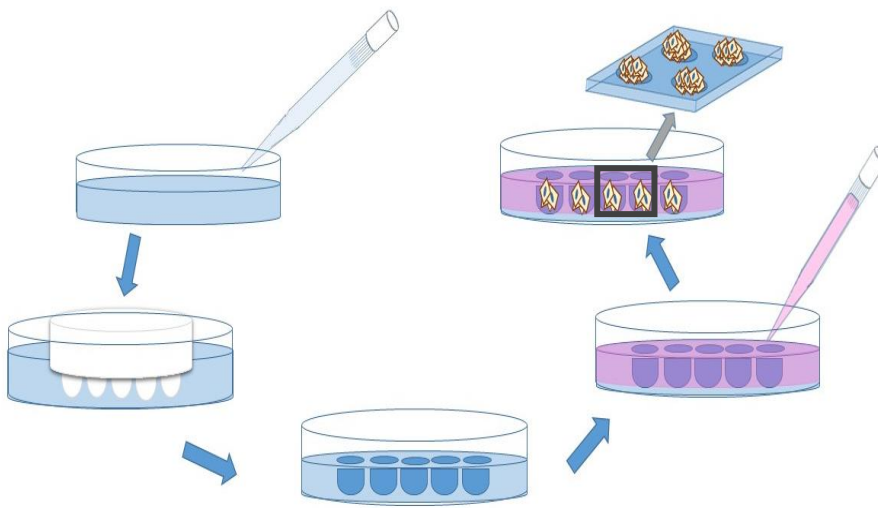


Figure 5.1: Schematic for the gellan gum based microwell fabrication

5.3.1 Gellan gum based microwell fabrication

In this study, gellan-gum based microwells were fabricated by the in-house developed computer controlled spheroid maker following the steps as shown in the schematic (Figure 5.1). After the cells were detached from the adherent monolayer from cell culture flask, hNSC and hIPSC suspensions were prepared to be seeded into the microwells in various seeding densities to generate the different sized cell spheroids with high uniformity using the in-house developed

spheroid maker (Figure 5.2). Moreover, the cells were evenly distributed and well attached to form robust spheroids.

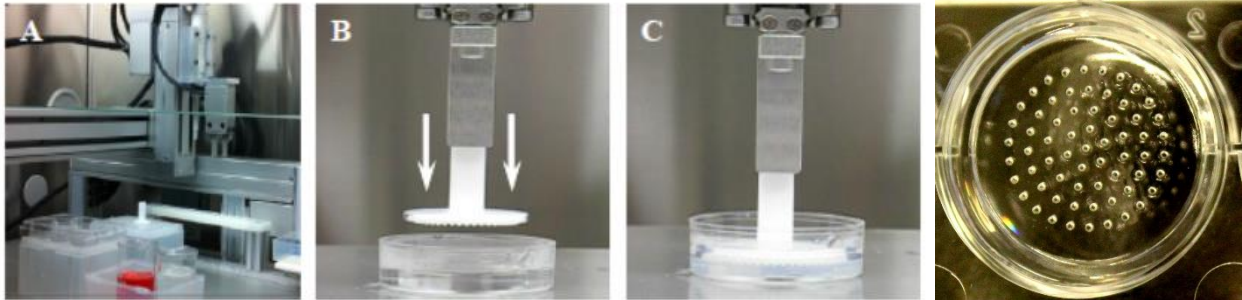


Figure 5.2: A. The Computer controlled spheroid maker, B and C. Process of microwells fabrication, D. Gellan gum Microwells

5.3.2 Rheological analysis

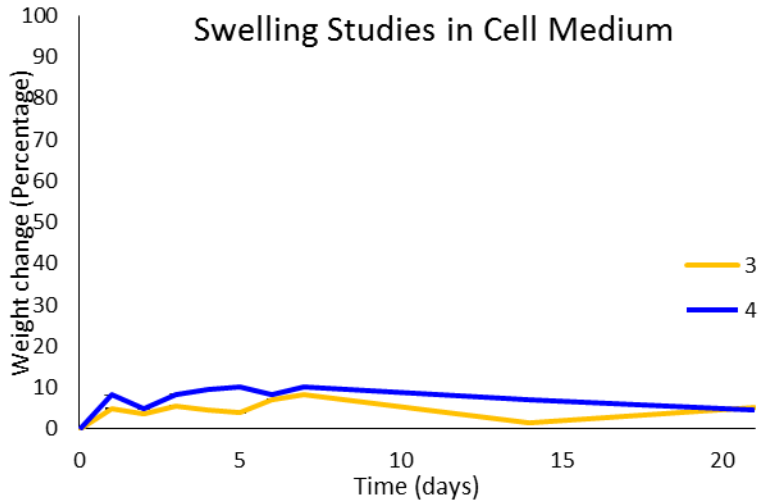
Hydrogels at various concentrations were made by dissolving the Phytigel™ in water and sterilized by autoclaving and used for fabrication of microwells. With an increase in the concentration, the G' was increased accordingly as calculated by the Oscillatory Frequency Sweep using a dynamic rheometer. Oscillatory Stress Sweep was used to determine the breaking stress at various concentrations and accordingly, the linear viscoelastic range (LVR) was determined. The elastic modulus was calculated from the values of G' for each condition of the hydrogel. The results are tabulated (Table 5.1).

Table 5.1: Rheological analysis of gellan gum concentrations to be used for microwell fabrication

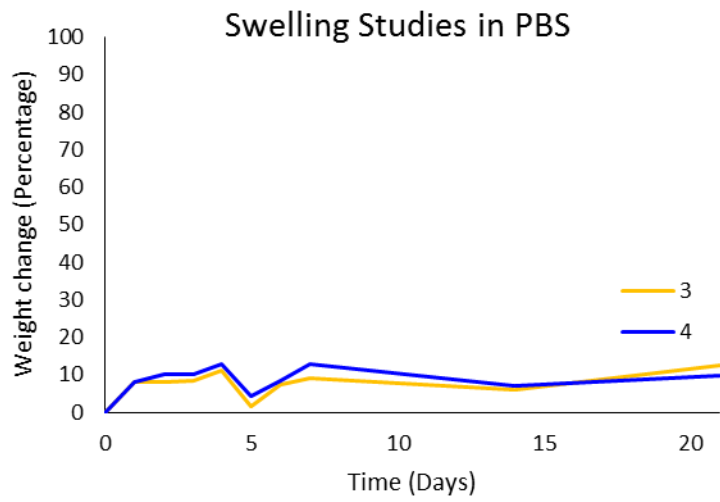
Conc	Linear Viscoelastic Range	Breaking Stress	G'	E = 3G'
2%	0.1-23 Pa	23.9 ± 3.2 Pa	2.2 ± 0.3 KPa	6.6 KPa
3%	0.1-34 Pa	34.1 ± 2.3 Pa	9.8 ± 1 KPa	29.4 KPa
3.5%	0.1-77 Pa	76.9 ± 4.4 Pa	41.5 ± 6 KPa	124.5 KPa

5.3.3 Swelling studies

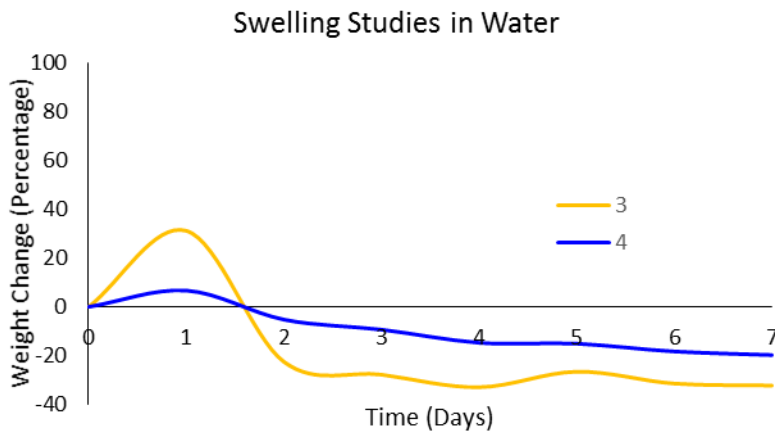
The swelling of hydrogels was studied by incubating them at 37°C and 5% CO₂. The hydrogels showed no more than 5-10% net increase in weight over a period of three weeks when incubated in PBS and DMEM-based cell culture medium and remained relatively stable over the course of study, thereby, not affecting the dimensions of microwells when incubated in PBS until the cell seeding (Figure 5.3). Deionized water (DI Water) was used as a negative control without any cations and it showed significant degradation.



a.



b.



c.

Figure 5.3: Dynamic swelling of the hydrogels of 3% and 4% was evaluated in cell culture medium (a) and PBS (b) to up to 21 days. Similar experiment was conducted simultaneously in DI water (c) as a negative control to observe the effect of cations on the swelling and potential degradation of the hydrogel

5.3.4 Human Embryoid body formation

Five different cell seeding densities of 20,000, 25,000, 30,000, 35,000 and 40,000 human foreskin-fibroblast derived pluripotent stem cells per microwell were studied to test their efficiency in forming uniform sized hEBs. Within the first one hour after the cell seeding, the cells were aggregated within the microwells and did not adhere to the surface of the gellan gum hydrogel which were not the microwells (Figure 5.4, A-E). Within 24 hours, the cells that were settled within the microwells showed a prominent core that will eventually give rise to the uniform hEBs (Figure 5.4, F-J). After the extraction from the microwells, the hEBs were added to a suspension culture which, in the next 24 hours, gave rise to uniform sized collection of hEB which had the outer layer sloughed off, which was not a part of the core (Figure 5.5, A-E). The rate of formation of the hEB was dependent on the cell seeding density to the microwells and the optimum range of the cell seeding density was observed to within the 25,000 to 40,000 cells per microwell (Figure 5.5F). The viability of the cells constituting the hEBs was shown using the Live-Dead Assay which show that the majority of the constituent cells were alive and eliminated the doubts of core necrosis in the size range tested in this study (Figure 5.6). The pluripotency of the hiPSCs within the hEBs was confirmed by studying the marker expression of the proteins exclusive to the three germ layer lineages by means of immunocytochemistry, Alpha fetoprotein (AFP) to the ectoderm, SOX1, to the endoderm and Brachyury to the mesoderm (Figure 5.7).

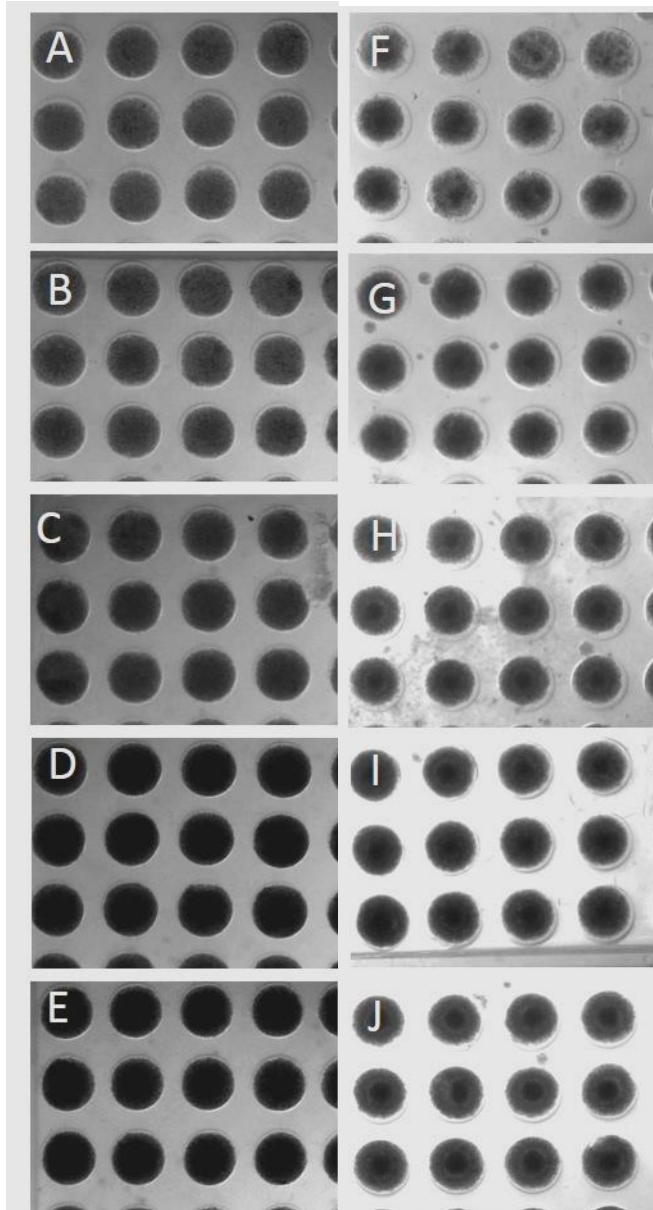


Figure 5.4: Condensation of the hiPSC suspension within the microwells immediately after seeding (A, B, C, D, E) and the compact core development within 24hours of culture in the microwells (F, G, H, I, J) for various cell seeding densities (top-bottom; 20k, 25k, 30k, 35k, 40k cells/microwell)

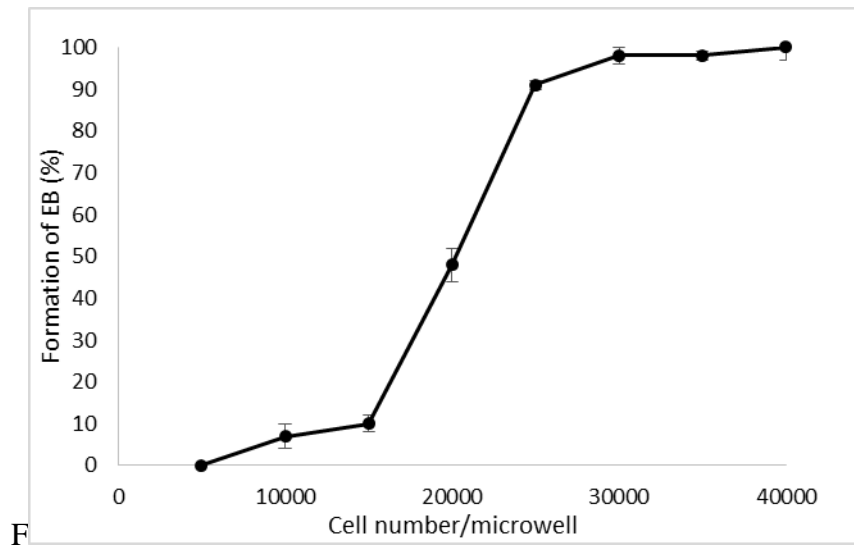
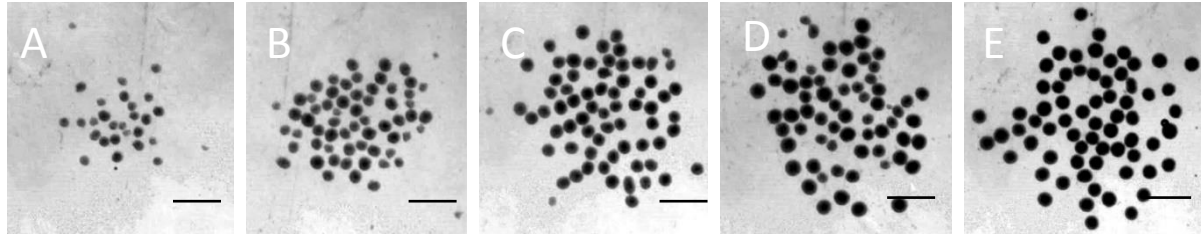


Figure 5.5: Compact and spherical hEBs were formed at various seeding densities and the size is directly proportional to the cell number per microwell, A-E, 20k, 25k, 30k, 35k, 40k cells/microwell and stayed intact after 24 hours of suspension culture with gentle agitation. **F.** The rate of formation of hEB was dependent on the cell seeding density to the microwells and the optimum range of cell seeding density was observed to be within 25k-40k cells/microwell; Scale bar: 500 μ m

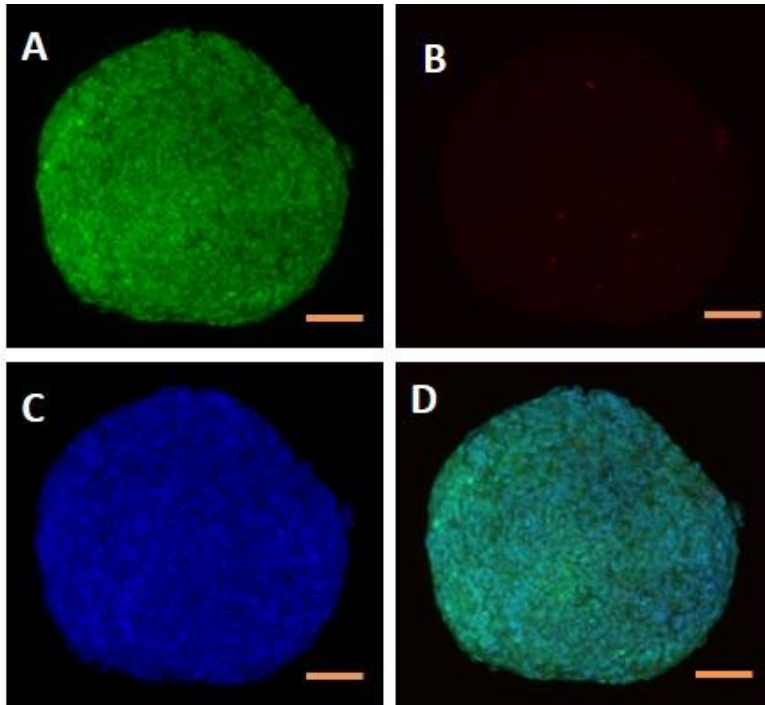


Figure 5.6: Cell viability of the hEBs was assessed by using Live-Dead assay with live cells stained with green fluorescent SYTO 10 (A) and dead cells with compromised cell membranes stained with red fluorescent ethidium homodimer-2 (B), DAPI staining for nuclei (C) and merge (D); Scale bar: 100 μ m

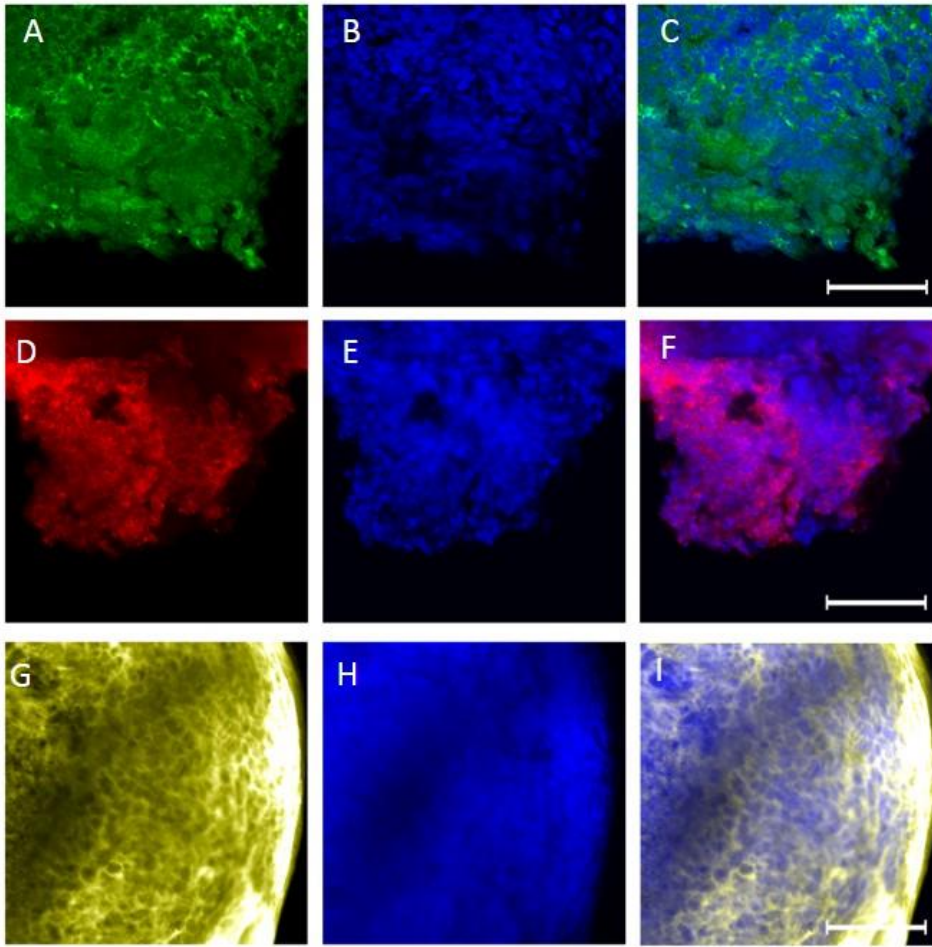


Figure 5.7: hEBs expressed the proteins specific to the three germ layer lineages with Alpha fetoprotein (AFP, endoderm-specific) (A-C), SOX1 (ectoderm-specific) (D-F) and brachyury (mesoderm-specific) (G-I); Scale bar: 100 μ m

5.3.5 Human neurosphere formation

Human neurospheres were formed in the similar manner as the hEBs with the different seeding densities to the microwell containing gellan gum hydrogel surfaces. The freshly extracted neurospheres retained their shape and structure in the suspension culture (Figure 5.8A). In suspension culture, the neurospheres showed an increase in the core diameter along with the overall diameter with the eventual sloughing off of the outer layer which was not a part of the prominent compact core (Figure 5.8, B-D). The size can be controlled by changing the cell seeding density to the microwell surface (Figure 5.9). The neurospheres had viable hNSCs as evident from the live-dead assay (Figure 5.10) which eliminates the question of core necrosis within the range of sizes examined in our study. The stemness of the neurospheres was confirmed with the positive nestin marker expression from the immunocytochemistry assay using the antibody against nestin (Figure 5.11). The uniformity of the cells within the neurosphere can be visualized using the CMFDA, cytotracker green expression of the cells and DAPI for the nuclei in a cross section of the neurosphere (Figure 5.12).

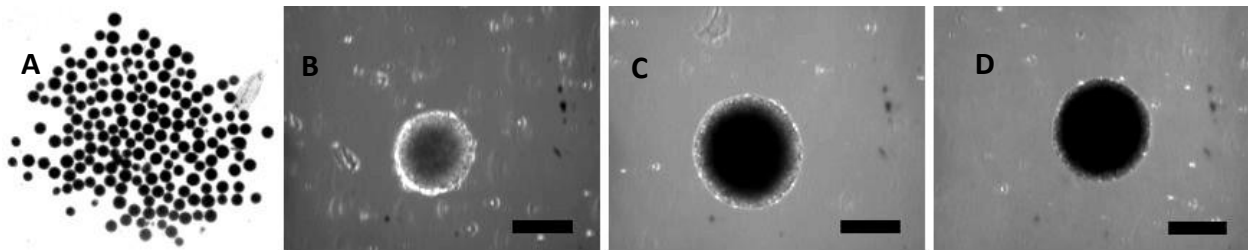


Figure 5.8: A. Freshly extracted human neurospheres from the microwells B-D. Increase in the size of the core and the overall size increase observed in the neurosphere from day 1

(B), day 2 (B) and day 4 (D) in suspension following the extraction from the microwells;

Scale bar: 200 μm

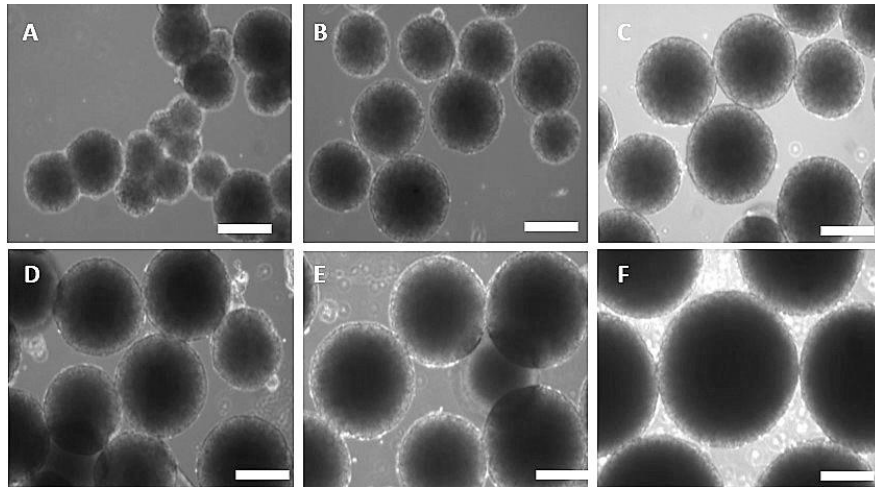


Figure 5.9: Compact and spherical human neurospheres were formed at various seeding densities and the size is directly proportional to the cell number per microwell, A-F, 125k, 250k, 500k, 750k, 1000k, 3000k cells per microwell; Scale bar: 200 μm

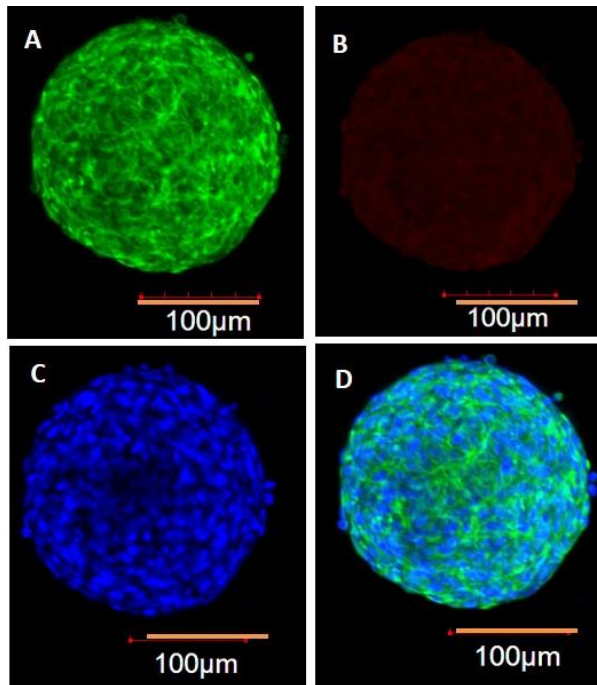


Figure 5.10: Cell viability of the neurospheres was assessed by using Live-Dead assay with live cells stained with green fluorescent SYTO 10 (A) and dead cells with compromised cell membranes stained with red fluorescent ethidium homodimer-2 (B), DAPI staining for nuclei (C) and merge (D); Scale bar: 100 µm

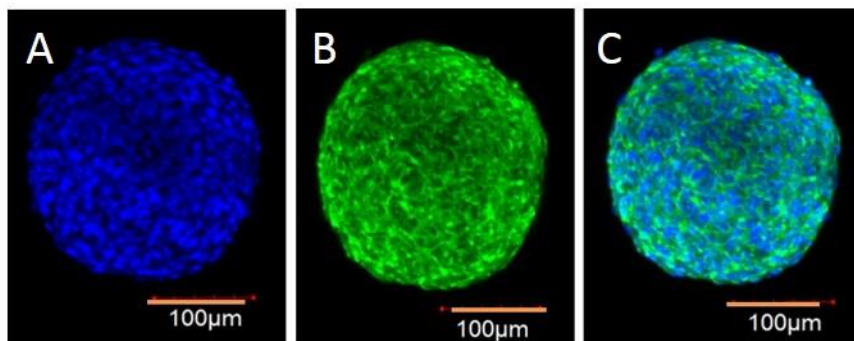


Figure 5.11: Human neurospheres expressed the nestin protein specific to the human neural stem cells with DAPI for nuclei (A), nestin antibody (B) and merge (C); Scale bar: 100 μ m

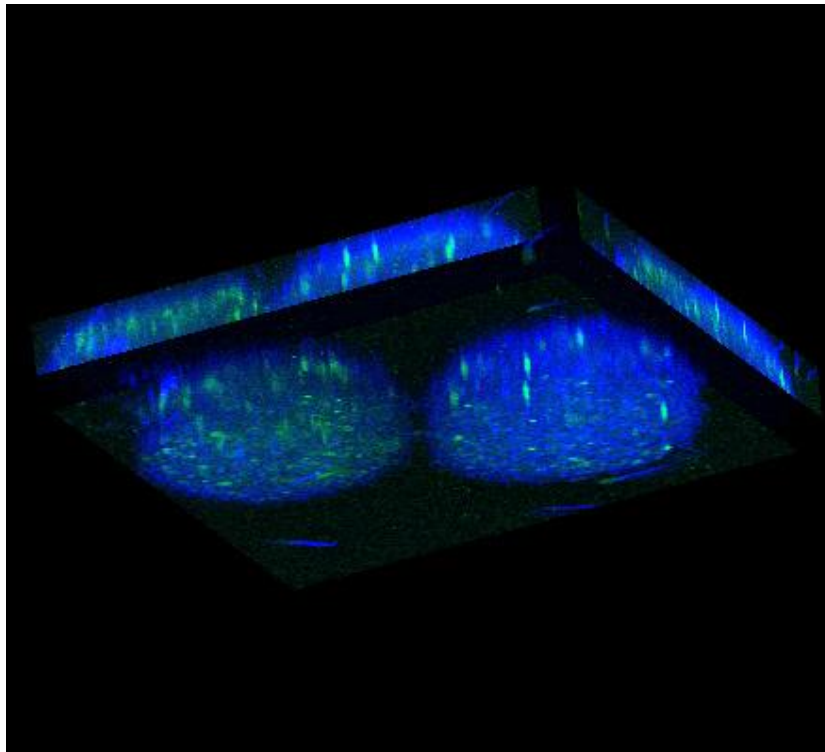


Figure 5.12: CMFDA stained cell bodies and DAPI stained nuclei of the human neurospheres were visible uniformly dispersed in the cross section of the human neurospheres proving the uniform cell distribution within the spheroids

5.4 DISCUSSION

In this study, we have developed a highthroughput technology to generate optically transparent microwells using gellan gum as the non-adhesive hydrogel. These microwells are used to create

different cell spheroids of different sizes useful for tissue printing and toxicology studies [12, 25]. The ultimate goal of creating human stem cell spheroids using a gellan gum mold is to standardize the procedure of generating human neurospheres from hNSCs, and hEBs from hiPSC in an efficient high-throughput reproducible manner. Using this method, human stem cell spheroids of different sizes can be generated by modifying the cell seeding density for their formation. The gellan gum is a novel hydrogel that is used for the imprinting of microwells. Gellan gum at the concentration from 2% and higher shows the mechanical properties that can withstand the stress of imprinting of the features without leading to deformation of the gel. An important feature of gellan gum based microwells is its transparency, which is a stand-out advantage, in applications dealing with light microscopy. The transparency of the gel based microwells decreases with increase in gel concentration. The gellan gum can also be dissolved in PBS to normalize the cell culture conditions. The monovalent and bivalent cations of the PBS render additional mechanical strength to the microwells and depending on the cell type, the mechanical strength of the base material is tunable. Gellan gum has provided an advantage of being non-cell adhesive at the concentrations of 2-4% potentially due to the higher crosslinking, which resulted in negligible pore size. This has promoted an increase in the cell-cell adhesion, and discouraged the cell-matrix adhesion.

The control of the spheroid sizes by means of modifying a simple criterion as the cell seeding density is especially beneficial to use it for applications like drug testing where in, the dosage dependency and time points can be analyzed on spheroids with cells at uniform growth conditions to get a statistically significant data. The highthroughput arraying technology developed in this study allows us to get as many microwells as required per each condition, depending on the type of stamp used for the microprinting studies. The precision at which the

stamp is imprinted can also be controlled giving rise to uniform size microwells eliminating the chances of manual errors or variations from study to study.

To test the functioning of this technology, we have used human induced pluripotent stem cells and human neural stem cells. Both the cell lines have a natural tendency to assemble into spheroid structures giving rise to the typical cell-cell interactions essential for the next stages of differentiation. Human pluripotent stem cells assemble into spheroids known as the embryoid bodies which are essential to give rise to the differentiated cell types from the lineages of the three germ layers of ectoderm, endoderm and mesoderm. In our study, we have shown the successful hEB formation by seeding dissociated single cell suspension of ROCKi-free hiPSC suspension to the microwells which assembled into the spheroids within 24 hours. The absence of xeno-factors, such as ROCKi and mechanical stress, by means of centrifugation is especially beneficial to get the intact, well organized hEBs that are not prone to the ambiguous downward signaling molecules released due to the ROCKi which may bias the cell differentiation fate of the pluripotent stem cells incorporated within the hEB or mechanical damage due to the unnatural centrifugation. Successful hEB formation was shown in a particular range of cell seeding density per microwell. All the hEBs showed the marker expression particular to the three germ layer lineages confirming their pluripotency.

The next cell type we worked with is the human neural stem cells. Human neural stem cells have different applications in the treatment of physical and neurological disorders of central nervous system including, traumatic brain injury and neurodegenerative disorders like Parkinson's disease, Alzheimer's disease [26-30]. One of the promising approaches to treat these disorders is by neuron replacement studies which use neural stem cells [30]. To solve the problem of long term cell survival of the transplanted neurons, we suggest using human neural stem cell

spheroids, neurospheres, which provide the necessary cell-cell interactions which will help in dealing with the anoikis. Also, the cell number per unit volume is considerable higher for a sphere, making the number of viable cells that survive the transplantation procedure much higher in comparison to the single cell seeding injection to the site of injury.

In our study, we showed successful human neurosphere formation which can be of different sizes depending on the cell seeding density to the microwells. Higher concentrations of hNSC seeding resulted in neurospheres of larger diameter. The cells in the neurospheres were able to maintain their stemness as evident from the nestin protein expression throughout the cells of the neurospheres. These can, in turn, undergo differentiation into neuron, astrocytes or other types of cells of neuronal lineage depending on the applications and the small molecules added to induce the differentiation.

5.6 CONCLUSIONS

In this study, uniform human stem cell based spheroids were successfully fabricated by using a computer controlled high-throughput microwells generated on non-adhesive gellan gum based hydrogels. The tunable mechanical properties of the gellan gum based on the concentration of the gellan gum and the concentration of the cations in the solvent make it a highly favorable material to generate cell spheroids of different lineages. Using these microwells, we showed successful formation of uniform hEBs from dissociated single cell suspension of the hiPSCs in the absence of xenofactors like ROCKi or mechanical stress from centrifugation. The second cell spheroids that were generated were the uniform neurospheres from the human neural stem cells with potential *in vivo* applications to treat central nervous system disorders. The automated microwell formation and the subsequent automated seeding of cells to the microwells will

change the course of the *in vitro* methods used to generate hybrid three-dimensional multicellular microtissues and can be the game-changer in scalable automatic biofabrication of large-size tissues or organs.

5.7 REFERENCES

1. Haycock, J.W., *3D cell culture: a review of current approaches and techniques*. Methods Mol Biol. **695**: p. 1-15.
2. Minchinton, A.I. and I.F. Tannock, *Drug penetration in solid tumours*. Nat Rev Cancer, 2006. **6**(8): p. 583-92.
3. Shao, Y., J. Sang, and J. Fu, *On human pluripotent stem cell control: The rise of 3D bioengineering and mechanobiology*. Biomaterials, 2015. **52**: p. 26-43.
4. Antoni, D., et al., *Three-Dimensional Cell Culture: A Breakthrough in Vivo*. Int J Mol Sci, 2015. **16**(3): p. 5517-5527.
5. Alberts B, J.A., Lewis J, et al, *The Extracellular Matrix of Animals*. 4th ed. Molecular Biology of the Cell. 2002, New York: Garland Science.
6. Lin, R.Z. and H.Y. Chang, *Recent advances in three-dimensional multicellular spheroid culture for biomedical research*. Biotechnol J, 2008. **3**(9-10): p. 1172-84.
7. Smalley, K.S., M. Lioni, and M. Herlyn, *Life isn't flat: taking cancer biology to the next dimension*. In Vitro Cell Dev Biol Anim, 2006. **42**(8-9): p. 242-7.
8. Guven, S., et al., *Multiscale assembly for tissue engineering and regenerative medicine*. Trends Biotechnol, 2015.

9. Whatley, B.R., et al., *Fabrication of a biomimetic elastic intervertebral disk scaffold using additive manufacturing*. *Biofabrication*, 2011. **3**(1): p. 015004.
10. Jakab, K., et al., *Tissue engineering by self-assembly and bio-printing of living cells*. *Biofabrication*. **2**(2): p. 022001.
11. Murphy, S.V. and A. Atala, *3D bioprinting of tissues and organs*. *Nat Biotechnol*. **32**(8): p. 773-85.
12. Mironov, V., et al., *Organ printing: tissue spheroids as building blocks*. *Biomaterials*, 2009. **30**(12): p. 2164-74.
13. Seol, Y.J., et al., *Bioprinting technology and its applications*. *Eur J Cardiothorac Surg*. **46**(3): p. 342-8.
14. Rengier, F., et al., *3D printing based on imaging data: review of medical applications*. *Int J Comput Assist Radiol Surg*, 2010. **5**(4): p. 335-41.
15. Ventola, C.L., *Medical Applications for 3D Printing: Current and Projected Uses*. *P T*, 2014. **39**(10): p. 704-11.
16. Ozbolat, I.T. and Y. Yu, *Bioprinting toward organ fabrication: challenges and future trends*. *IEEE Trans Biomed Eng*, 2013. **60**(3): p. 691-9.
17. Gross, B.C., et al., *Evaluation of 3D printing and its potential impact on biotechnology and the chemical sciences*. *Anal Chem*, 2014. **86**(7): p. 3240-53.
18. Smith, A.M., et al., *An initial evaluation of gellan gum as a material for tissue engineering applications*. *J Biomater Appl*, 2007. **22**(3): p. 241-54.

19. Ferris, C.J., et al., *Modified gellan gum hydrogels for tissue engineering applications*. *Soft Matter*. **9**(14): p. 3705-3711.
20. Oliveira, J.T., et al., *Gellan gum injectable hydrogels for cartilage tissue engineering applications: in vitro studies and preliminary in vivo evaluation*. *Tissue Eng Part A*, 2010. **16**(1): p. 343-53.
21. Silva-Correia, J., et al., *Rheological and mechanical properties of acellular and cell-laden methacrylated gellan gum hydrogels*. *J Biomed Mater Res A*, 2013. **101**(12): p. 3438-46.
22. Li, X., et al., *Engineering neural stem cell fates with hydrogel design for central nervous system regeneration*. *Progress in Polymer Science*. **37**(8): p. 1105-1129.
23. Watanabe, K., et al., *A ROCK inhibitor permits survival of dissociated human embryonic stem cells*. *Nat Biotechnol*, 2007. **25**(6): p. 681-6.
24. Pettinato, G., et al., *ROCK inhibitor is not required for embryoid body formation from singularized human embryonic stem cells*. *PLoS One*. **9**(11): p. e100742.
25. Thoma, C.R., et al., *3D cell culture systems modeling tumor growth determinants in cancer target discovery*. *Adv Drug Deliv Rev*, 2014. **69-70**: p. 29-41.
26. Zhao, P., et al., *Solving the puzzle of Parkinson's disease using induced pluripotent stem cells*. *Exp Biol Med (Maywood)*, 2014. **239**(11): p. 1421-32.
27. Jaber, M., et al., *Cell transplantation in the damaged adult brain*. *Rev Neurol (Paris)*, 2013. **169**(11): p. 838-43.

28. Elliott Donaghue, I., et al., *Cell and biomolecule delivery for tissue repair and regeneration in the central nervous system*. J Control Release, 2014. **190**: p. 219-27.
29. Kim, S.U., H.J. Lee, and Y.B. Kim, *Neural stem cell-based treatment for neurodegenerative diseases*. Neuropathology, 2013. **33**(5): p. 491-504.
30. Martinez-Morales, P.L., et al., *Progress in stem cell therapy for major human neurological disorders*. Stem Cell Rev, 2013. **9**(5): p. 685-99.

6. OVERALL CONCLUSIONS AND FUTURE DIRECTIONS

6.1 Conclusions

The major impact of this work is in the development and characterization of a novel application of the polysaccharide, gellan gum in the generation of the shear-thinning *in vitro* cell propagation system. This provides the simulation of the nature bio-mechanical environment of the cells to the research models bridging the gap between the *in vitro* and *in vivo* research, thereby, saving a vast amount of time and resources. This will, invariably, provide a reliable platform to get solutions to a variety of existing research questions.

Chapter 3: In this chapter, the preparation and characterization of gellan-gum based hydrogels that are shear-thinning was shown and it was observed that with their high rates of growth-factor entrapment and diffusivity of molecules of different size ranges, they form excellent scaffolding materials for the adhesion and propagation of different cell types. The rheological analysis on the scaffolds have shown the shear thinning and recovery abilities of the hydrogel. These hydrogels will now be used for the applications in the development of a three-dimensional *in vitro* passaging model for the cells, providing a much closer microenvironment as the extracellular matrix of the natural tissues.

Chapter 4: Within this chapter, the ability of the gellan gum based shear-thinning hydrogels to allow for cell adhesion, proliferation, and viability was tested with four different cell types, human induced pluripotent stem cells, human neural stem cells, primary cell line of human endothelial cells and the mouse insulinoma line for the pancreatic β -cells. In all the cell types investigated, it was observed that the cells could successfully assembly into organoid structures, i.e. hollow tubules for the hECs, neurospheres for the hNSCs and islet-like structures for the β -cells. The cell viability of the human induced pluripotent stem cells can be considered as the

indicator for the biocompatibility of the material to majority of the cell types, as the hiPSCs are counted amongst the difficult cells to propagate on novel substrates. In the future studies, the hydrogels with the cells are used for the further development into the organoids to be used for tissue engineering and regenerative medicine applications.

Chapter 5: In this chapter, uniform human stem cell based spheroids were successfully fabricated by using a computer controlled high-throughput microwells generated on non-adhesive gellan gum based hydrogels. The tunable mechanical properties of the gellan gum based on the concentration of the gellan gum and the concentration of the cations in the solvent make it a highly favorable material to generate cell spheroids of different lineages. Using these microwells, we showed successful formation of uniform hEBs from dissociated single cell suspension of the hiPSCs in the absence of xenofactors like ROCKi or mechanical stress from centrifugation. The second cell spheroids that were generated were the uniform neurospheres from the human neural stem cells with potential *in vivo* applications to treat central nervous system disorders. The automated microwell formation and the subsequent automated seeding of cells to the microwells will change the course of the *in vitro* methods used to generate hybrid three-dimensional multicellular microtissues and can be the game-changer in scalable automatic biofabrication of large-size tissues or organs.

6.2 Future Directions

Hydrogels with functional peptides

In chapter 3, the exceptional encapsulation abilities of the hydrogel were noted. The slow and sustained release of the growth factor, VEGF was observed. Similar studies can be performed using other growth factors like G-CSF, BDNF or GDNF in order to develop cell-specific niches. Synthetic peptides, specific to improve cell adhesion or viability of the particular cell types can also be incorporated within the hydrogel to make it a universal cell propagation model.

Chemical modification of gellan gum

The presence of multiple side chains in gellan gum can be taken into consideration in order to develop gellan gum based shear thinning hydrogels with lower degradation rates, higher structural stability, tunable sol-gel transitions etc. The interactions with cations further allows for tuning the storage modulus of the hydrogels in order to make it specific for the different cell types, ranging from the soft tissues of synovial fluid, fat tissue to the hard, mineralized tissues of bone, cartilage.

Generation of Vasculature Niche

The VEGF and Silk Fibroin have been shown to develop an excellent scaffold when incorporated into the gellan gum hydrogels. This study can be further extended in order to develop controlled vascular genesis by means of addition of synthetic peptides with the cell adhesion region or the cell viability region of the growth factors in question.

Optimizing the hydrogel system to allow for cellular coculture

The tunable mechanical properties of the hydrogels can be taken into consideration in order to develop hydrogel system which allows for coculture of different cell types, providing a different gradient of growth factors within each section of the hydrogel, catering to the specific cell types.

Co-culture of cells with endothelial cells can be useful for the organ replacement therapies with a built-in vasculature in the scaffold, allowing for the ease of translation.

Bioprinting

In the current study, the successful formation of cell spheroids in a high-throughput manner has been detailed. It is desired to apply this technology for the automated lining of the spheroids into patterns in order to develop complex three-dimensional models to generate novel solutions to the existing problems in the fields of tissue engineering and regenerative medicine.